Synthesis and Characterization of Ruthenium(II) Complexes with 3-Amino-2-(phenylazo)pyridine Ligand

Supojjanee Sansook

A Thesis Submitted in Partial Fulfillment of the Requirements
for the Degree of Master of Science in Inorganic Chemistry
Prince of Songkla University
2008

Thesis Title	Synthesis and Characterization of Ruthenium(II) Complexes with 3-Amino-2-(phenylazo)pyridine Ligand
Author	Miss Supojjanee Sansook
Major Program	Inorganic Chemistry

Major Advisor

……..……..

(Asst. Prof. Dr. Kanidtha Hansongnern)

Examining Committee :

……..……..……..Chairperson

(Assoc. Prof. Dr. Suthathip Siripaisanpipat)

……..……..…….

(Asst. Prof. Dr. Kanidtha Hansongnern)

……..……..…….

(Asst. Prof. Dr. Chaveng Pakawatchai)

……..……..…….

(Dr. Walailak Puetpaiboon)

The Graduate School, Prince of Songkla University, has approved this thesis as partial fulfillment of the requirements for the Master of Science Degree in Inorganic Chemistry

…..…..……..

(Assoc. Prof. Dr. Krerkchai Thongnoo)

Dean of Graduate School

ชื่อวิทยานิพนธ์ การสังเคราะห์และศึกษาโครงสร้างของสารประกอบเชิงซ้อนของ ruthenium (II) กับลิแกนด์ 3-Amino-2-(phenylazo)pyridine

ผู้เขียน นางสาวสุพจนี แสนสุข
สาขาวิชา เคมีอนินทรีย์
ปีการศึกษา 2551

บทคัดย่อ

ได้มีการสังเคราะห์ลิแกนด์ 3-amino-2-(phenylazo)pyridine หรือ 3aazpy ซึ่งเป็นลิแกนด์ที่มีหมู่ฟังก์ชันเอโซอิมีน การทำปฏิกิริยาระหว่างลิแกนด์ชนิดนี้กับ $RuCl_3.3H_2O$ ในตัวทำละลาย *N,N*-dimethylformamide จะได้สารประกอบเชิงซ้อน $[Ru(3aazpy)_2Cl_2]$ สองไอโซเมอร์ สารดังกล่าวสามารถแยกออกมาได้โดยเทคนิคคอลัมน์โครมาโทกราฟฟี ได้ทำการศึกษาโครงสร้างของสารแต่ละตัวโดยเทคนิคการวิเคราะห์หาปริมาณธาตุ (elemental analysis) เทคนิคอินฟราเรดสเปกโทรสโกปี (Infrared spectroscopy) เทคนิคนิวเคลียร์แมกเนติกเรโซแนนซ์สเปกโทรสโกปี (NMR spectroscopy) เทคนิคการวัดการดูดกลืนแสง (UV-Vis spectroscopy) และศึกษาไฟฟ้าเคมีโดยเทคนิคไซคลิกโวลแทมเมทรี (cyclic voltammetry) นอกจากนี้ยังได้ยืนยันโครงสร้างของ 3aazpy และผลิตภัณฑ์พลอยได้ 2-amino-3-(phenylazo)pyridine, 2a3pp โดยเทคนิคการเลี้ยวเบนของรังสีเอกซ์อีกด้วย

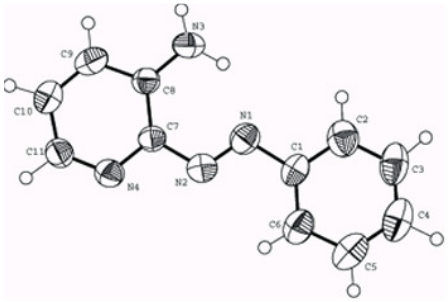

3-amino-2-(phenylazo)pyridine

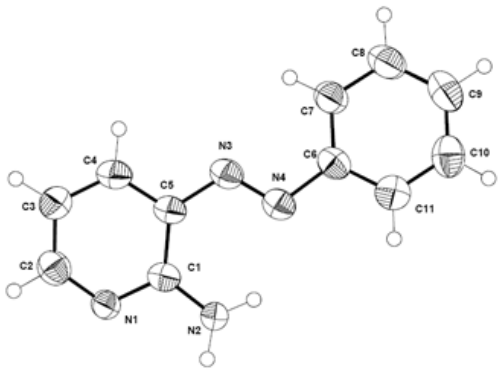

2-amino-3-(phenylazo)pyridine

Thesis Title	Synthesis and Characterization of Ruthenium(II) Complexes with 3-Amino-2-(phenylazo)pyridine Ligand
Author	Miss Supojjanee Sansook
Major Program	Inorganic Chemistry
Academic Year	2008

ABSTRACT

The azoimine functionalized ligand 3-amino-2-(phenylazo)pyridine (3aazpy) was synthesized. The reaction between 3aazpy and $RuCl_3.3H_2O$ in *N,N*-dimethylformamide afforded two isomers of the $[Ru(3aazpy)_2Cl_2]$ complexes. The complexes have been chromatographically separated. They have been characterized by elemental analyses, Infrared spectroscopy, NMR spectroscopy, UV-Vis absorption spectroscopy and cyclic voltammetry. The 3aazpy ligand and 2-amino-3-(phenylazo)pyridine (2a3pp) have been confirmed by X-ray crystallography.

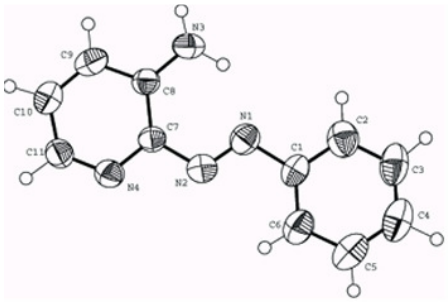

3-amino-2-(phenylazo)pyridine

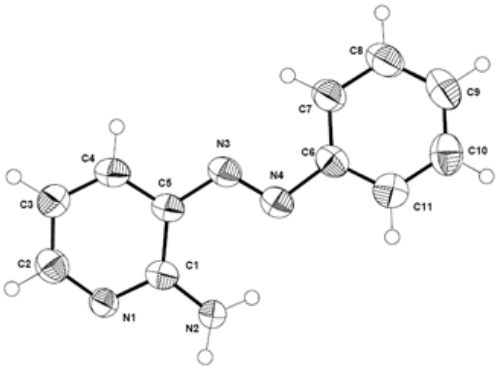

2-amino-3-(phenylazo)pyridine

ACKNOWLEDGEMENTS

I would like to thank my advisor, Asst. Prof. Dr. Kanidtha Hansongnern who provided support, knowledge, useful discussion and kindness during the laboratory work and the preparation of this thesis.

I am very grateful to Asst. Prof. Dr. Chaveng Pakawatchai for X-ray crystallographic data and helpful advice.

I would like to thank examination committee members, Assoc. Prof. Dr. Suthatip Siripaisanpipat, Dr. Walailak Puetpaiboon for their valuable time. I am grateful to Department of Chemistry, Faculty of Science, Prince of Songkla University for all necessary laboratory apparatus and chemicals supplies used throughout this research.

I would like to thank Dr. Uraiwan Changsaluk and Dr. Luksamee Sahavisit for helpful suggestion of this research.

I am very grateful to the Center of Excellence for Innovation in Chemistry (PERCH-CIC): Commision on Higher Education, Ministry of Education and Graduate School, Prince of Songkla University for financial support.

I would like to thank all members of CH 439. Their friendship, kindness and help have been valuable to me.

Finally, I would like to thank Mr. Ruk and Mrs. Sunee Sansook, my parent for love, care and encouragement.

THE RELEVANCE OF THE RESEARCH WORK

In this research, two isomers of ruthenium(II) complexes with the bidentate ligand, 3-amino-2-(phenylazo)pyridine (3aazpy) were synthesized and characterized by spectroscopic techniques. The redox properties of these compounds were studied by cyclic voltammetric technique.

Result from this work helps us to understand a variety of techniques used for the synthesis and characterization of compounds. In addition, these compounds may be developed into producing more effective catalysts, medicinal drug and other applications.

CONTENTS

CONTENTS (Continued)

LIST OF TABLES

LIST OF TABLES (Continued)

LIST OF ILLUSTRATIONS

LIST OF ILLUSTRATIONS (Continued)

LIST OF ILLUSTRATIONS (Continued)

ABBREVIATIONS AND SYMBOLS

Å	= Angstrom unit
A.R. grade	= Analytical reagent grade
3aazpy	= 3-Amino-2-(phenylazo)pyridine
2a3pp	= 2-Amino-3-(phenylazo)pyridine
azpy	= 2-(phenylazo)pyridine
CH_3CN	= Acetonitrile
$CHCl_3$	= Chloroform
CH_2Cl_2	= Dichloromethane
cm^{-1}	= Wave number
COSY	= Correlation spectroscopy
CV	= Cyclic voltammetry
d	= Doublet
dd	= Doublet of doublet
DEPT	= Distortionless Enhancement by Polarization Transfer
DMF	= *N, N*-Dimethylformamide
DMSO	= Dimethyl sulfoxide
g	= Gram
h	= Hour
HMQC= Heteronuclear Multiple Quantum Correlation experiment	
Hz	= Hertz
IR	= Infrared
J	= Coupling constant
K	= Kelvin
mg/mL	= Milligram per milliliter
mL	= Milliliter
MLCT	= Metal-to-ligand charge transfer
mmol	= Millimole
mV/s	= Millivolt per second
MW.	= molecular weight

ABBREVIATIONS AND SYMBOLS (Continued)

nm	= Nanometer
NMR	= Nuclear Magnetic Resonance
s	= Singlet
t	= Triplet
TBAH	= Tetrabutylammonium hexafluorophosphate
TMS	= Tetramethylsilane
UV-Vis	= Ultraviolet-Visible
°	= Degree
λ_{max}	= Maximum wavelength
ε	= Molar extinction coefficient
δ	= Chemical shift relative to TMS

1 INTRODUCTION

1.1 Introduction

The chemistry of azoimine (-N=N-C=N-) ligand has been studied for several years. The advantage of the azoimine functional unit is that it has a strong ability to stabilize low valence metal redox states, such as Cu(I), Ru(II), Os(II). Thus the chemistry of complexes having azoimine ligand induced some researchers to synthesize a new ligand containing azoimine unit. 2-(phenylazo)pyridine or azpy is one of the most interesting ligand in the azoimine functional unit because of its σ-donor and π-acceptor properties.

The ruthenium(II) complexes with azoimine ligands were investigated because of their potential application in many chemical reactions. For example, the complexes of $[Ru(azpy)_2Cl_2]$ (azpy = 2-(phenylazo)pyridine) have been used as catalysts in epoxidation reactions (Barf, *et al*., 1995). Its structure is shown in Figure 1.

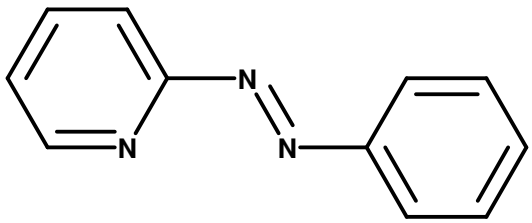

Figure 1. The structure of 2-(phenylazo)pyridine, (azpy)

In addition, the *cis*- and *trans*- isomeric complexes of $[Ru(azpy)_2Cl_2]$ showed in the vitro cytotoxicity activity in tumor-cell lines (Velders, *et al*., 2000). Moreover, the complexes of α-$Ru(azpy)_2(NO_3)_2$ showed strong binding to DNA-model bases (Holtze *et al*.,2000). The $[Ru(papm)_2Cl_2]$ complex which consists another azoimine functionalized ligand, 2-(phenylazo)pyrimidine, has an important activity of antibiotics and antimicrobials (Santra, *et al*., 1999).

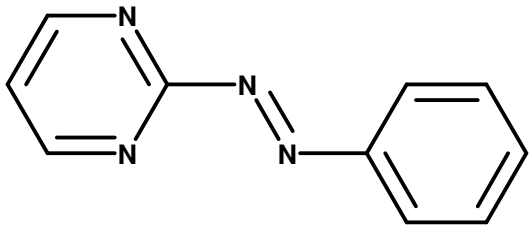

Figure 2. The structure of 2-(phenylazo)pyrimidine (azpym).

In this work, it was of interest to synthesize the complexes of Ru(II) with 3-amino-2-(phenylazo)pyridine (3aazpy) ligand. The 3aazpy is an azpy related ligand with containing an amino group (-NH_2) at the third position on the pyridine ring. The 3aazpy compound acts as a bidentate ligand that can coordinate to a metal ion through the lone electron pairs of the pyridine and the azo nitrogen atoms, forming a stable chelating 5-membered ring. The 3aazpy derived from the condensation reaction between 2, 3-diaminopyridine and nitrosobenzene provides the π-acidic azoimine fragment for metal coordination. The complexes of ruthenium(II) with 3aazpy were synthesized. Theoretically, the type of the RuL_2Cl_2, complex formula has five geometrical isomers: *trans-cis-cis* (*tcc*); *trans-trans-trans* (*ttt*); *cis-trans-cis* (*ctc*); *cis-cis-trans* (*cct*); and *cis-cis-cis* (*ccc*) by considering the order of the coordinating pairs of Cl, N(pyridine), and N(azo), respectively. From this work, we were able to isolate only two of the five isomers. The chemical properties of these ruthenium(II) complexes having the general formula [$Ru(3aazpy)_2Cl_2$] were described. The structure of the 3aazpy is shown in Figure 3.

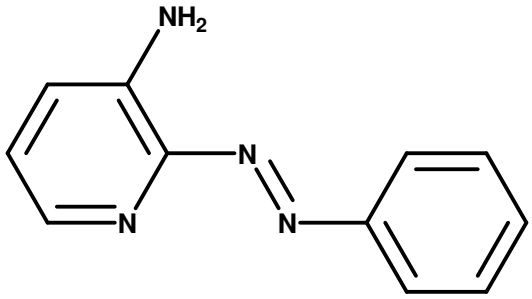

Figure 3. The structure of 3-amino-2-(phenylazo)pyridine (3aazpy)

1.2 Review of Literatures

Krause and Krause, (1980) studied dichlorobis(2-(phenylazo)pyridine)-ruthenium(II) complexes, $[Ru(azpy)_2Cl_2]$. Three isomers of $[Ru(azpy)_2Cl_2]$ were obtained from reaction between 2-(phenylazo)pyridine (azpy) and $RuCl_3.3H_2O$. There were two *cis*-isomers (α and β) and one *trans*-isomer (γ). These complexes were characterized by IR spectroscopy, UV-Visible absorption spectroscopy and ^{13}C NMR techniques. The results from cyclic voltammetric data showed that the azpy ligand was a better π-acceptor than the bpy ligand (bpy = 2,2'-bipyridine).

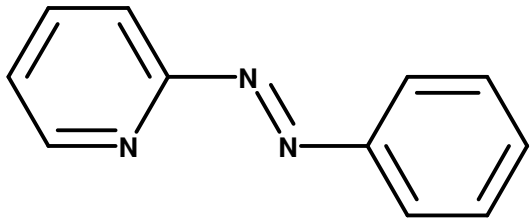

azpy

Krause and Krause, (1984) synthesized and characterized the complexes of $Ru(Naz)_2Cl_2$ (Naz = 2-(4'-nitrophenyl)azo)pyridine by infrared spectroscopic, UV-Vis absorption spectroscopic and differential pulse voltammetric techniques. In comparison with $Ru(azpy)_2Cl_2$ complexes, the Naz ligand can stabilize ruthenium(II) better than the azpy ligand. This was due to the inductive of the nitrogen group in Naz ligand as it is stronger π-acceptor property than the azpy ligand.

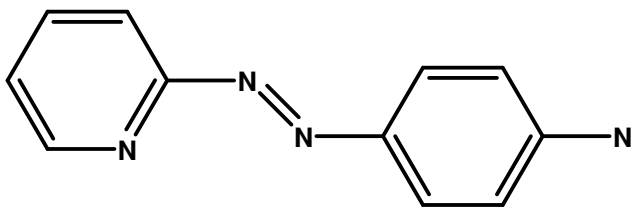

Naz

Sheldon and Barf, (1995) studied the ruthenium-catalyzed epoxidation of olefins using a variety of nitrogen-containing ligands. They reported that in the epoxidation of *trans*-stibene with $NaIO_4$ as oxygen donor and $Ru(azpy)_2Cl_2$ complexes was used as catalysts.

Santra, *et al*., (1999) describe the synthesis, spectral studied, redox properties and single crystal X-ray structure of $[Ru(aapm)_2Cl_2]$ (aapm = 2-(arylazo)pyrimidine). They synthesized a new member of azoimine family, 2-(arylazo)pyrimidine (aapm). Pyrimidine was chosen because of its higher π-acidity than that found in conventional widely used pyridine bases and also due to its biochemical importance.

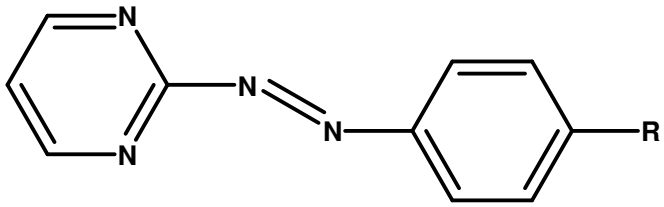

aapm

Velder, *et al*., (2000) describe the remarkably different cytotoxicity data of three isomeric dichlororuthenium(II) complexes of the type $[Ru(azpy)_2Cl_2]$, in which azpy stands for the bidentate ligand, 2-(phenylazo)pyridine. Although the mechanism of action antitumor-active ruthenium compounds was not fully understood, it was thought that, similar to the platinum drugs, the chloride complexes can be hydrolyzed in vivo, allowing the Ru to finally bind to the nucleobases of the DNA.

Hotze, *et al*., (2000) reported the new water-soluble compound α-$[Ru(azpy)_2(NO_3)_2]$. The solid-state structure of this compound has been determined by X-ray crystallography. The binding of DNA-model bases 9-ethylguanine (9egua) and guanosine (guo) to this complex has been studied.

Santra, *et al*., (2001) reported two classes of mixed-ligand ruthenium(II)-arylazopyrimidine complexes incorporating one and two 2-(arylazo)pyrimidine (aapm) ligand. Triphenylphosphine and chloride act as coligands. $Ru(PPh_3)_3Cl_2$ was used as starting complex of ruthenium. In dichloromethane, the mixing of $Ru(PPh_3)_2(aapm)Cl_2$ whereas the reaction in EtOH under reflux yields $[Ru(PPh_3)_2(aapm)_2]^{2+}$ as the major species. The complexes were characterized by spectroscopic studies and in one case, $Ru(PPh_3)_2(aapm)Cl_2$, the structure was established by X-ray crystallography.

Santra, *et al*., (2001) reported first structurally characterized coordination polymer of silver(I) with 2-(arylazo)pyrimidine (aapm). 2-(arylazo)pyrimidine belonged to neutral binucleating N,N'-chelating ligand. They posses active azoimine function and were efficient agents to stabilize low valent metal redox state. Presence of metal-related pyrimidine-N was responsible for self-assembly to generate coordination polymer.

Senapoti, *et al*., (2002) reported the synthesis, spectral studies, redox properties and single-crystal X-ray structure of one of the isomers of osmium(II) complexes of 2-(arylazo)pyrimidines (aapm). The electronic properties of $OsCl_2(papm)_2$ were different from that of ruthenium(II)-arylazopyrimidine complexes and have been interpreted from theoretical calculations using EHMO approximation.

Kamar, *et al*., (2002) described the synthesis and properties of a series of chromium(II) and chromium(III) complexes of the isomeric 2-[(N-arylamino)phenylazo]pyridine ligands. Optical properties of these were markedly different from those of the parent chromium-pap complexes.

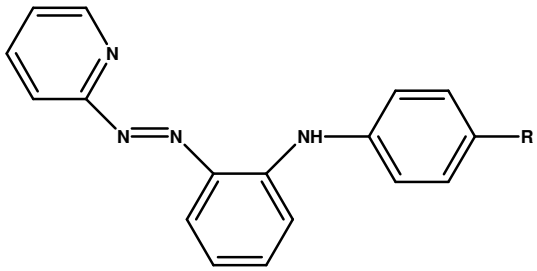

2-[(N-arylamino)phenylazo]pyridine

Lu, *et al*., (2003) described the synthesis and X-ray characterization of *tcc*- and *ccc*-[Ru(paiq)$_2$Cl$_2$] (paiq = 1-phenylazoisoquinoline) complexes. A study of some coordinated bond lengths of these complexes with other similar complexes of ruthenium(II) has been summarized and compared.

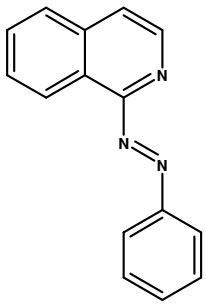

1-(phenylazo)isoquinoline

Hansongnern, *et al*., (2003) reported the synthesis and single-crystal X-ray structure of 2-(4'-*N*,*N*-diethylaminophenylazo)pyrimidine. This compound containing pyridine with the azo moiety.

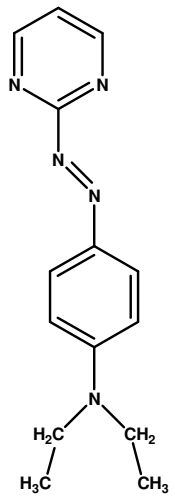

2-(4'-*N*,*N*-Diethylaminophenylazo)pyrimidine

Velders, *et al*., (2004) reported the isolation of the fourth isomer, δ-[$Ru(azpy)_2Cl_2$]. The isomeric structure of δ-[$Ru(azpy)_2Cl_2$] has been determined by ^{1}H-NMR spectroscopy and single-crystal X-ray diffraction analysis.

Bohle, *et al*., (2007) reported the synthesis and single-crystal X-ray structure of *trans*-bis(2-aminophenyl)diabenzene. This compound is a member of the azobenzene family.

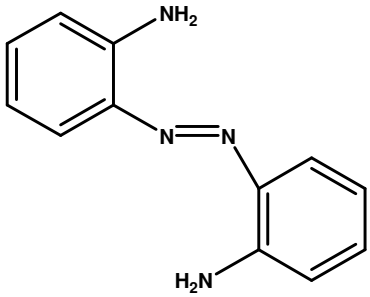

trans-Bis(2-aminophenyl)diazene

1.3 Objective

1. To synthesize the 3-amino-2-(phenylazo)pyridine (3aazpy) ligand and the isomeric complexes of $[Ru(3aazpy)_2Cl_2]$
2. To characterize and to analyze the chemistry of the 3aazpy ligand and the $[Ru(3aazpy)_2Cl_2]$ complexes.

2 MATERIALS AND METHODS

2.1 Materials

2.1.1 Chemical substances

Materials from Fluka

2,3-Diaminopyridine, $C_5H_7N_3$, A.R. grade

Nitrosobenzene, C_6H_5NO, A.R.grade

Tetrabutylammonium hexafluorophosphate, $[NBu_4]PF_6$, A.R.grade

Lithium chloride anhydrous, LiCl, A.R. grade

Materials from Merck

Silica gel 60 (0.040-0.063 nm) GF_{254}

Sodium hydroxide, NaOH, A.R. grade

Materials from Aldrich

Ruthenium(III) chloride hydrate, $RuCl_3.3H_2O$, A.R. grade

2.1.2 Solvents

Solvent from BHD Laboratory Supplies

Chloroform, $CHCl_3$, A.R. grade

Solvents from Lab.Scan analytical science

Acetonitrile, CH_3CN, A.R. grade

Dichloromethane, CH_2Cl_2, A.R. grade

Dimethyl sulfoxide, DMSO, A.R. grade

Hexane, C_6H_{14}, A.R. grade

Solvents from Merck

Methanol, CH_3OH, A.R grade

Ethanol, C_2H_5OH, A.R. grade

Hydrochloric acid, HCl, A.R. grade

Solvent from M&B Laboratory Chemical

Dimethylformamide, $HCON(CH_3)_2$, A.R. grade

2.2 Instruments

2.2.1 Melting Point Apparatus

Melting points of all compounds were measured on an Electrothermal Melting point apparatus (Electrothermal 9100).

2.2.2 Elemental Analysis

Elemental analytical data were obtained by using a CE Instruments Flash 1112 Series EA CHNS-O Analyzer

2.2.3 Infrared Spectroscopy

Infrared spectra were collected by using KBr pellets on a Perkin Elmer Spectrum GX FT-IR Spectrophotometer from 400 - 4,000 cm^{-1}.

2.2.4 UV-Visible Absorption Spectroscopy

UV-Visible absorption spectra were recorded in the range 200-800 nm by Hewlett Peckard 8425A diode array spectrophotometer.

2.2.5 Nuclear Magnetic Resonance Spectroscopy

1D and 2D NMR spectra were recorded in $CDCl_3$ solution with Fourier Transform NMR spectrometer 500 MHz, Model UNITY INOVA, Varian. Tetramethylsilane ($Si(CH_3)_4$) was used as an internal standard.

2.2.6 Cyclic Voltammetry

Electrochemical experiments were carried out using cyclic voltammetric technique. The program was Echem 1.5.1. Cyclic voltammograms were obtained using a glassy carbon working electrode, a platinum wire auxiliary electrode and a platinum disc reference electrode. The supporting electrolyte was tetrabutylammonium hexafluorophosphate, $[NBu_4]PF_6$ **,** (TBAH) in dichloromethane. At the end of each experiment, ferrocene was added as an internal standard. The argon was bubbled through the solution prior to each measurement.

2.2.7 X-ray Diffractometry

The structure of 3-amino-2-(phenylazo)pyridine ligand and 2-amino-3-(phenylazo)pyridine were determined by Smart APEX CCD diffractometer with the Xtal 3.7.1 program system.

2.3 Synthesis of ligand

3-amino-2-(phenylazo)pyridine (3aazpy)

The 3-amino-2-(phenylazo)pyridine (3aazpy) ligand was prepared by condensation reaction. 2,3-Diaminopyridine (214 mg, 2 mmol) reacted with nitrosobenzene (217 mg, 2.1 mmol) in the mixture of 30 M NaOH (3 mL) and 35 mL of benzene solution. The reaction mixture was heated in the water bath at 60-65 °C with stirring for 30 min and then refluxed for 14 h. The mixture was extracted with benzene. The brown reaction mixture was evaporated to 3 mL and transferred to silica gel column packed with hexane. The two red-orange band was eluted with hexane-ethyl acetate (9:1) mixture , which were collected and evaporated to dryness. The total yield is 37 %

2.4 Syntheses of complexes

ctc and *ccc*- [$Ru(3aazpy)_2Cl_2$]

The *ctc* and *ccc*-[$Ru(3aazpy)_2Cl_2$] complexes were prepared by mixing of $RuCl_3.3H_2O$ (20.7 mg, 0.10 mmol) and 3-amino-2-(phenylazo)pyridine ligand (59 mg, 0.29 mmol) in dimethyl formamide (10 mL) at reflux for 8 h. The solvent was removed. The residue was purified by column chromatography. The complexes were eluted with a hexane:chloroform (3:2) mixture. The blue band and dark-green band were eluted respectively. The pure complexes were collected and evaporated to dryness.

The isolated product consisted of two isomers (*ctc* and *ccc*-[$Ru(3aazpy)_2Cl_2$]). The yield of *ctc* isomer is 22 % (13 mg) and that of *ccc* isomer is 16 % (9 mg).

3 RESULTS AND DISCUSSION

3.1 Syntheses of ligand and complexes

The 3-amino-2-(phenylazo)pyridine (3aazpy) ligand was synthesized by the condensation of the 2,3-diaminopyridine and the nitrosobenzene in 1:1 mole ratio in the mixture of sodium hydroxide and benzene solution. The reaction was refluxed for 14 h. Then, the mixture was extracted with benzene and purified by column chromatography. The two red-orange product were isolated.

The isolated product consisted of two compounds, 3-amino-2-(phenylazo)pyridine (3aazpy) and 2-amino-3-(phenylazo)pyridine (2a3pp). The reaction is shown in equation (1)

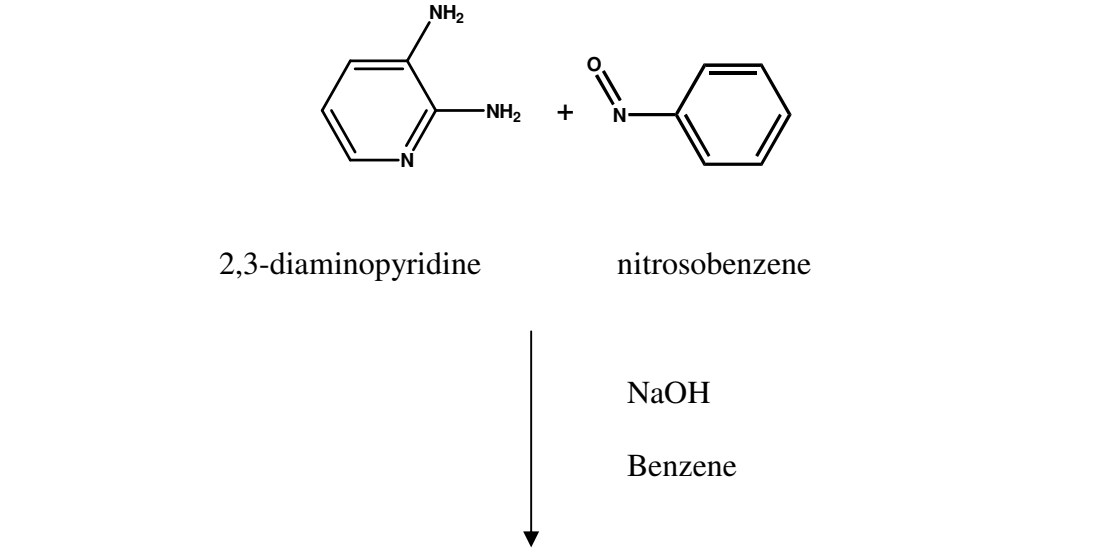

2,3-diaminopyridine nitrosobenzene

3-amino-2-(phenylazo)pyridine (3aazpy) + 2-amino-3-(phenylazo)pyridine (2a3pp) **(1)**

The yield of 3aazpy is 20 % and that of the 2a3pp is 17 %. The physical properties of the 3aazpy and 2a3pp are listed in Table 1.

Table 1. The physical properties of 3aazpy and 2a3pp

Compound	Physical properties		
	Appearance	Color	Melting point (°C)
3aazpy	solid	dark red-orange	117-119
2a3pp	solid	red-orange	148-149

The melting point of the 3aazpy ligand was in the range 117-119 °C. The solubility of 10 mg of ligand was tested in 5 mL of various solvents. The ligand was very soluble in almost all solvents (CH_2Cl_2, $CHCl_3$, CH_3CN, EtOAc, Acetone).

The 3-amino-2-(phenylazo)pyridine (3aazpy) ligand is a bidentate ligand containing the azoimine functional group, -N=N-C=N-, which has N-N donor atoms. Reaction of 3aazpy with $RuCl_3.3H_2O$ in DMF produced the complexes of $[Ru(3aazpy)_2Cl_2]$. The reactions afforded two isomers. They were *ctc* and *ccc*-$[Ru(3aazpy)_2Cl_2]$ complexes. The coordination number of these complexes was six-coordinated. The physical properties of the complexes are summarized in Table 2.

Table 2. The physical properties of the $[Ru(3aazpy)_2Cl_2]$ complexes

Compound	Physical properties		
	Appearance	Color	Melting point (°C)
ctc-$[Ru(3aazpy)_2Cl_2]$	solid	blue	> 330
ccc-$[Ru(3aazpy)_2Cl_2]$	solid	purple	> 330

The solubility of 10 mg of $[Ru(3aazpy)_2Cl_2]$ complexes was tested in 10 mL of various solvents. The results showed that complexes were slightly soluble in MeOH, EtOH, toluene, and acetone. It was completely soluble in dichloromethane, chloroform, and acetonitrile but insoluble in ether and water.

3.2 Characterization of ligand and complexes

The chemistry of the 3aazpy ligand , 2a3pp and complexes was determined by using these techniques.

3.2.1 Elemental analysis
3.2.2 Infrared spectroscopy
3.2.3 UV-Visible absorption spectroscopy
3.2.4 Nuclear Magnetic Resonance spectroscopy (1D and 2D)
3.2.5 Cyclic Voltammetry
3.2.6 X-ray Crystallography

3.2.1 Elemental analysis

Elemental analysis is a technique to study the composition of elements in a compound. It is shown that the analytical data of the compounds corresponded to the calculated values. The elemental analysis data are listed in Table 3.

Table 3. Elemental analysis data of the 3aazpy ligand , 2a3pp and the $[Ru(3aazpy)_2Cl_2]$ complexes

Compounds	% C		% H		% N	
	Calc.	Found	Calc.	Found	Calc.	Found
3aazpy	66.65	66.01	5.08	5.11	28.26	27.76
2a3pp	66.65	66.80	5.08	5.15	28.26	27.99
ctc-$[Ru(3aazpy)_2Cl_2]$	46.48	46.43	3.55	3.60	19.71	19.43
ccc-$[Ru(3aazpy)_2Cl_2]$	46.48	46.45	3.55	3.57	19.71	19.52

3.2.2 Infrared spectroscopy

Infrared spectroscopy is a technique to study the functional groups of compounds. Infrared spectra were collected by using KBr pellets in the range 4000-400 cm^{-1}. The important vibrational frequencies are C=C, C=N, N=N (azo) stretching modes and C-H bending in monosubstituted benzene.

Infrared spectroscopy of the 3aazpy ligand

The infrared spectroscopic data of the 3aazpy ligand are listed in Table 4.

Table 4. Infrared spectroscopic data of the 3aazpy ligand

Vibration modes	Frequencies (cm^{-1})
C=C, C=N stretching	1613 (s) 1476 (m)
N=N stretching	1399 (m)
C-H bending in monosubstituted benzene	802 (m) 773 (s) 687 (m)

s = strong, m = medium

The infrared spectrum of 3aazpy exhibited intense bands at 1600-400 cm^{-1}. The ligand showed medium peaks at 1613-1476 cm^{-1}, corresponding to C=C and C=N stretching in the pyridine ring of the ligand. The sharp band at 1399 cm^{-1} was assigned to the N=N stretchings,which was had a lower frequency than that in azpy (1421 cm^{-1}).This stretching mode was used to be considered the π-acid property in azo complexes. It was found that the N=N bond of the free azpy ligand is stronger than that of 3aazpy ligand. In addition, this vibrational band is expected to be of higher frequency than that in the complexes due to the coordination of ligand to ruthenium metal. The infrared spectrum is shown in Figure 4.

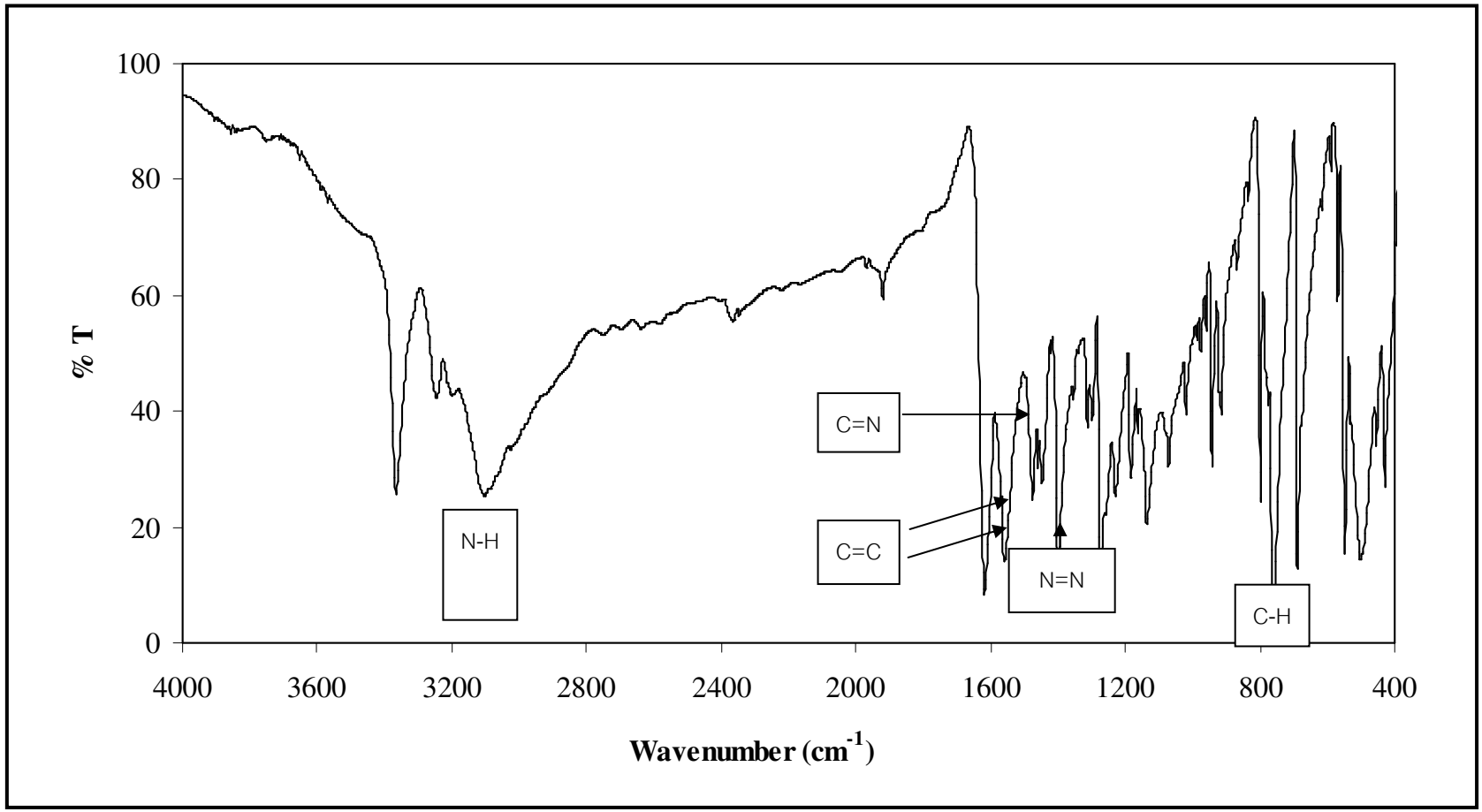

Figure 4. IR spectrum of 3aazpy.

Infrared spectroscopy of the 2a3pp

The infrared spectroscopic data of the 2a3pp are listed in Table 5.

Table 5. Infrared spectroscopic data of the 2a3pp

Vibration modes	Frequencies (cm^{-1})
C=C, C=N stretching	1617 (s) 1599 (s) 1474 (m) 1446 (m)
N=N stretching	1399 (s)
C-H bending in monosubstituted benzene	799 (m) 759 (s) 688 (s)

s = strong, m = medium

The infrared spectrum of 2a3pp exhibited intense bands at 1620-400 cm^{-1}. The compound showed medium peaks at 1617-1446 cm^{-1} , corresponding to C=C and C=N stretching in pyridine ring. The sharp band at 1399 cm^{-1} was assigned to the N=N stretchings, which had a lower frequency than in azpy (1421 cm^{-1}). The infrared spectrum is shown in Figure 5.

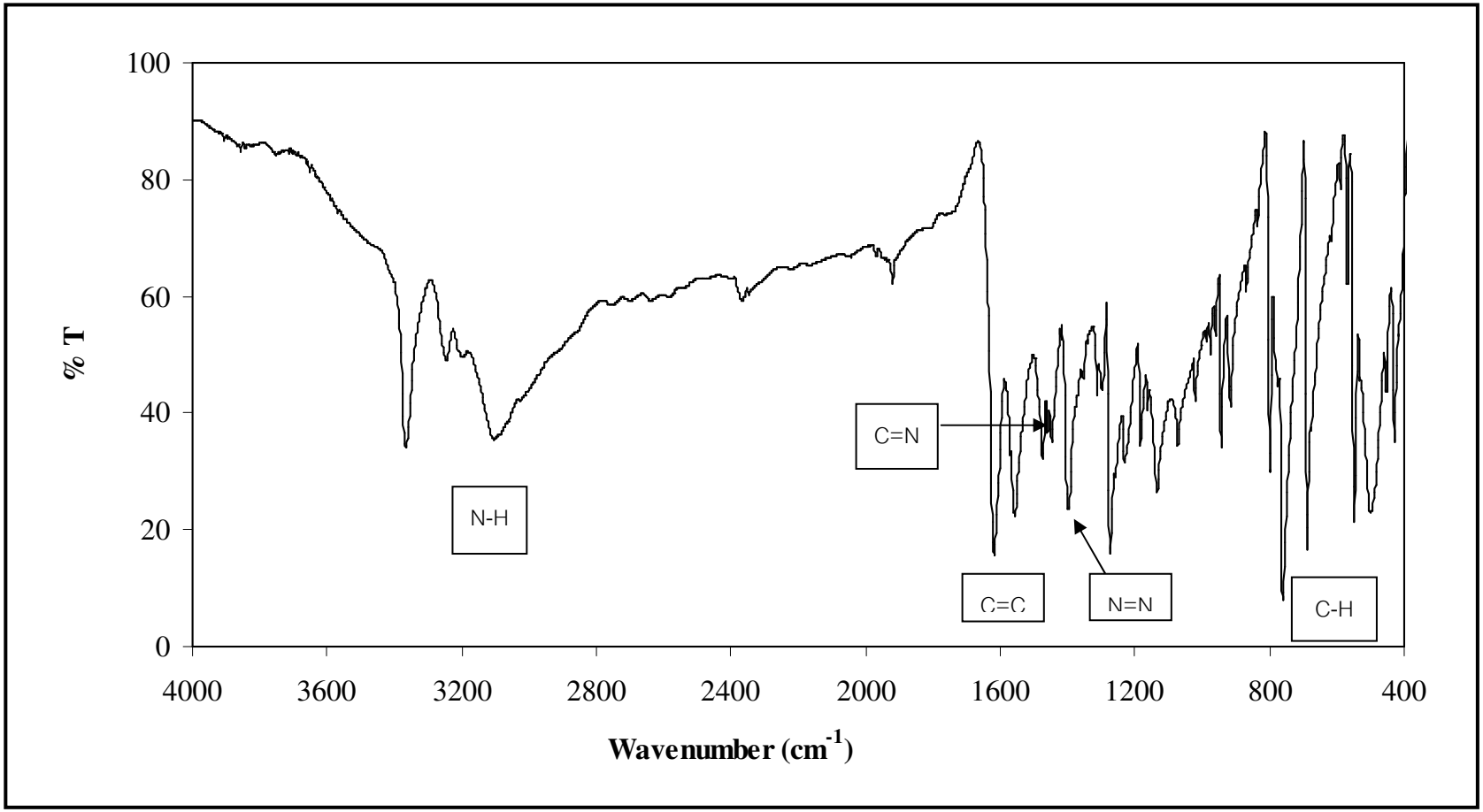

Figure 5. IR spectrum of 2a3pp.

Infrared spectroscopy of the $[Ru(3aazpy)_2Cl_2]$ complexes

The infrared spectroscopic data of the complexes are listed in Table 6.

Table 6. Infrared spectroscopic data of $[Ru(3aazpy)_2Cl_2]$ complexes

Vibration modes	Frequencies (cm^{-1})	
	ctc-$[Ru(L)_2Cl_2]$	*ccc*-$[Ru(L)_2Cl_2]$
C=C, C=N stretching	1585 (m) 1536 (m) 1422 (m)	1584 (m) 1535 (m) 1442 (m)
N=N stretching	1317 (s) 1285 (s)	1305 (s) 1287 (s)
C-H bending in monosubstituted benzene	840 (m) 767 (m) 689 (m)	840 (m) 762 (m) 688 (m)

s = strong, m = medium

In the complexes, the infrared spectra exhibited medium peaks at 1585-1422 cm^{-1}. These frequencies were assigned to the C=C and the C=N vibrational modes. The ν(N=N) (1305-1317 cm^{-1}) is red shift by 94-82 cm^{-1} , compared to the free ligand value (1399 cm^{-1}) which is a good indication of N-coordination.

It is noted that the N=N stretching modes in the complexes appeared at lower frequency than that in the free ligand. It was due to the π-back bonding occurring from the t_{2g} orbitals of metal to the π* orbitals of azo. From this result, the bond order of N=N (azo) decreased and the bond length increased, so the vibrational energies decreased. In addition, ν(N=N) of the *ctc*-[$Ru(3aazpy)_2Cl_2$] appeared at the higher frequency than the *ccc*-[$Ru(3aazpy)_2Cl_2$]. It indicated that the 3aazpy in *ctc* could accept electrons from the t_{2g}(Ru) orbitals to its π* orbitals less than *ccc* (*ccc* > *ctc*). The infrared spectra of the [$Ru(3aazpy)_2Cl_2$] isomers are shown in Figure 6 and 7, respectively.

The N=N stretching mode [$Ru(azpy)_2Cl_2$] appears between 1303-1323 cm^{-1} and an azo mode at 1424 cm^{-1} (free azpy) indicates conjugation the shift to lower energy in the complexes indicates less double-bond character in the N=N group. The N=N stretching mode in [$Ru(3aazpy)_2Cl_2$] gave similar results to those in [$Ru(azpy)_2Cl_2$] (*Inorg Chem*. 1980, 19, 2600-2603).

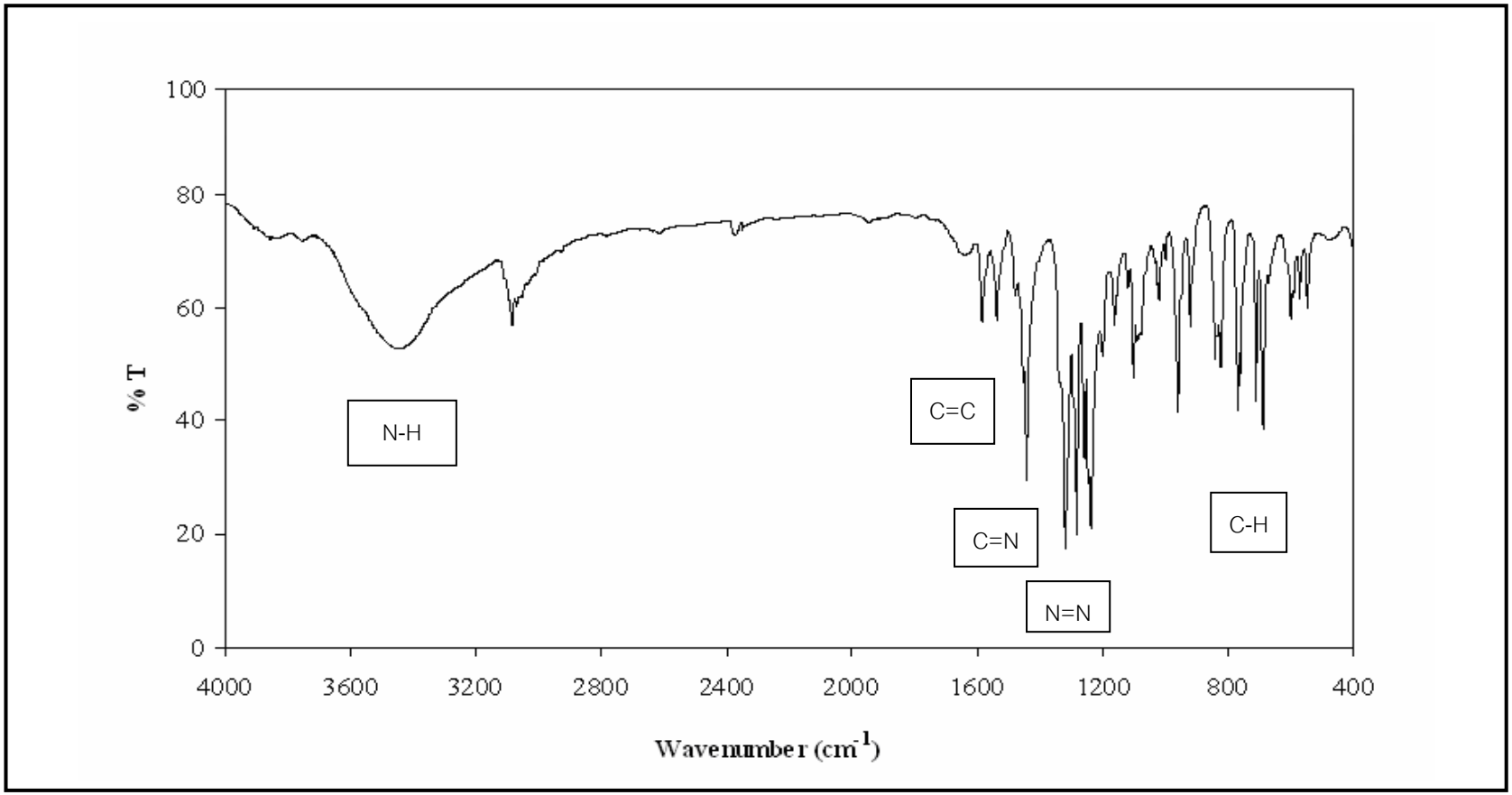

Figure 6. IR spectrum of *ctc*-[Ru(3aazpy)$_2$Cl$_2$].

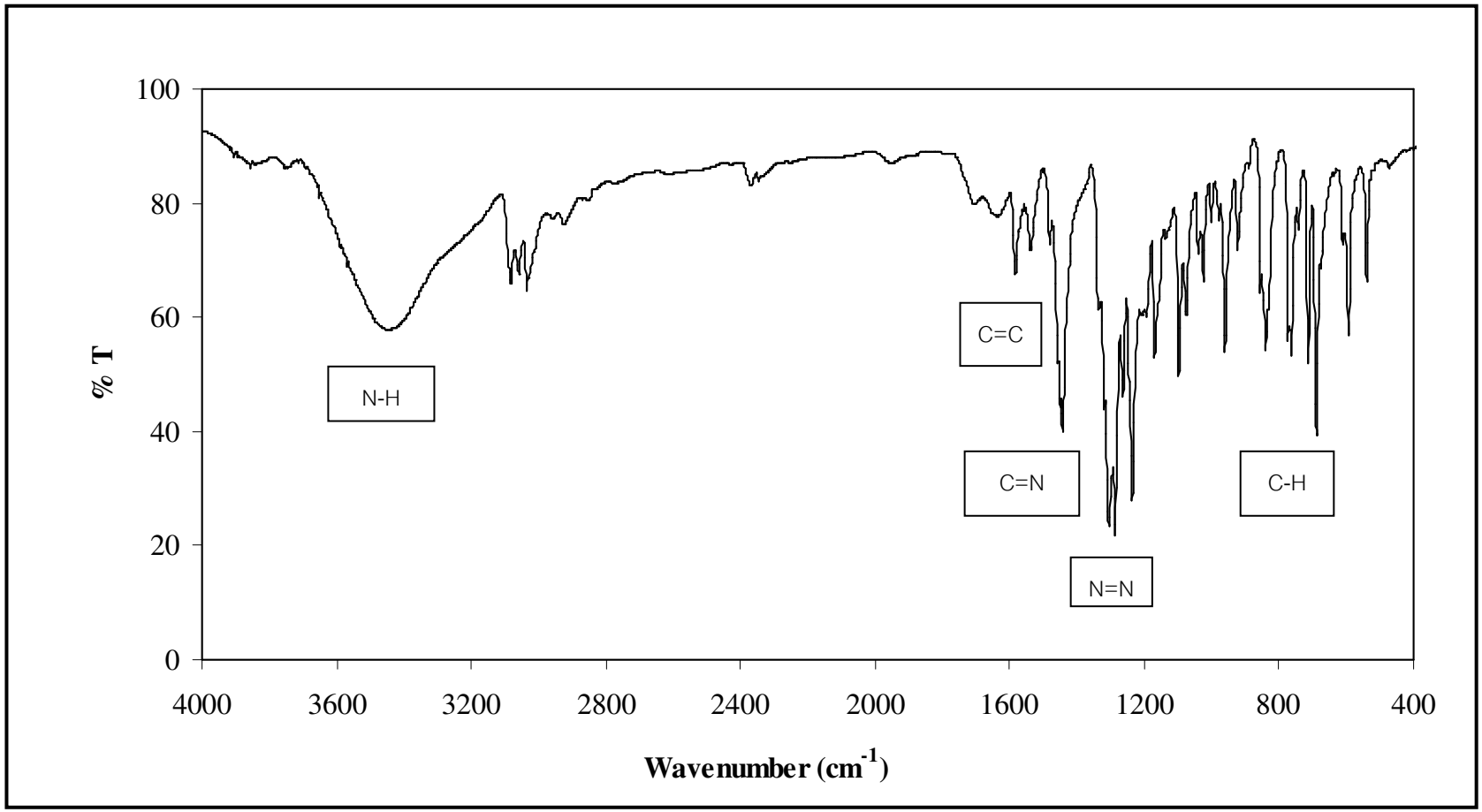

Figure7. IR spectrum of *ccc*-[Ru(3aazpy)$_2$Cl$_2$].

3.2.3 UV-Visible absorption spectroscopy

UV-Visible absorption spectroscopy is a technique to study the electronic transitions of compound. The electronic absorption spectra of the complexes in five solvents were recorded in the range of 200-800 nm. The spectral data are given in Table 7. The absorption spectra of all compounds in CH_2Cl_2, $CHCl_3$, CH_3CN, DMF and DMSO are shown in Figure 8 to Figure 11.

Table 7. UV-Visible absorption spectroscopic data of the ligand, 2a3pp and the complexes.

Compounds	λ_{max} nm, ($\varepsilon^a \times 10^4$ $M^{-1}cm^{-1}$)				
	CH_2Cl_2	$CHCl_3$	CH_3CN	DMF	DMSO
3aazpy	237 (1.1) 288 (0.7) 407 (0.8)	245 (0.7) 288 (0.5) 406 (0.5)	234 (1.2) 286 (0.7) 412 (0.7)	278 (1.4) 424 (0.9)	276 (2.3) 427 (0.9)
2a3pp	238 (1.4) 298 (0.8) 394 (1.0)	245 (1.2) 298 (0.8) 393 (1.1)	234 (1.2) 296 (0.6) 396 (0.8)	298 (0.9) 408 (1.1)	298 (0.8) 410 (0.9)
ctc-[Ru(3aazpy)$_2$Cl$_2$]	331 (3.3) 582 (1.0)	331 (1.8) 597 (0.8)	230 (2.3) 327 (2.3) 586 (0.9)	331 (3.2) 592 (1.3)	331 (2.5) 589 (1.1)
ccc-[Ru(3aazpy)$_2$Cl$_2$]	355 (2.1) 592 (1.3)	361 (1.6) 584 (0.8)	347 (1.4) 576 (0.7)	351 (2.0) 580 (1.0)	351 (1.6) 578 (0.8)

[a] Molar extinction coefficient

UV-Visible spectral studies of the free ligand displayed absorption at 276-288 nm ($\varepsilon \approx 11200\ M^{-1}cm^{-1}$) which was assigned to $\pi \longrightarrow \pi^*$ transition and the band in visible region, 406-427 nm ($\varepsilon \approx 7600\ M^{-1}cm^{-1}$) was assigned to $n \longrightarrow \pi^*$. These bands are due to the intraligand charge transition. Figure 8 shows the UV-Visible absorption spectrum for the 3aazpy ligand in CH_2Cl_2 solvent and Figure 9 shows UV-Visible absorption spectrum for the 2a3pp in CH_2Cl_2 solvent.

The two *cis* complexes, *ctc*-[$Ru(3aazpy)_2Cl_2$] and *ccc*-[$Ru(3aazpy)_2Cl_2$] displayed intense bands in UV region within the range 327-361 nm, intraligand charge transfer transition and at 576-597 nm, metal-to-ligand charge transfer transition. The electronic spectra of *cis* complexes in the visible region (576-597 nm) which existed in two isomeric forms. The *cis* complexes displayed two different intense band characters. The most intense bands were in the range of 327-361 nm and the less intense bands were in the range of 576-597 nm. Figure 10 and 11 show the UV-Visible absorption spectra for all the two complexes in CH_2Cl_2 solvent.

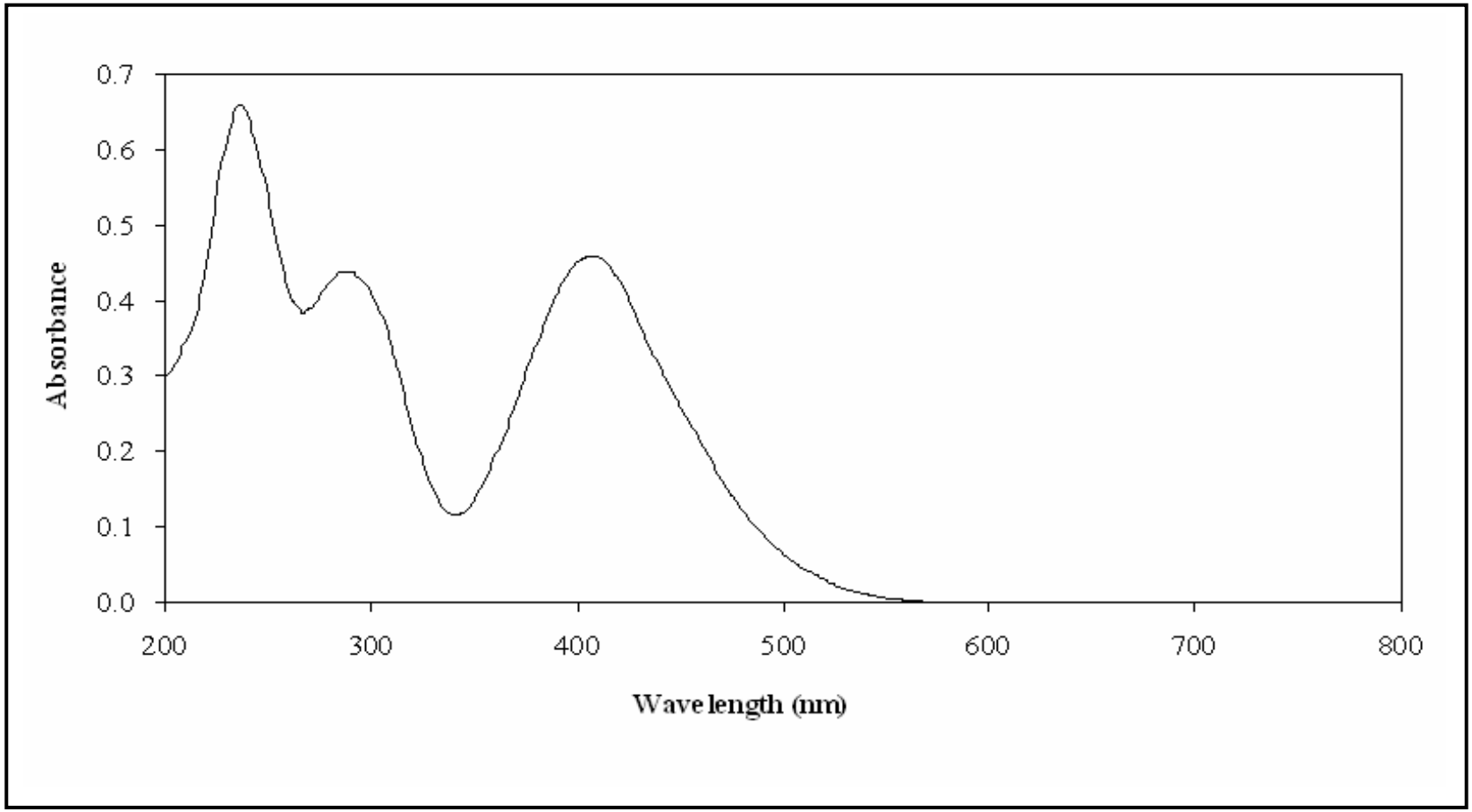

Figure 8. UV-Visible absorption spectrum of 3aazpy in CH_2Cl_2.

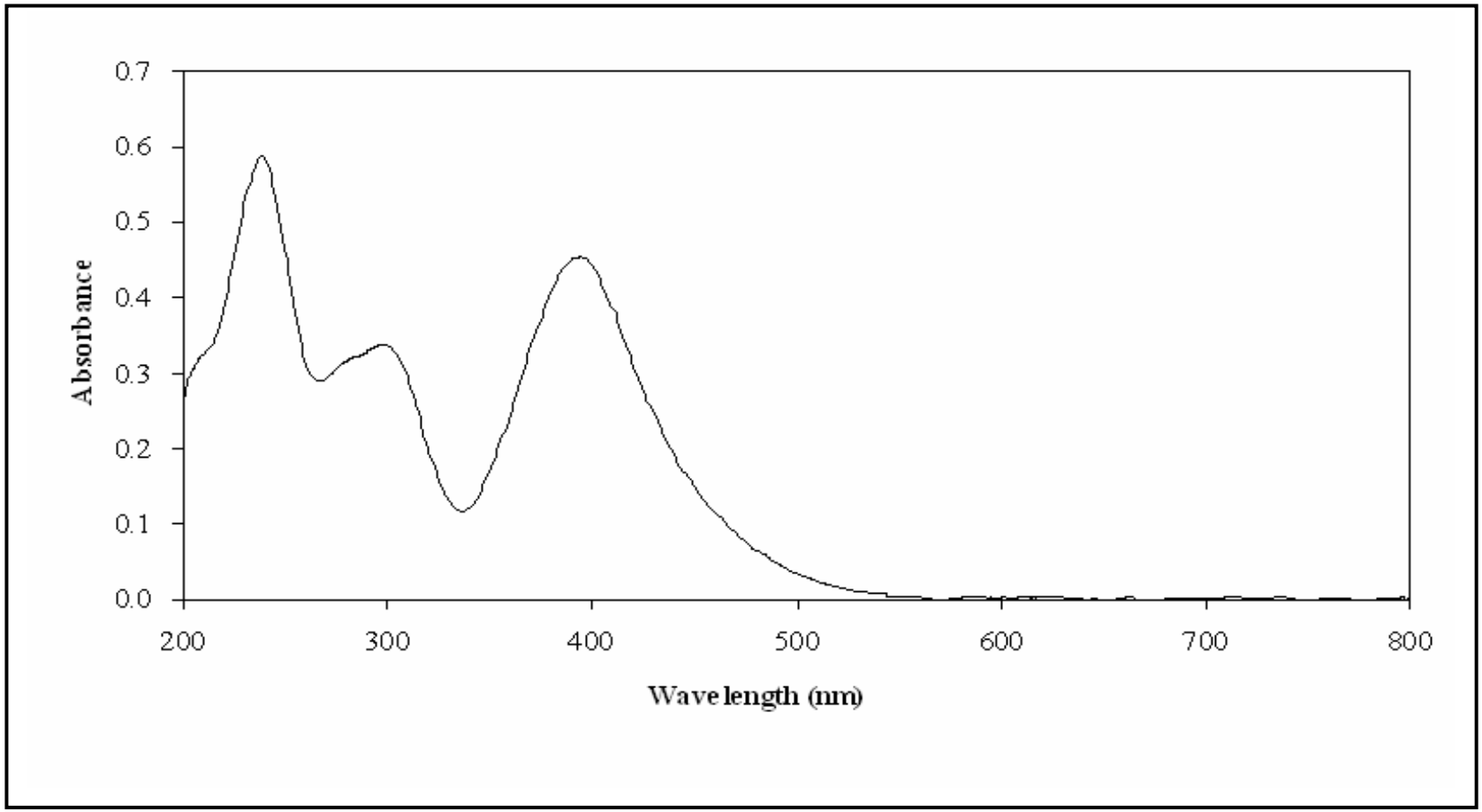

Figure 9. UV-Visible absorption spectrum of 2a3pp in CH_2Cl_2.

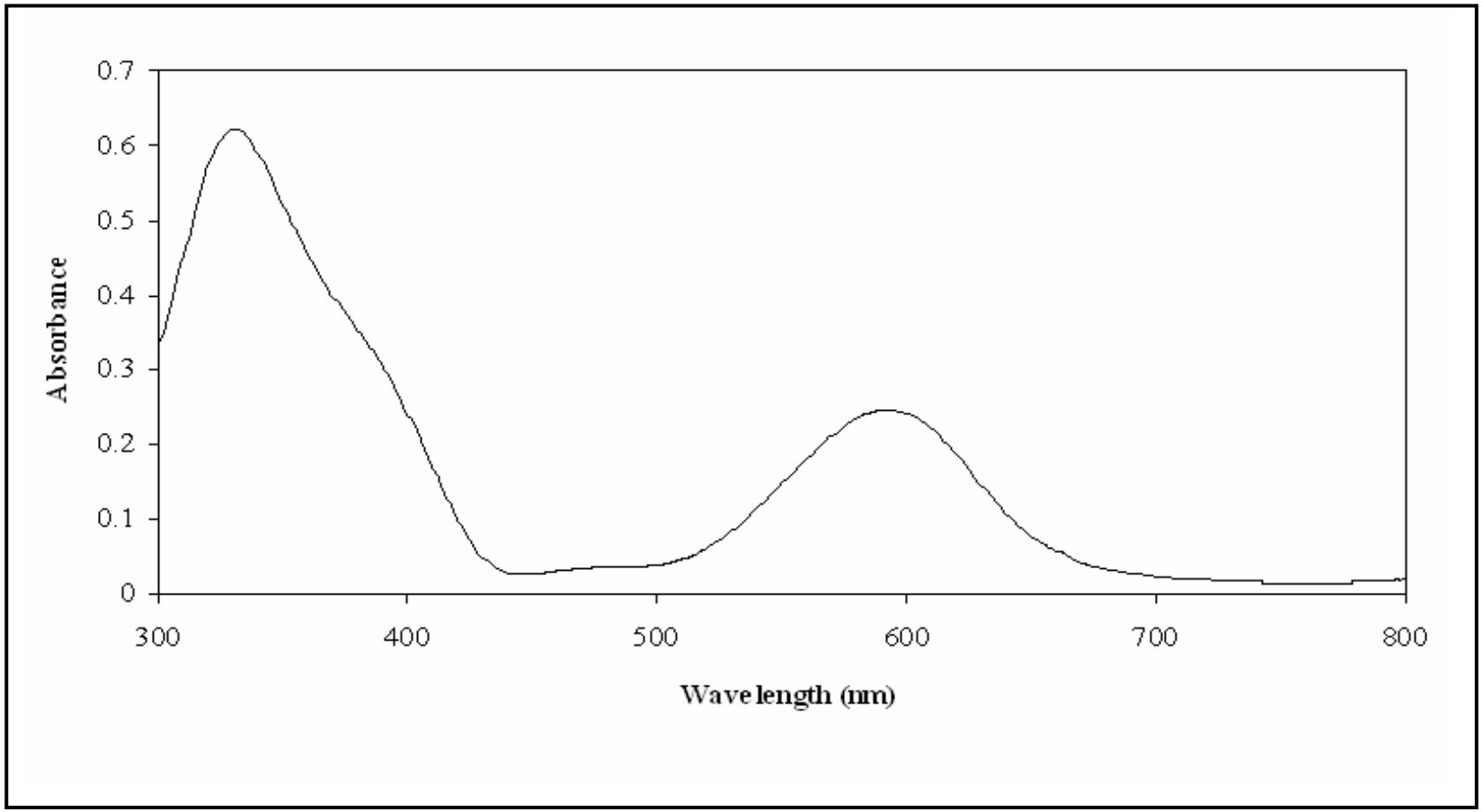

Figure 10. UV-Visible absorption spectrum of *ctc*-[Ru(3aazpy)$_2$Cl$_2$] in CH_2Cl_2.

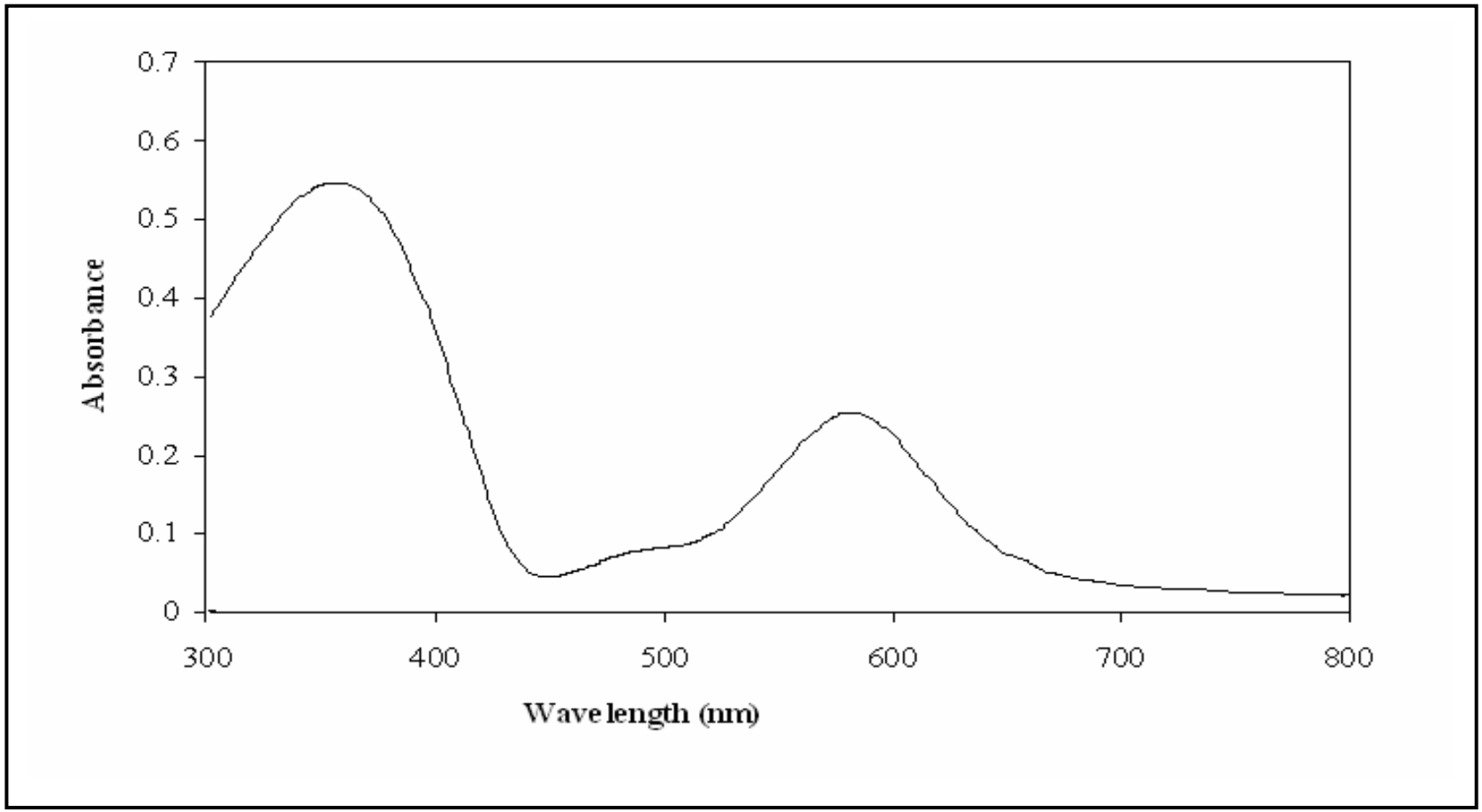

Figure 11. UV-Visible absorption spectrum of *ccc*-[Ru(3aazpy)$_2$Cl$_2$] in CH_2Cl_2.

3.2.4 Nuclear Magnetic Resonance spectroscopy (1D-2D)

Nuclear Magnetic Resonance (NMR) spectroscopy is a technique to determine the molecular structure of a compound. The structures of ligand and complexes were investigated by using 1D and 2D NMR spectroscopic techniques (^{1}H NMR, ^{1}H-^{1}H COSY NMR, ^{13}C NMR, DEPT NMR and ^{1}H-^{13}C HMQC NMR). The NMR spectra of all compounds were recorded in $CDCl_3$ on UNITY INOVA 500 MHz. The tetramethylsilane ($Si(CH_3)_4$) was used as an internal reference.

The 3-amino-2-(phenylazo)pyridine (3aazpy) has ten protons on the molecule. The ^{1}H NMR spectrum of 3aazpy showed seven signals (Figure 12). The highest field signal was assigned to H11 (-NH_2). The most downfield of H6 was due to the nitrogen atoms which was located close to it. The protons H4 and H5 appeared as multiplet peak at 7.1 ppm. The signal of proton H9 and H10 showed as multiplet peaks at the same position due to both protons being located close to each other. In the phenyl ring, the proton H8 were two equivalent protons. The signal occurred as a doublet peak at 7.9 ppm. This resonance appeared at the lower field than the proton H9 and H10 because it located next to the azo nitrogen, the ^{1}H NMR spectrum of the 3aazpy ligand was shown in Figure 12. In addition, the peak assignment was supported by using simple correlation ^{1}H-^{1}H COSY NMR spectroscopy. The ^{1}H-^{1}H COSY NMR signals are presented in Figure 13.

The ^{13}C NMR (Figure 14) results corresponded to those from DEPT NMR (Figure 15), which showed only methane carbon signals. The ^{13}C NMR spectrum of the 3aazpy ligand gave 9 signals for 11 carbons. The quaternary carbon C2 of the pyridine ring appeared at the most downfield. The signal at 146 ppm was due to the quaternary carbon C7 on the phenyl ring. The intense peak at 139 ppm referred to the quaternary carbon C4. The signal of carbon C6 occurred at the lower field than that of other methane carbons because it is located next to the nitrogen atoms. The carbon signals at 122 and 129 ppm were attributed to the two equivalent carbon C8 and C9. The signals of carbon C3, C5, and C10 appeared at 139, 125, and 131 ppm, respectively. The ^{13}C NMR signals assignments were based on the ^{1}H-^{13}C

HMQC NMR spectrum (Figure 16), which exhibited a correlation between ^{1}H NMR spectrum and ^{13}C NMR spectrum.

Nuclear Magnetic Resonance spectroscopy of the 3-amino-2-(phenylazo)pyridine ligand

Table 8. ^{1}H and ^{13}C NMR spectroscopic data of the 3aazpy ligand

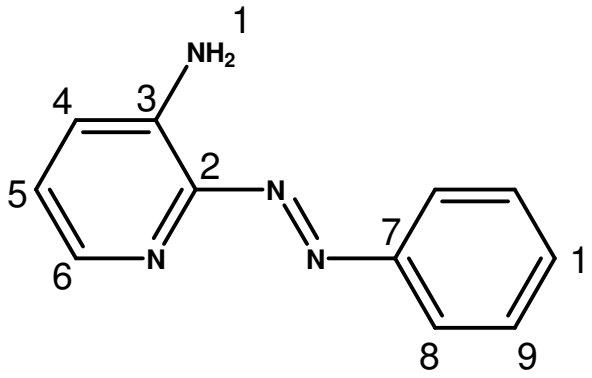

H-position	^{1}H NMR			^{13}C NMR δ (ppm)
	δ (ppm)	*J* (Hz)	Number of H	
6	8.1 (*dd*)	4, 2	1	138
8	7.9 (*d*)	7	2	122
9 10	7.5 (*m*)	-	3	129 131
4 5	7.1 (*m*)	-	2	126 125

Table 8. (Continued)

H-position	^{1}H NMR			^{13}C NMR δ (ppm)
	δ (ppm)	J (Hz)	Number of H	
11	5.9 (*s*)	-	2	-
Quaternary carbons				152, C2 146, C7 139, C3

s = singlet, d = doublet, t = triplet, dd = doublet of doublet

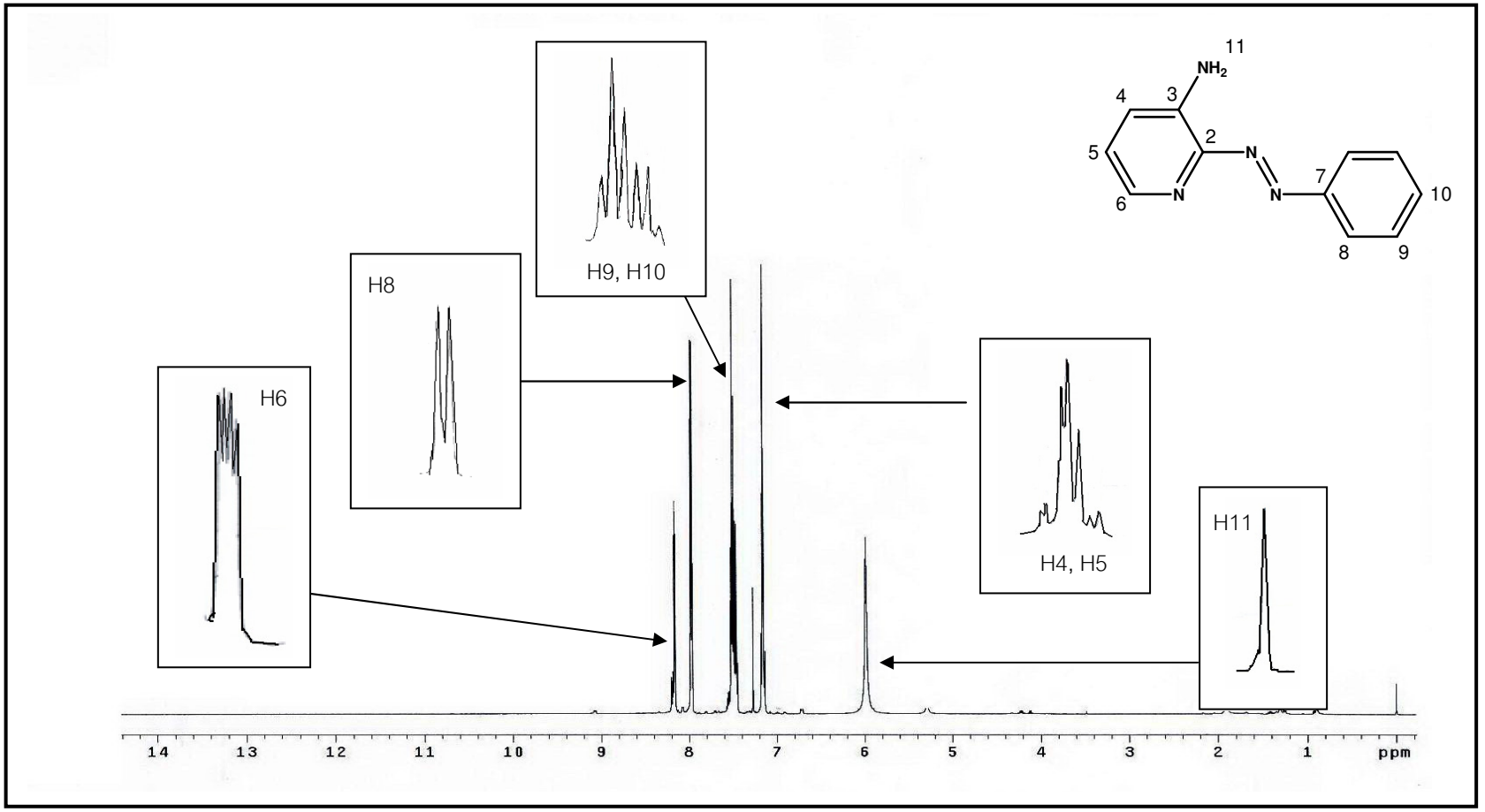

Figure 12. ^{1}H NMR spectrum of 3aazpy in $CDCl_3$.

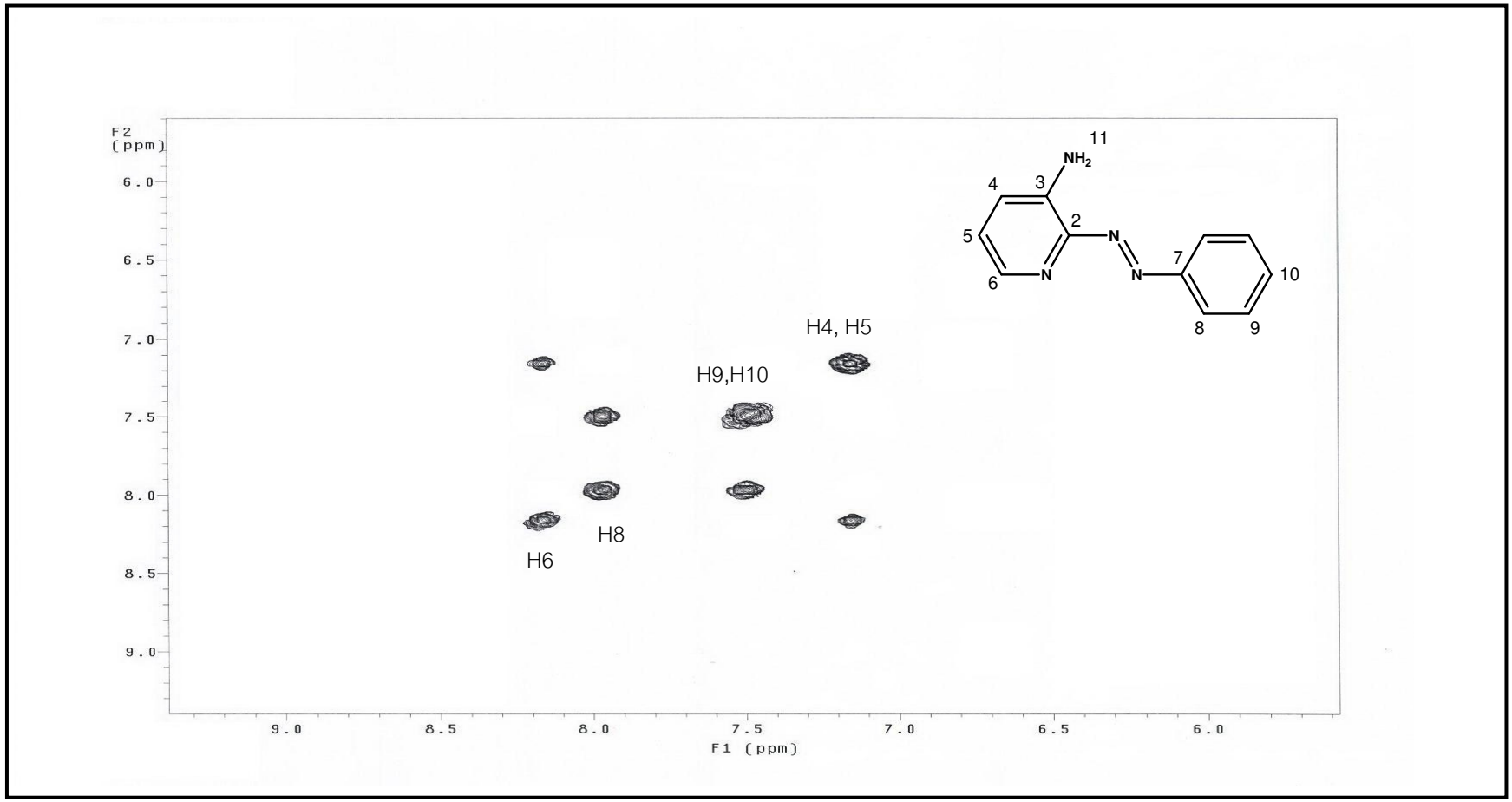

Figure 13. ^{1}H-^{1}H COSY NMR spectrum of 3aazpy in $CDCl_3$.

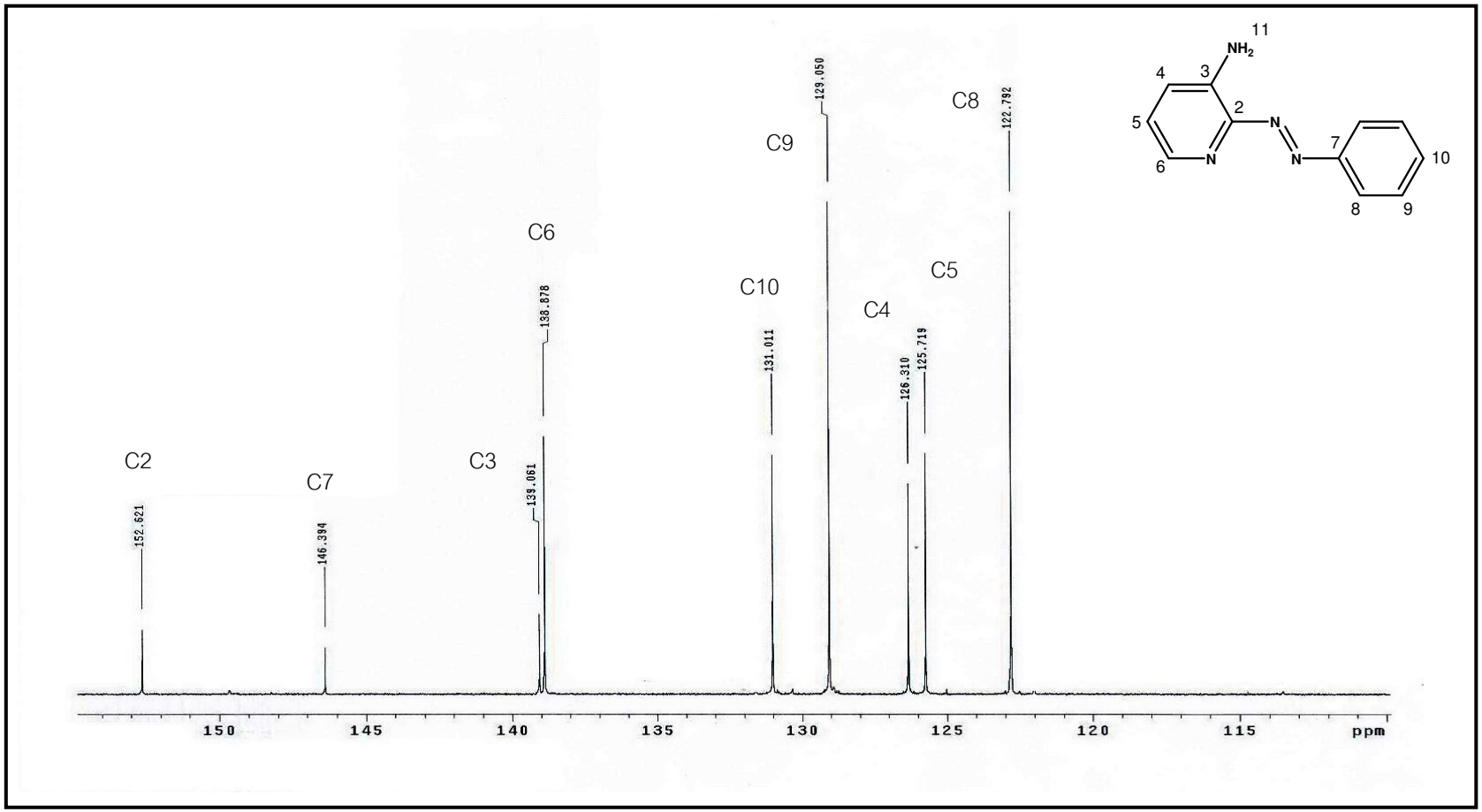

Figure 14. ^{13}C NMR spectrum of 3aazpy in $CDCl_3$.

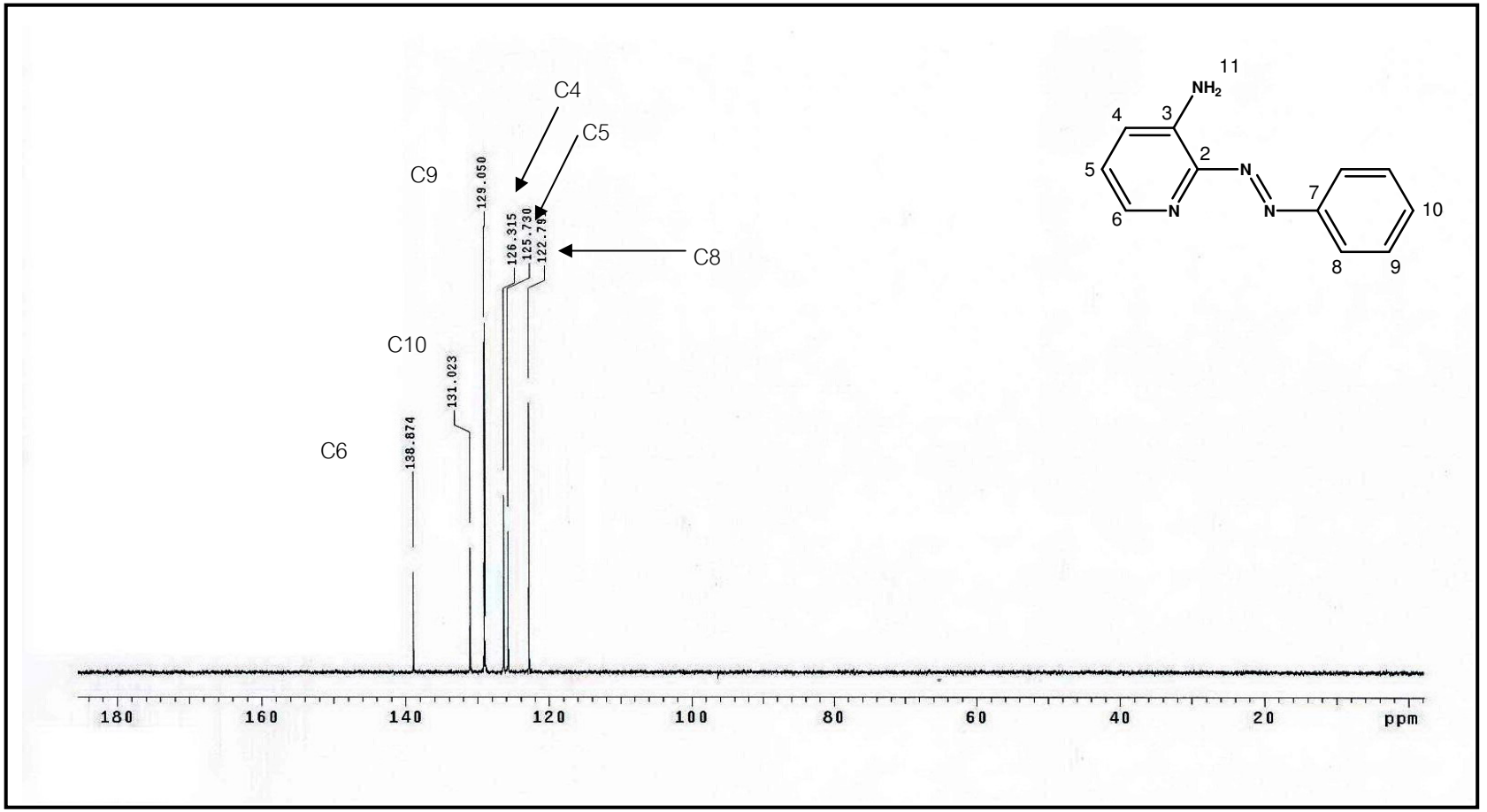

Figure 15. DEPT NMR spectrum of 3aazpy in $CDCl_3$.

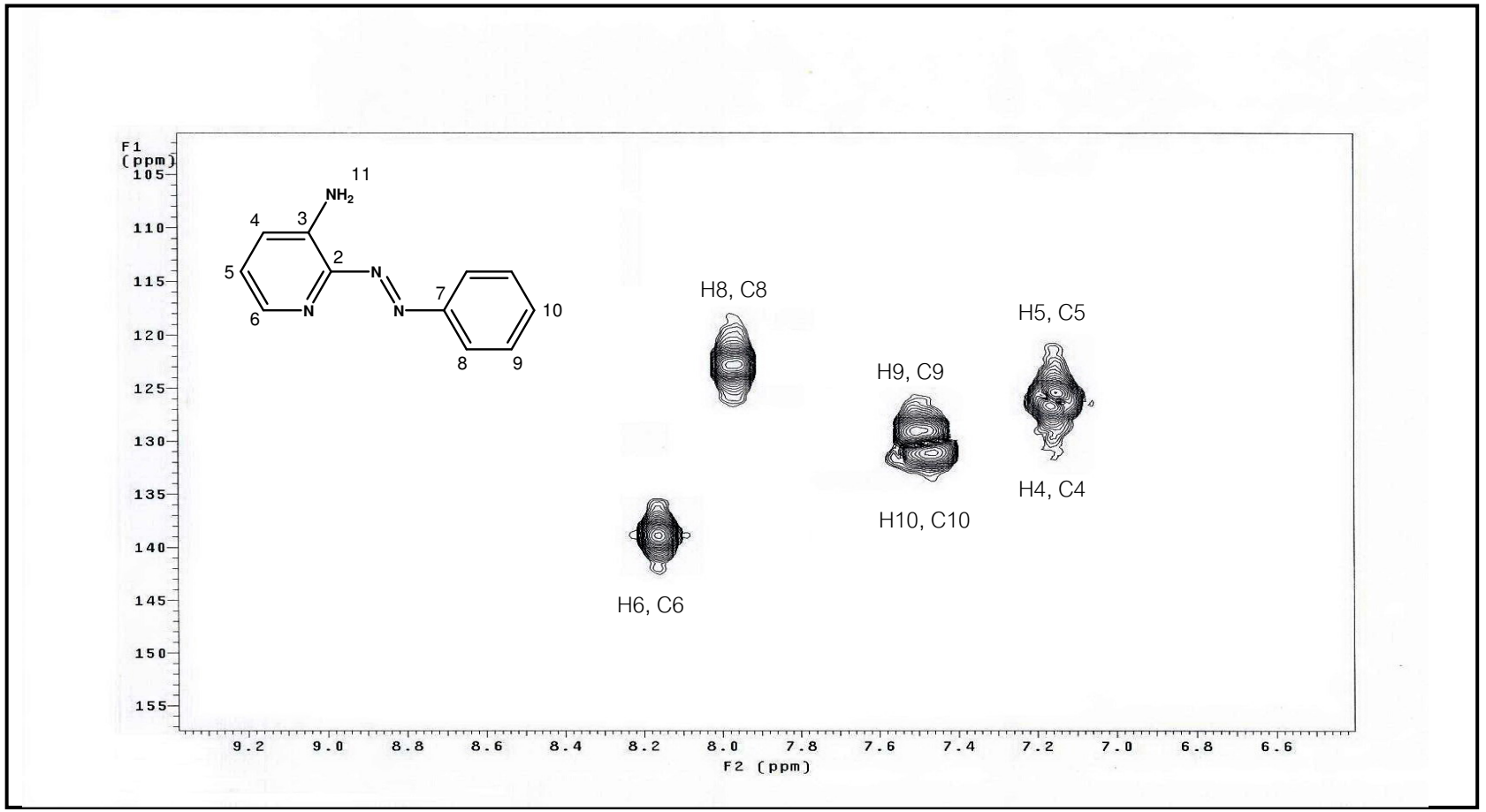

Figure 16. ^{1}H-^{13}C HMQC NMR spectrum of 3aazpy in $CDCl_3$.

The 2-amino-3-(phenylazo)pyridine (2a3pp) has ten protons on the molecule. The ^{1}H NMR spectrum of 2a3pp showed eight signals (Figure 17). The highest field signal was assigned to H11 ($-NH_2$). The most downfield of H6 was due to the nitrogen atoms which was located close to it. The proton H4 (δ = 8, 2 ppm) and H5 (δ = 8, 7.5 ppm) appeared as a doublet of doublet peak. In the phenyl ring, the proton H8 were two equivalent protons. The signal occurred as a doublet of doublet at 7.8 ppm. This resonance appeared at the lower field than the proton H9 and H10 because it located next to the azo nitrogen, the ^{1}H NMR spectrum of the 2a3pp was shown in Figure 17. In addition, the peak assignment was supported by using simple correlation ^{1}H-^{1}H COSY NMR spectroscopy. The ^{1}H-^{1}H COSY NMR signals are presented in Figure 18.

The ^{13}C NMR (Figure 19) results corresponded to those from DEPT NMR (Figure 20), which showed only methane carbon signals. The ^{13}C NMR spectrum of the 2a3pp gave 9 signals for 11 carbons. The quaternary carbon C2 of the pyridine ring appeared at the most downfield. The signal at 151 ppm was due to the quaternary carbon C7 of the phenyl ring. The peak at 131 ppm referred to the quaternary carbon C3. The signals of carbon C6 occurred at a lower field than that of other methane carbons because it is located next to the nitrogen atoms. The carbon signals at 122 and 129 ppm were attributed to the two equivalent carbon C8 and C9. The signals of carbon C4, C5, and C10 appeared at 138, 113, and 130 ppm, respectively. The ^{13}C NMR signals assignments were based on the ^{1}H-^{13}C HMQC NMR spectrum (Figure 21), which exhibited a correlation between ^{1}H NMR spectrum and ^{13}C NMR spectrum.

Nuclear Magnetic Resonance spectroscopy of 2-amino-3-(phenylazo)pyridine

Table 9. ^{1}H and ^{13}C NMR spectroscopic data of 2a3pp

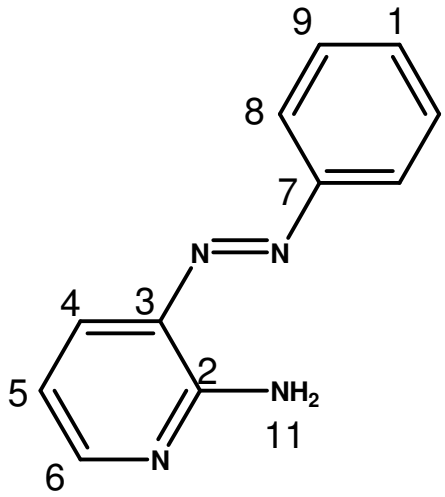

H-position	^{1}H NMR			^{13}C NMR δ (ppm)
	δ (ppm)	J (Hz)	Number of H	
6	8.2 (*dd*)	5, 2	1	151
4	8.1 (*dd*)	8, 2	1	138
8	7.8 (*dd*)	9, 1.5	2	122
9	7.5 (*t*)	7	2	129
10	7.4 (*t*)	7.5	1	130
5	6.8 (*dd*)	8, 7.5	1	113
11	1.8 (*s*)	-	2	-
Quaternary carbons				152, C2 151, C7 131, C3

s = singlet, d = doublet, t = triplet, dd = doublet of doublet

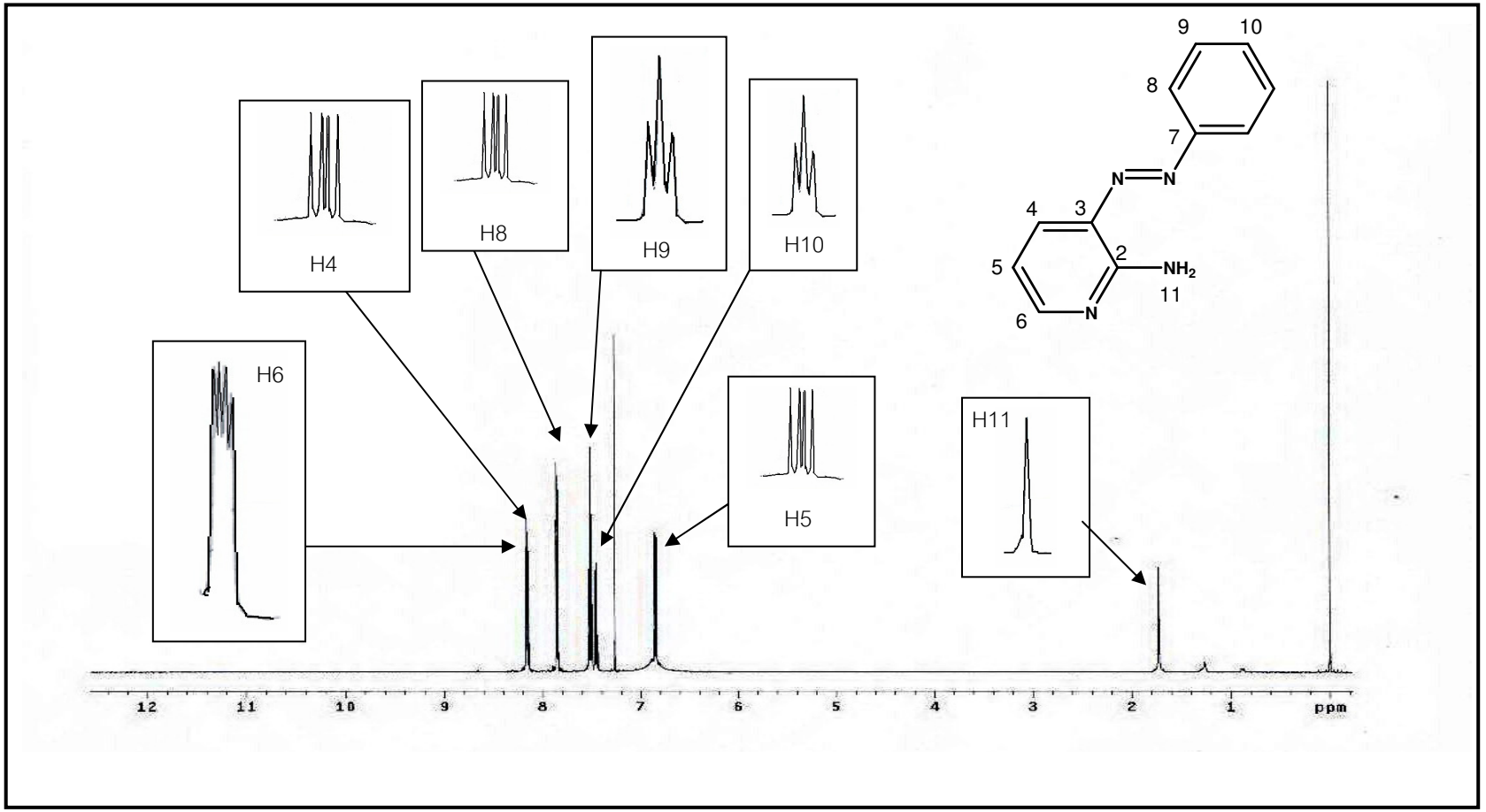

Figure 17. ^{1}H NMR spectrum of 2a3pp in $CDCl_3$.

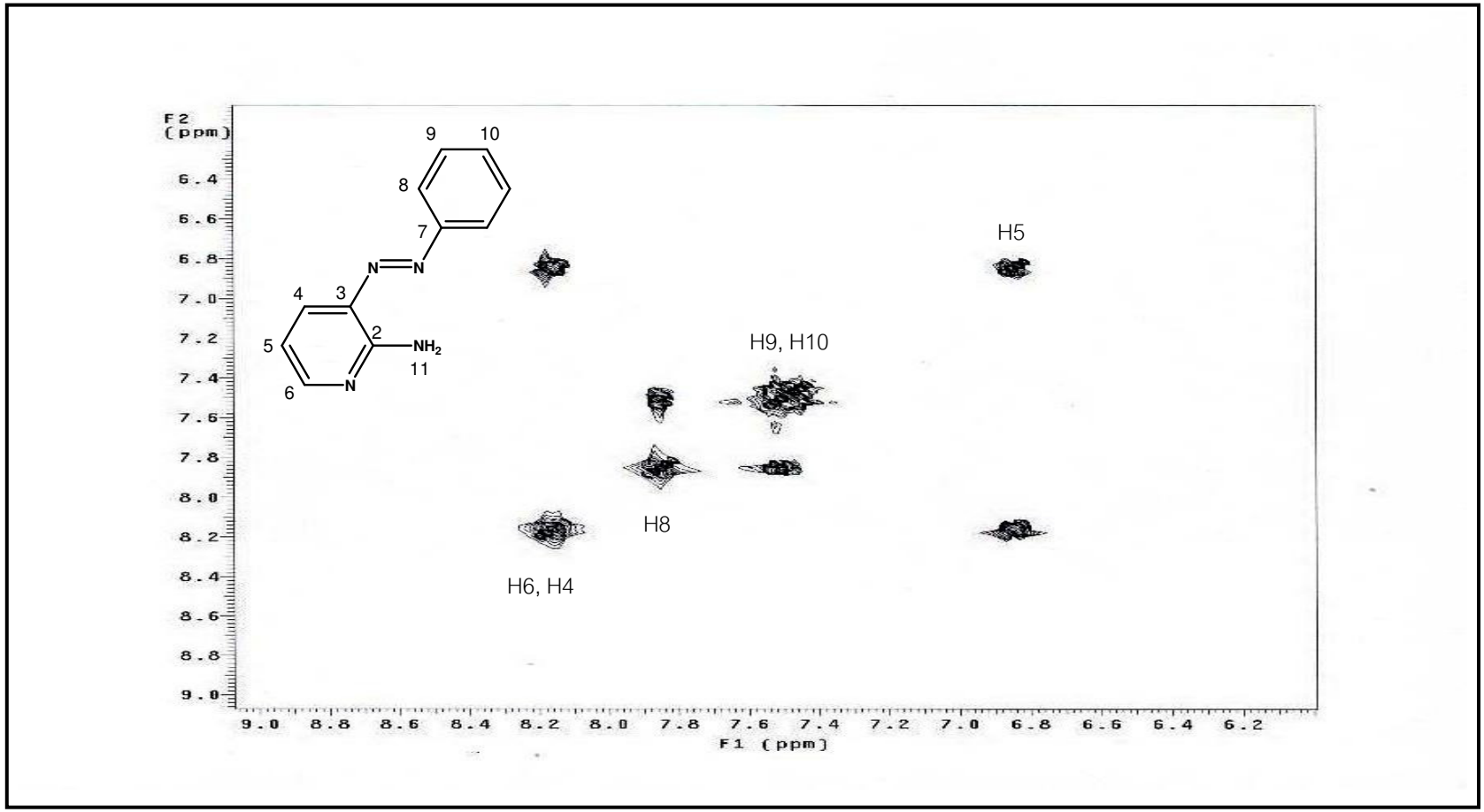

Figure 18. ^{1}H-^{1}H COSY NMR spectrum of 2a3pp in $CDCl_3$.

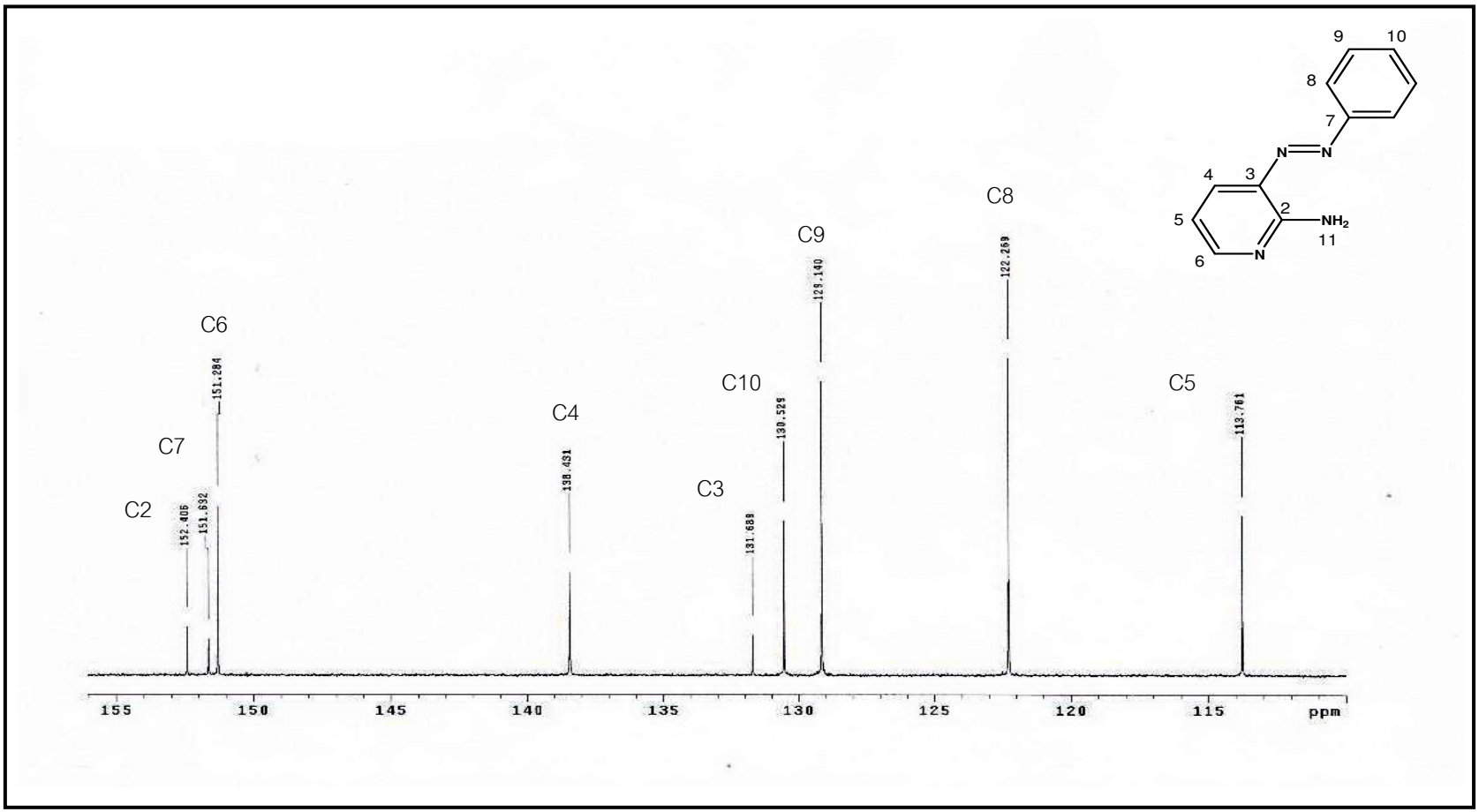

Figure 19. ^{13}C NMR spectrum of 2a3pp in $CDCl_3$.

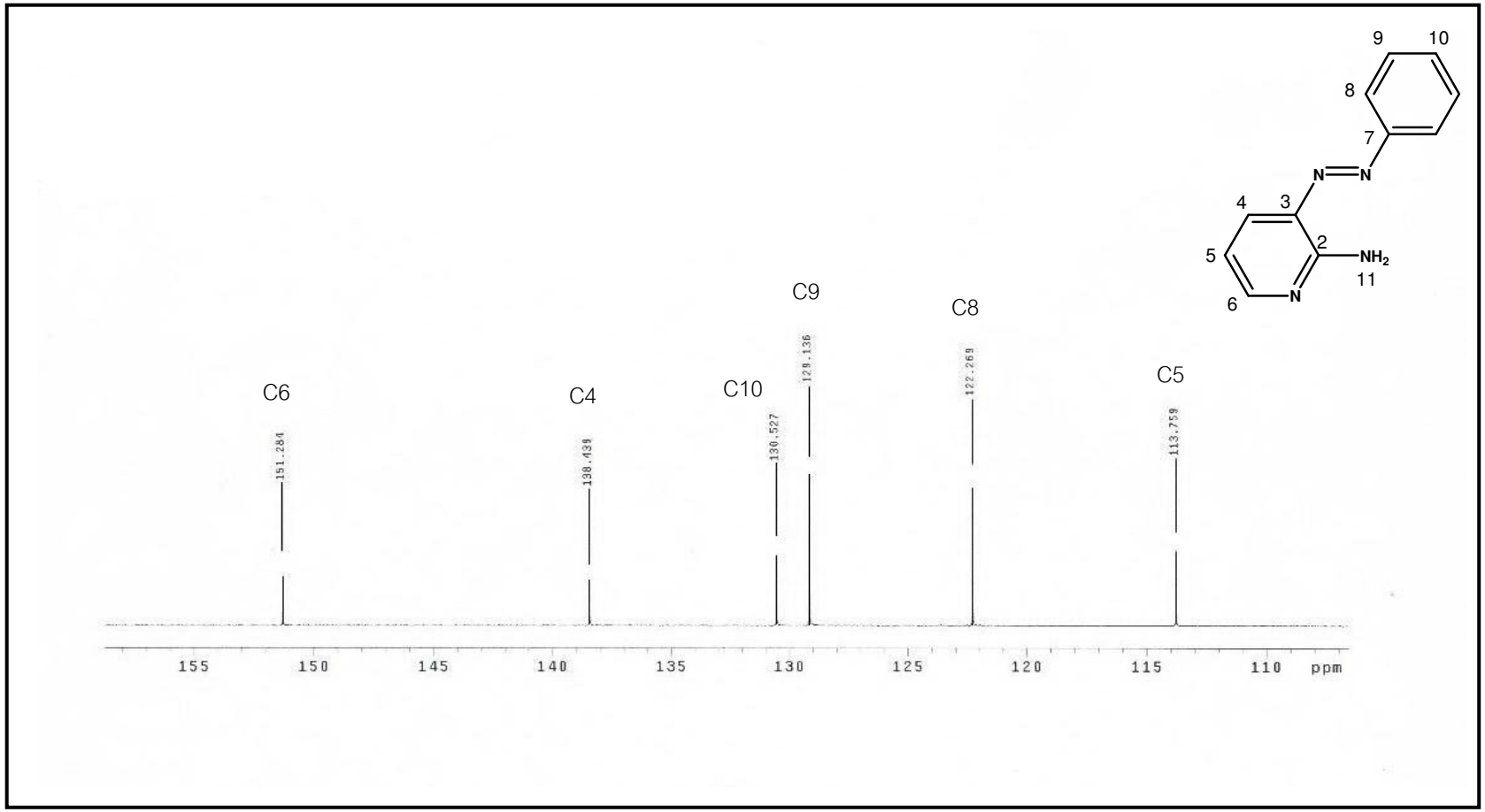

Figure 20. DEPT NMR spectrum of 2a3pp in $CDCl_3$.

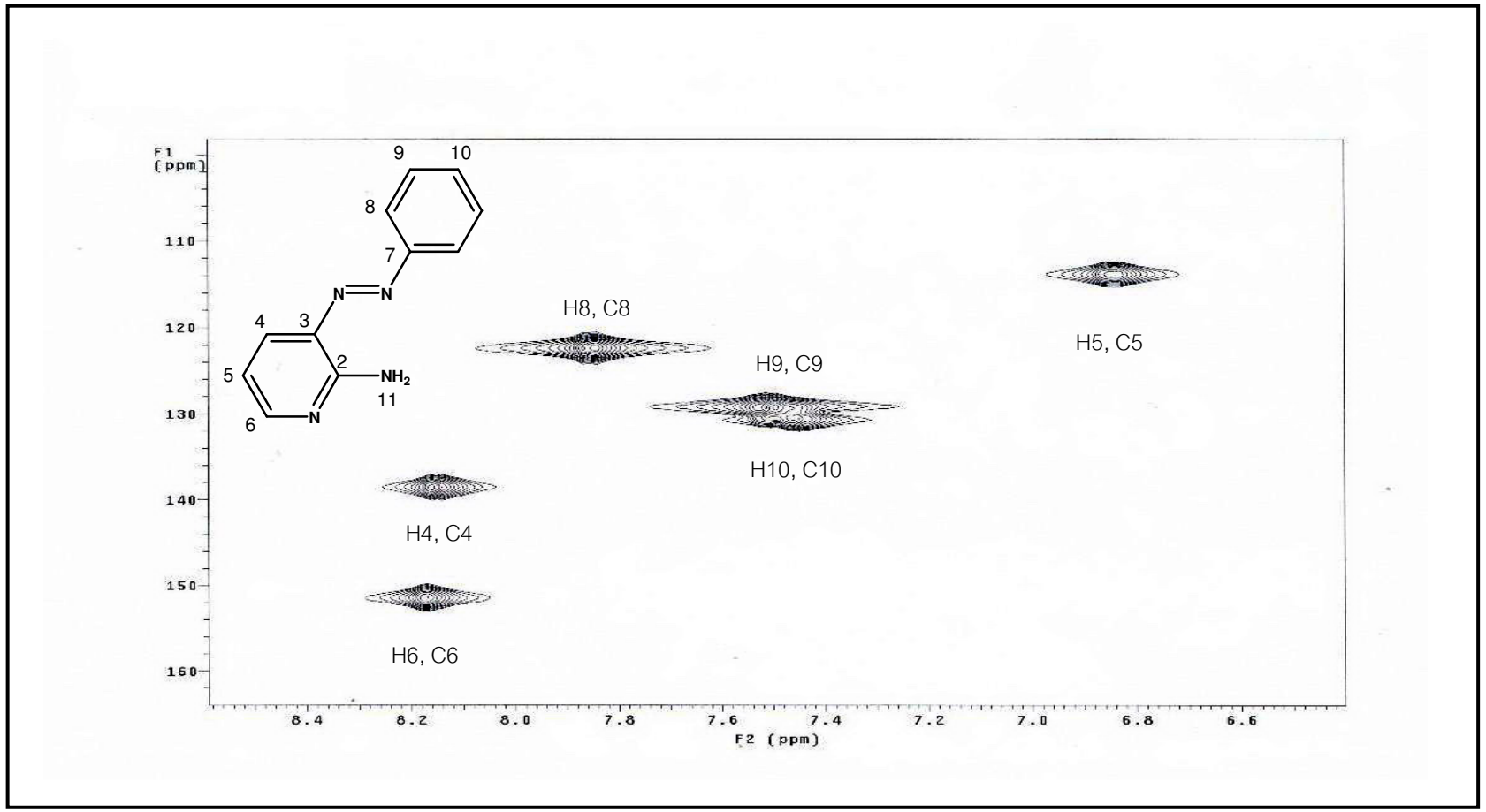

Figure 21. ^{1}H- ^{13}C HMQC NMR spectrum of 2a3pp in $CDCl_3$.

The ^{1}H NMR spectrum of the *ctc*-[Ru(3aazpy)$_2$Cl$_2$] complex showed only one set of protons similar to the free ligand. This result indicated that the complex was a symmetric molecule (C_2-symmetry). Moreover, the individual protons in the molecule showed different chemical shifts. The ^{1}H NMR spectrum of the *ctc*-[Ru(3aazpy)$_2$Cl$_2$] showed nine signals (Figure 22). It is interesting to note that the spectrum of the complex was divided into two parts (Table 11). The downfield portion was due to the pyridine protons (H4, H5, H6) and the upfield signals referred to phenyl protons (H8, H9, H10). The most downfield signal was assigned to H6. This is because of the influence of nitrogen atoms in the pyridine ring. The singlet peak at the highest field was referred to H11. The signal of proton H6 in the pyridine rings occurred at the lowest field due to the influence of coordinated nitrogen atoms.

The ^{13}C NMR of *ctc*-[Ru(3aazpy)$_2$Cl$_2$] is shown in Figure 24. The result of spectrum corresponded to the DEPT NMR spectrum (Figure 25). This trend is also found in free ligand. However, in complex, each signal slightly shifted to lower field or higher field than free ligand. The downfield signals at 157 ppm, 156 ppm, and 155 ppm were assigned to three quaternary carbons C2, C7, and C3, respectively. Moreover, the ^{13}C NMR signals assignment were based on the ^{1}H-^{13}C HMQC spectrum (Figure 26).

Nuclear Magnetic Resonance spectroscopy of *ctc*-[Ru(3aazpy)$_2$Cl$_2$] complex

Table 10. ^{1}H and ^{13}C NMR spectroscopic data of the *ctc*-[Ru(3aazpy)$_2$Cl$_2$] complex

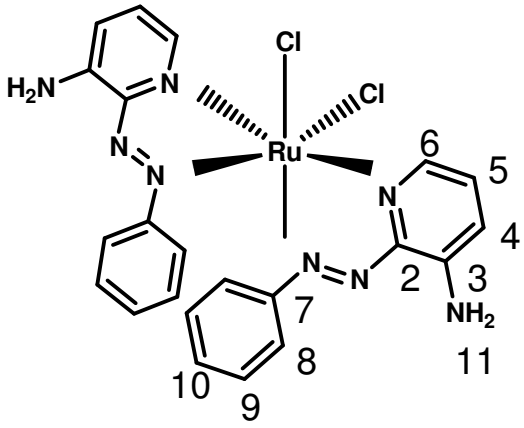

H-position	^{1}H NMR			^{13}C NMR δ (ppm)
	δ (ppm)	J (Hz)	Number of H	
6	9.38 (*d*)	2	1	152
4	8.33 (*d*)	8.5	1	126
5	8.08 (*dd*)	8.5, 2	1	140
8	7.78 (*d*)	7.5	2	125
10	7.49 (*t*)	7.5	1	131
9	7.2 (*t*)	7.5	2	128
11	1.59 (*s*)	-	2	-
Quaternary carbons				157, C2 156, C7 155, C3

s = singlet, d = doublet, t = triplet, dd = doublet of doublet

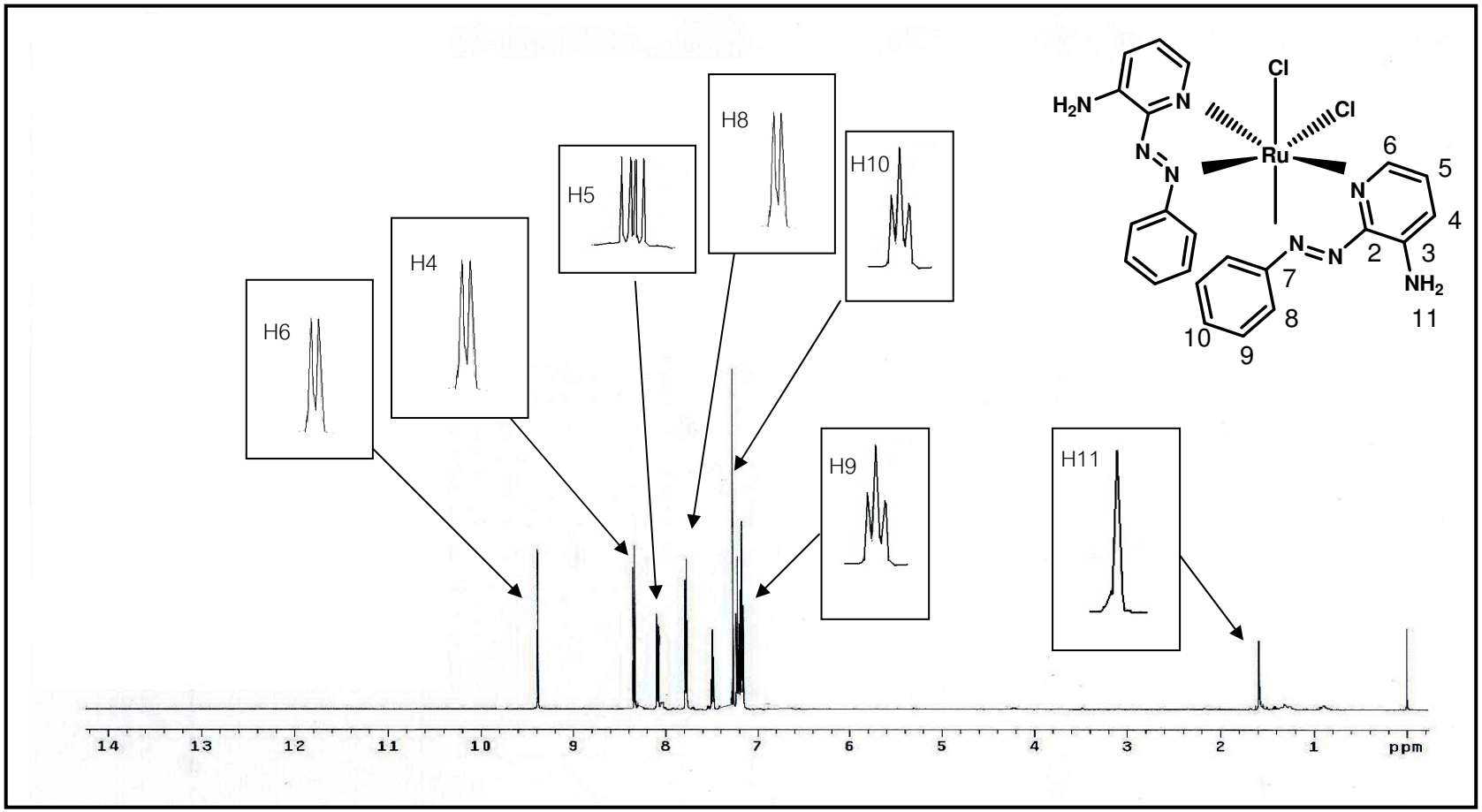

Figure 22. ^{1}H NMR spectrum of *ctc*-[Ru(3aazpy)$_2$Cl$_2$] in CDCl$_3$.

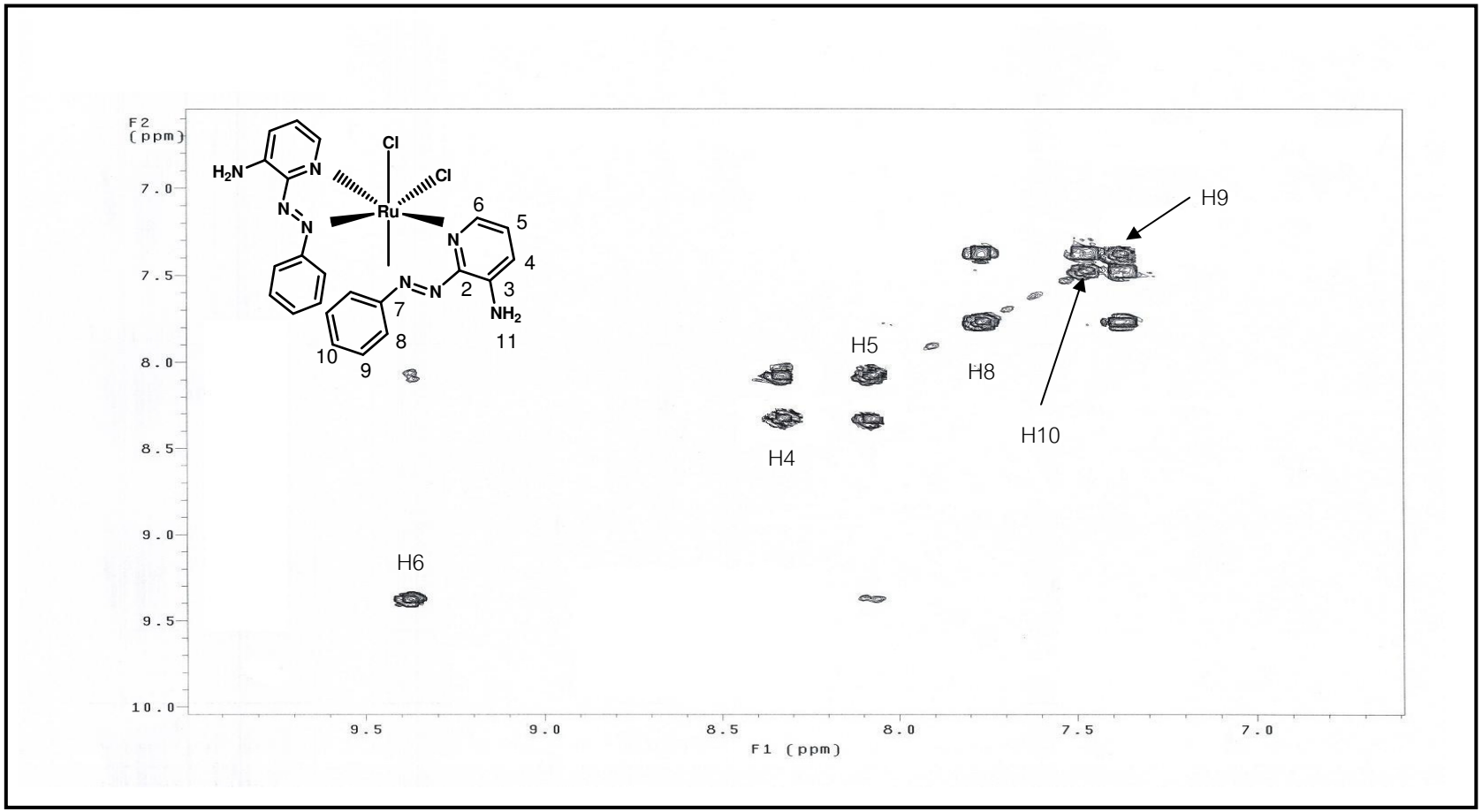

Figure 23. ^{1}H-^{1}H COSY NMR spectrum of *ctc*-[Ru(3aazpy)$_2$Cl$_2$] in $CDCl_3$.

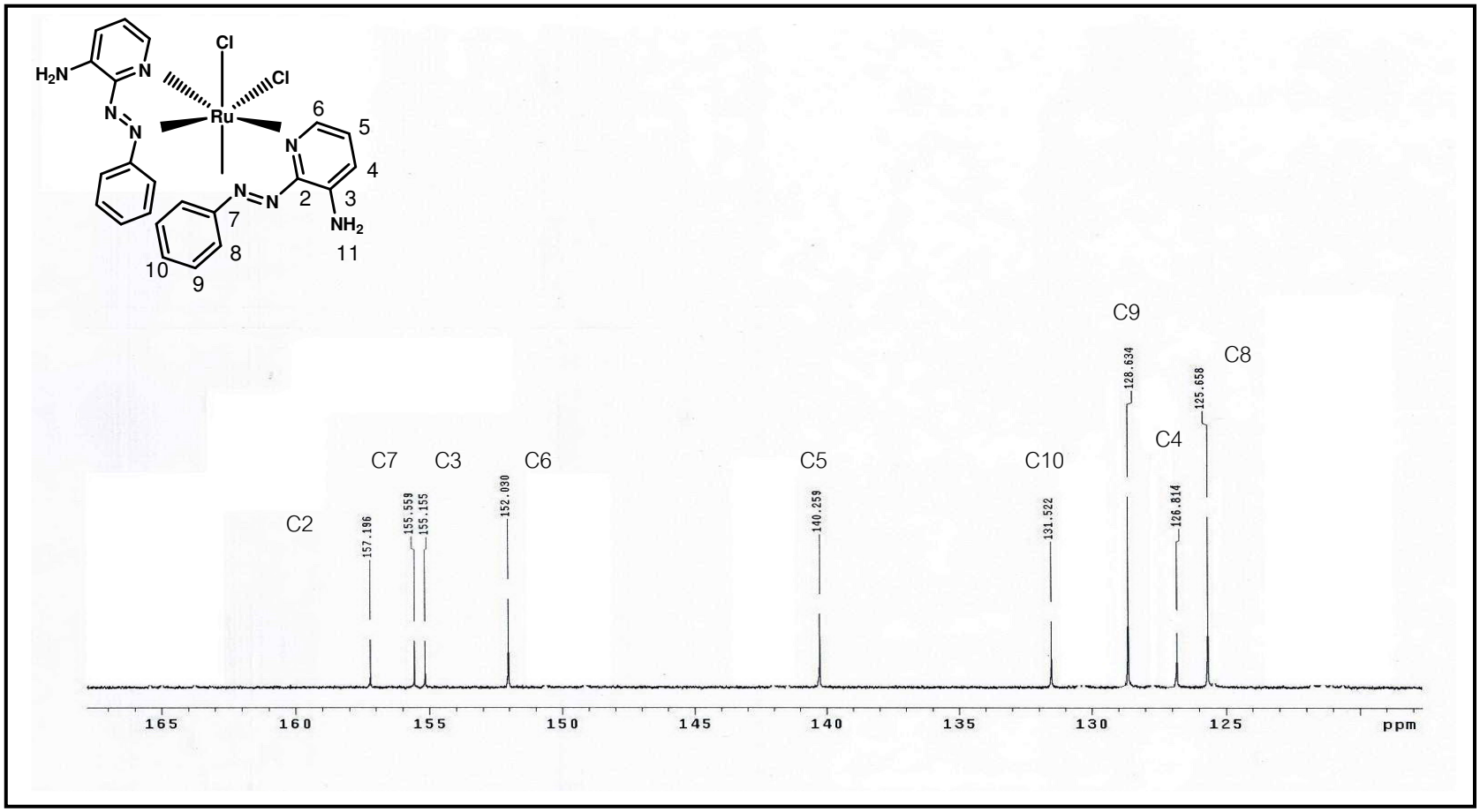

Figure 24. ^{13}C NMR spectrum of *ctc*-[Ru(3aazpy)$_2$Cl$_2$] in $CDCl_3$.

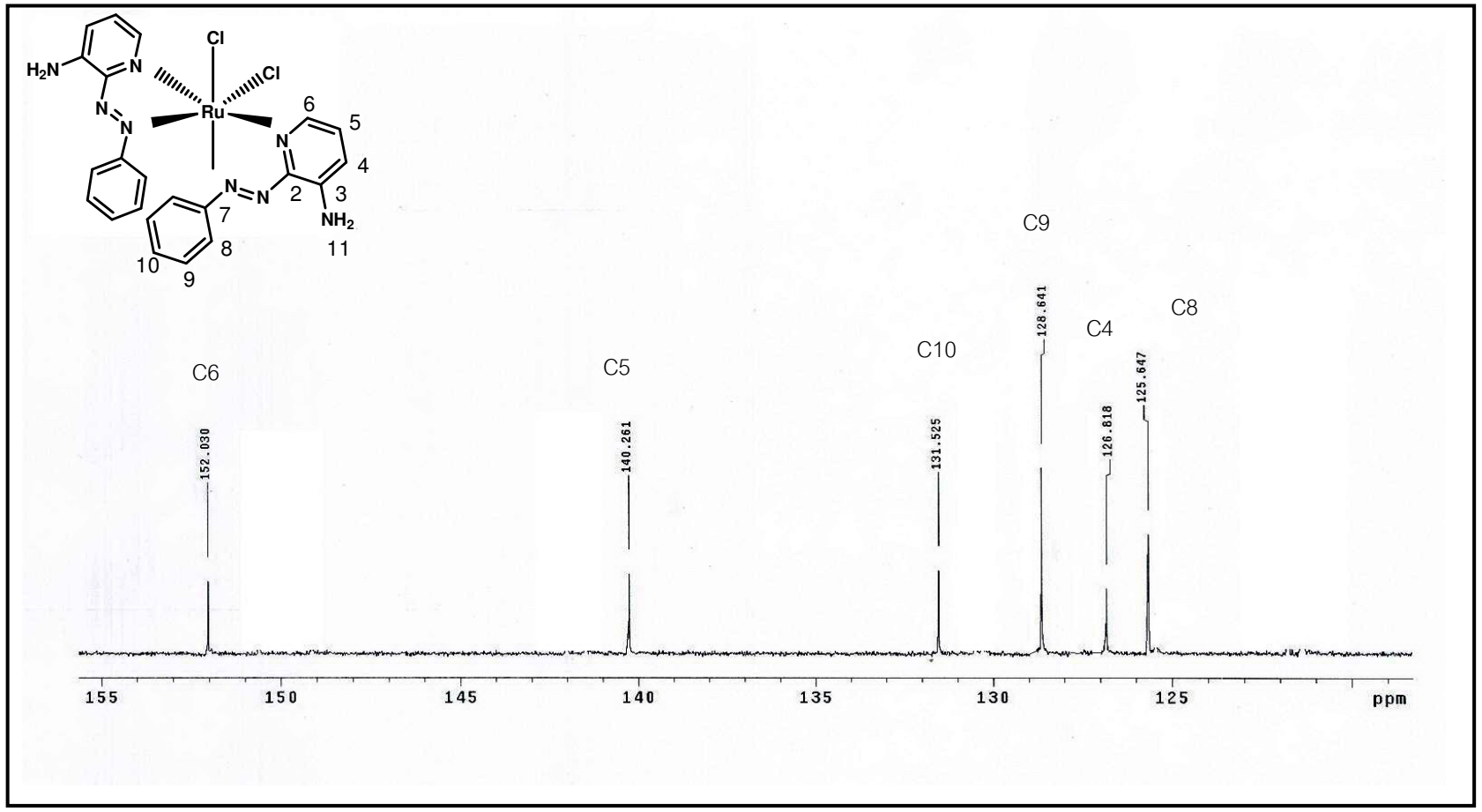

Figure 25. DEPT NMR spectrum of *ctc*-[Ru(3aazpy)$_2$Cl$_2$] in CDCl$_3$.

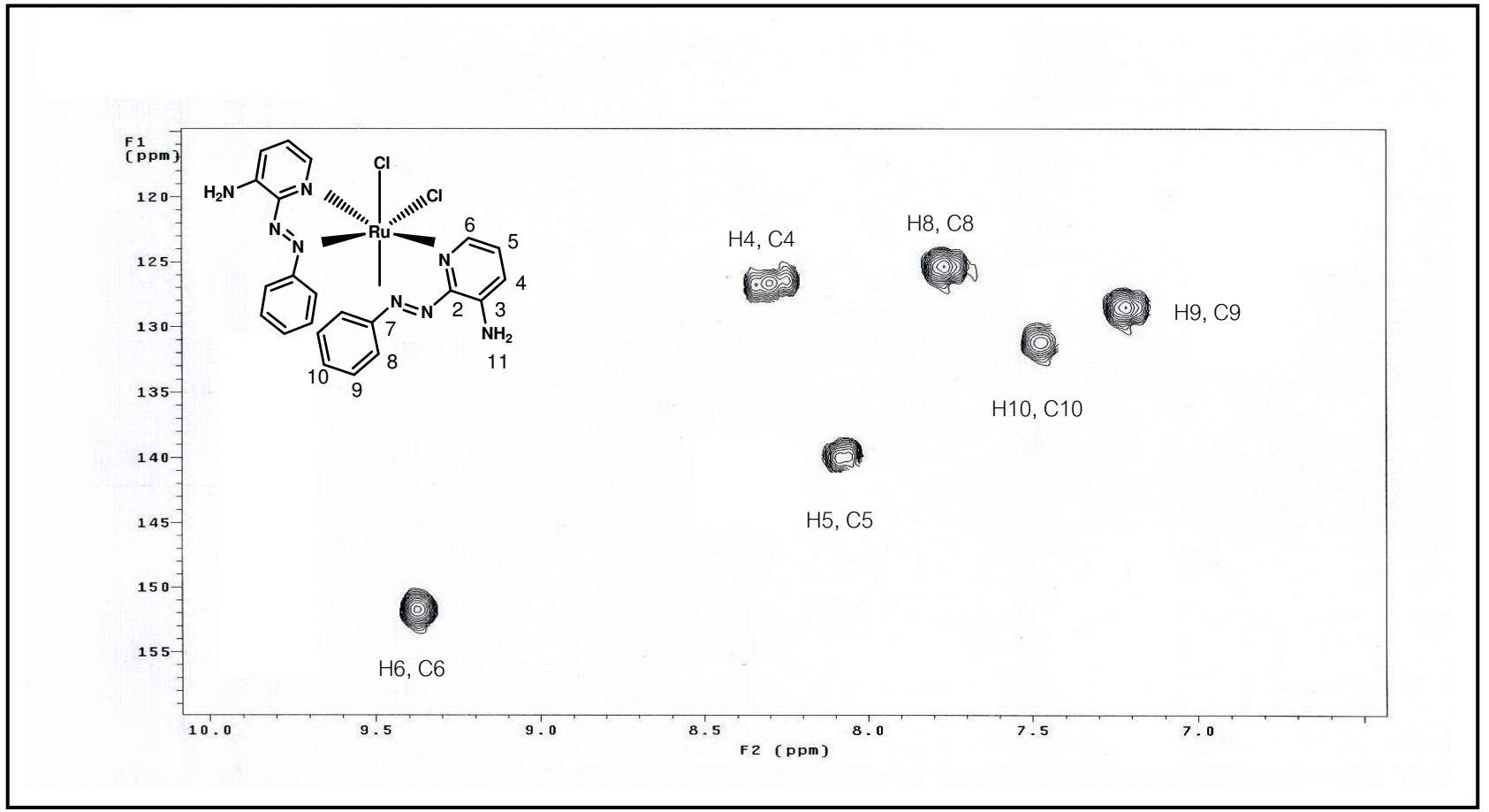

Figure 26. ^{1}H-^{13}C HMQC NMR spectrum of *ctc*-$[Ru(3aazpy)_2Cl_2]$ in $CDCl_3$.

The *ccc*-[Ru(3aazpy)$_2$Cl$_2$] is C_1-symmetrical and is expected to exhibit two sets of protons (Figure 27). This is indeed observed. The spectra showed that the pyridine protons are mostly affected when compared to the phenyl protons. The H6(b) and H4(a,b) signals are shifted downfield by approximate 1 ppm while, H9(a,b) and H10(a,b) are shifted upfield from those of the free ligand. Because the greater π-backbonding interaction to azo group will increase the electron density in the phenyl ring, this provided higher field phenyl protons. The pyridine protons H6(b) and H6(a) were observed at different chemical shifts. The proton H6 in pyridine ring a, appeared at the lower field than pyridine ring b, because it was trans to the N=N withdrawing group while proton H6 in pyridine ring b was trans to Cl. In addition, the proton signals in –NH_2, ring a and ring b, showed the same effect of the trans withdrawing group. The assignments of ^{1}H NMR were confirmed by using the ^{1}H-^{1}H COSY NMR spectrum (Figure 28).

The ^{13}C NMR spectrum is shown in Figure 29. The DEPT spectral data (Figure 30) showed only signals of methane carbons and supported the ^{13}C NMR result.

Nuclear Magnetic Resonance spectroscopy of the *ccc*-[Ru(3aazpy)$_2$Cl$_2$] complex

Table 11. ^{1}H and ^{13}C NMR spectroscopic data of the *ccc*-[Ru(3aazpy)$_2$Cl$_2$] complex

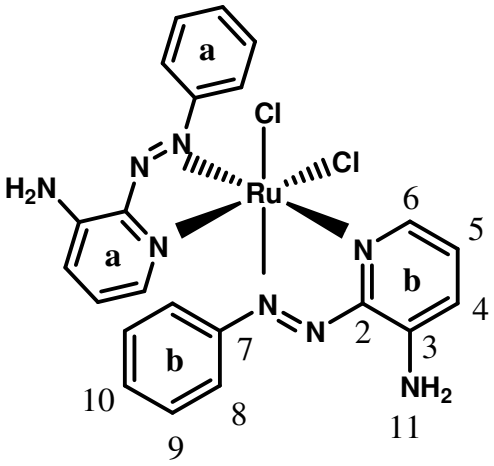

H-position	^{1}H NMR			^{13}C NMR δ (ppm)
	δ (ppm)	J (Hz)	Number of H	
6 (b)	9.7 (*d*)	2	1	150
4 (b)	8.4 (*d*)	8.5	1	125
4 (a) 5 (b)	8.2 (*d*)	9	2	4 (a) 126 5 (b) 142
5 (a)	8 (*dd*)	9, 1.5	1	141
8 (b)	7.7 (*d*)	8	2	125
10 (b)	7.5 (*t*)	7.5, 7	1	131
9 (b) 10 (a)	7.4 (*m*)	-	3	9 (b) 127 10 (a) 130

Table 11. (Continued)

H-position	^{1}H NMR			^{13}C NMR δ (ppm)
	δ (ppm)	*J* (Hz)	Number of H	
6 (a)	7.3 (*d*)	7	1	149
9 (a)	7.2 (*t*)	7.5, 8	2	128
8 (a)	6.7 (*d*)	8	2	121
11 (b)	1.6 (*s*)	-	2	-
11 (a)	1.3 (*s*)	-	2	-
Quaternary carbons				165, C2(b) 163, C2(a) 157, C7(b) 155, C7(a) 121, C3(b) 120, C3(a)

s = singlet, d = doublet, t = triplet, dd = doublet of doublet

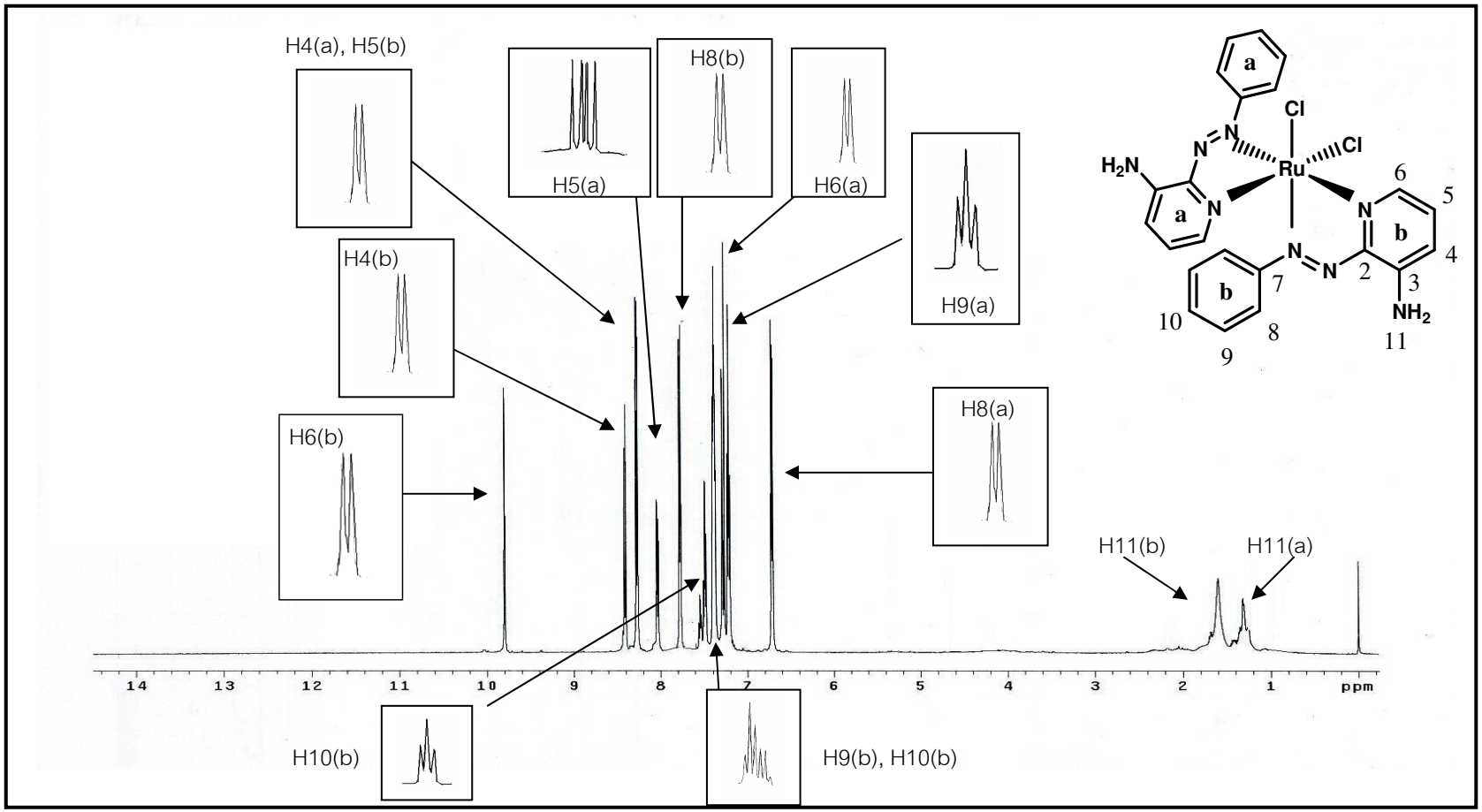

Figure 27. ^{1}H NMR spectrum of *ccc*-[Ru(3aazpy)$_2$Cl$_2$] in CDCl$_3$.

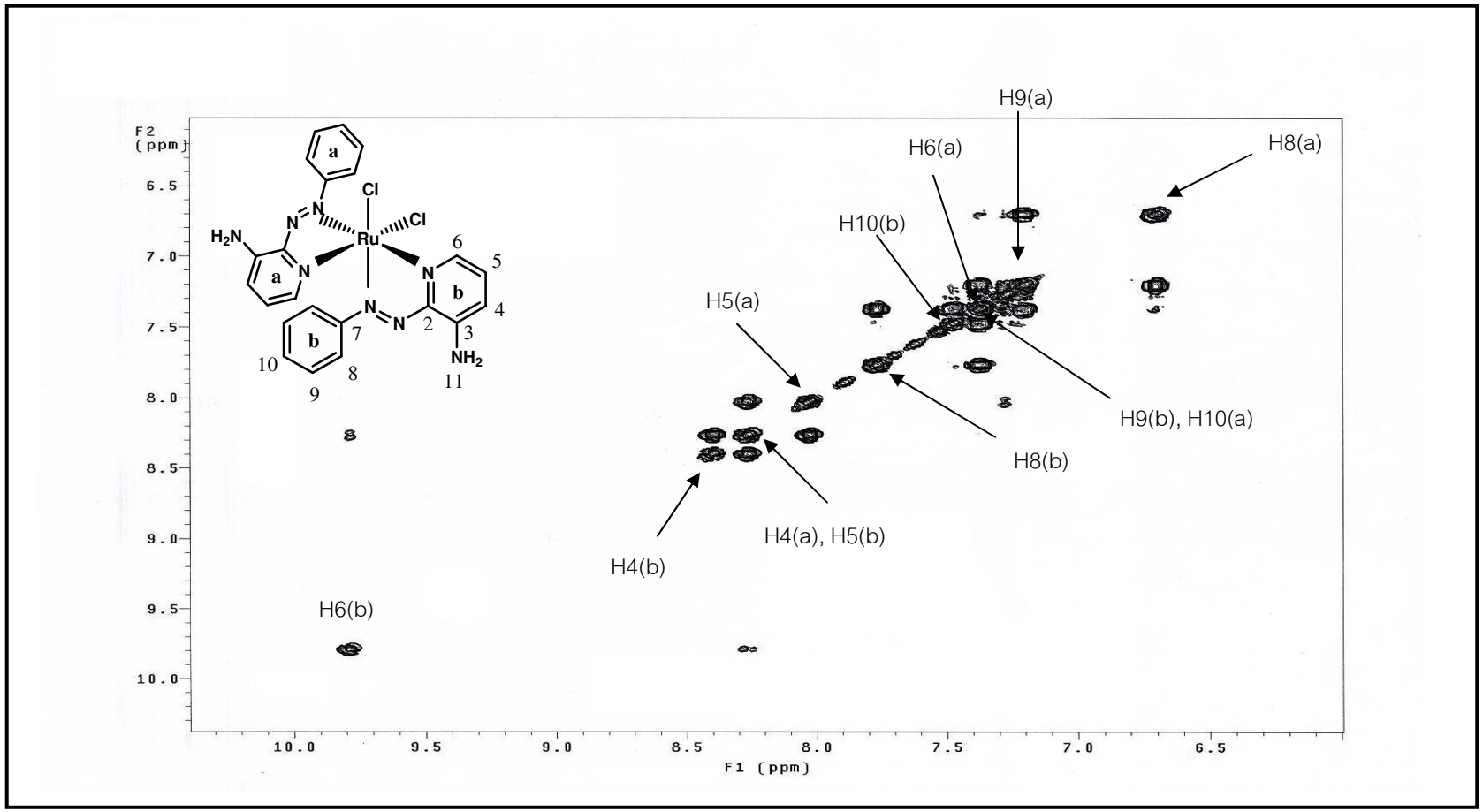

Figure 28. ^{1}H-^{1}H COSY NMR spectrum of *ccc*-[Ru(3aazpy)$_2$Cl$_2$] in CDCl$_3$.

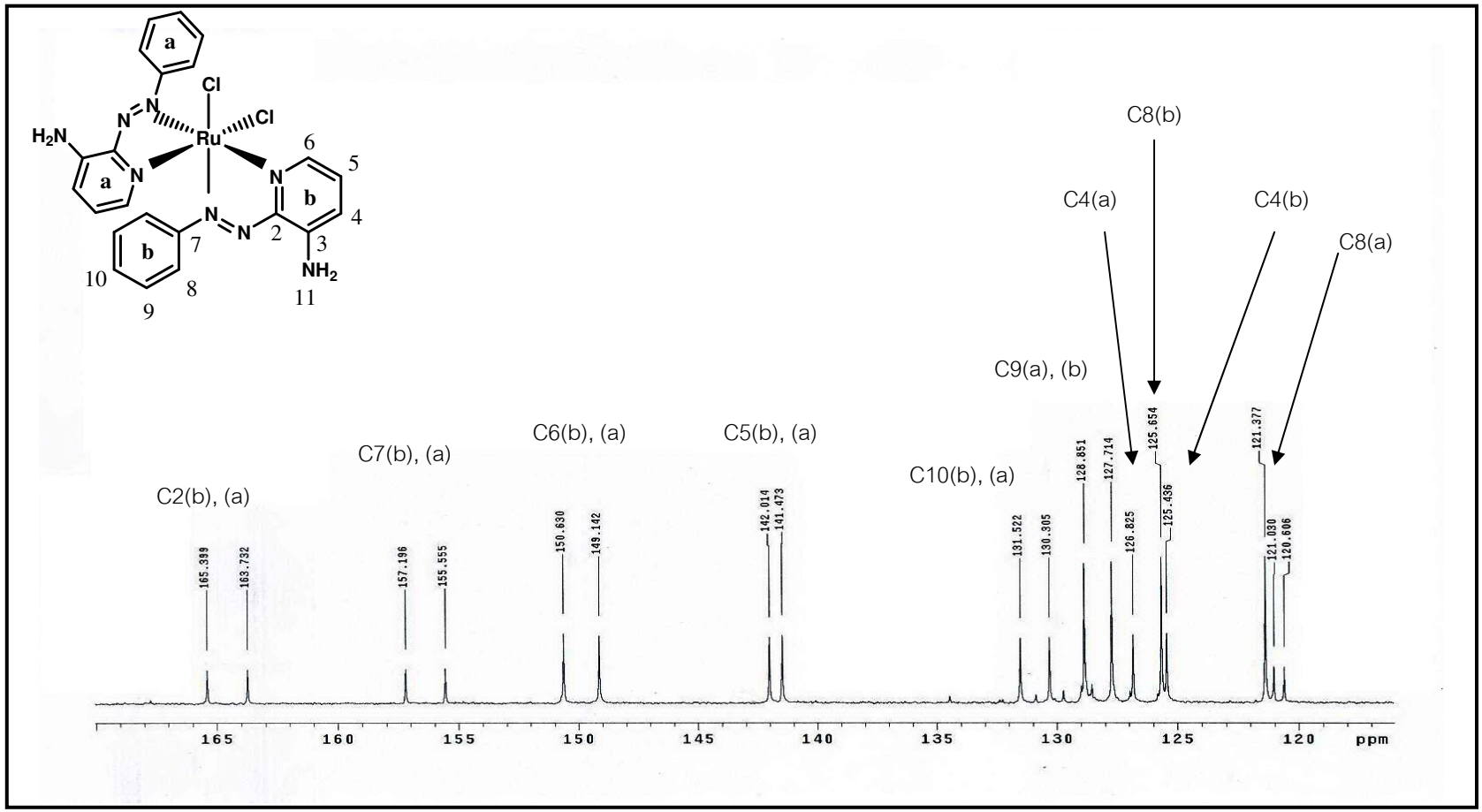

Figure 29. ^{13}C NMR spectrum of *ccc*-[Ru(3aazpy)$_2$Cl$_2$] in $CDCl_3$.

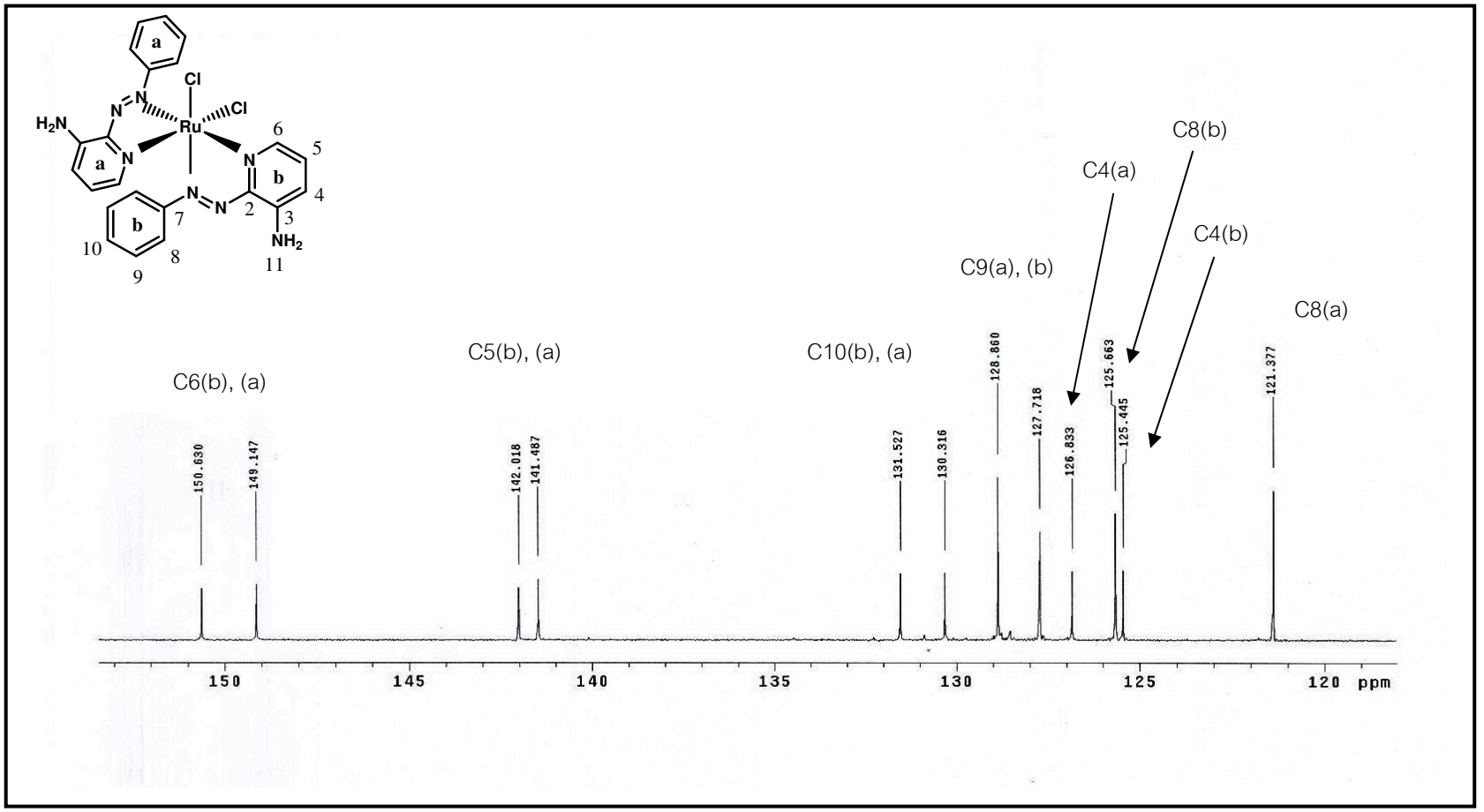

Figure 30. DEPT NMR spectrum of *ccc*-[Ru(3aazpy)$_2$Cl$_2$] in CDCl$_3$.

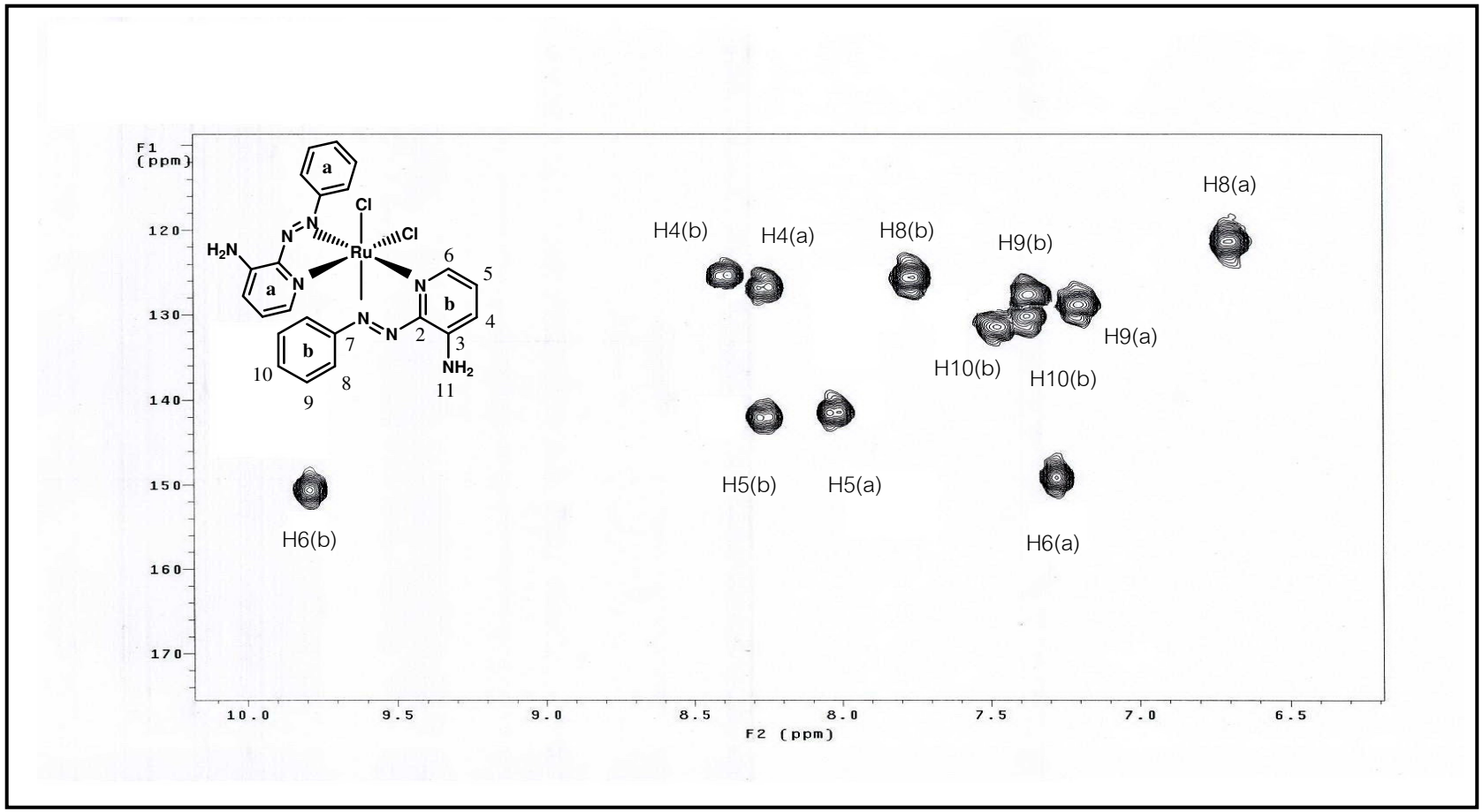

Figure 31. ^{1}H-^{13}C HMQC NMR spectrum of *ccc*-[Ru(3aazpy)$_2$Cl$_2$] in $CDCl_3$.

3.2.5 Cyclic Voltammetry

Electrochemical properties of all the complexes were studied by cyclic voltammetry at a glassy carbon working electrode and were examined in dichloromethane using tetrabutylammonium hexafluorophosphate (TBAH) as supporting electrolyte at the scan rate of 100 mV/s. Voltammetric data are given in Table 12 and selected voltammograms are shown in Figure 32 to 35. The voltammograms displayed $Ru^{III/II}$ couple at the positive side and ligand reductions at the negative side. The potentials were compared with the potential of a ferrocene couple.

In this experiment, different scan rates were used to check the couple ΔEp of the redox reaction. The couple having equal anodic current (i_{pa}) and cathodic current (i_{pc}) was referred to as a reversible couple. On the other hand, the unequal currents were referred unequally transfer of reduction and oxidation peaks. This led to an irreversible couple. When different scan rates were applied, these currents gave equal anodic and cathodic currents at higher scan rates, which led to quasi-reversible couple.

Table 12. Cyclic voltammetric[a] data for 3aazpy ligand, 2a3pp and the two complexes in 0.1 M TBAH dichloromethane at scan rate of 100 mV/s.

Compound	$E_{1/2}$ (V) (ΔE_p (mV))	
	Oxidation	Reduction
3aazpy	0.57 [b]	-1.78 (96)
2a3pp	0.99 [b]	-1.75 (94)
ctc-[$Ru(3aazpy)_2Cl_2$]	1.61 [b] 0.96 (70)	-0.79 (105) -1.18 (115)
ccc-[$Ru(3aazpy)_2Cl_2$]	1.70 [b] 0.85 (95)	-0.89 (150) -1.29 (135)

[a] $E_{1/2} = (E_{pa} + E_{pc})/2$, where E_{pa} and E_{pc} are anodic and cathodic peak potentials, respectively; $\Delta E_p = E_{pa}-E_{pc}$; [b] anodic peak potential, V

In the potential range +0.5 to +1.5 V at a scan rate of 100 mV/s in dichloromethane, one electron oxidation response was observed corresponding to the Ru(II) ⟶ Ru(III) couple. The oxidation process is shown in equation (1).

$$Ru(3aazpy)_2Cl_2 \longrightarrow Ru(3aazpy)_2Cl_2^{+} + e^{-} \qquad (1)$$

The *ctc* isomer showed a slightly higher Ru(III)/Ru(II) couple (0.11 V) than that of the *ccc* isomer. These were also supported by electronic spectral data.

In the potential range 0 to -2.0 V, reductive responses were observed under similar conditions using a glassy carbon working electrode. The reduction potentials were compared with the results from the free ligand. The free ligand showed one reversible two electron reduction responses with peak to peak separation at 96 mV, corresponding to the couple in equation (2)

$$3aazpy \underset{}{\overset{2e^-}{\rightleftharpoons}} 3aazpy^{2-}$$

The potential of this couple was -1.78 V. All the two complexes displayed two reversible, two electron reduction, one reversible, one electron oxidation and one irreversible peak of one electron.

Moreover, the reduction potential showed a positive shift from the free ligand value. The first reduction couple of the *ctc* complex (-0.79 V) occurred at a higher potential than that in the *ccc* complex (-0.89 V). These results showed that the *ctc* isomer accepted electron better than the other isomer. In addition, it could be concluded that the 3aazpy ligand in the *ctc* complex was more easily reduced than the *ccc* complex.

In the $[Ru(3aazpy)_2Cl_2]$ complexes, the ability of 3aazpy ligand to stabilize the complex is as follow:

$$ccc < ctc$$

In addition, The results of voltammetry were supported by the electronic spectral data shown in Table 13.

Table 13. Comparison of electronic and redox properties of $[Ru(3aazpy)_2Cl_2]$ complexes

Properties	*ctc*-isomer	*ccc*-isomer
Ru(III)/Ru(II), $E_{1/2}$ (V)	0.96	0.85
MLCT band, λ_{max} (nm)	582	592

The oxidation potentials of each complexes are positive than that of the $[Ru(azpy)_2Cl_2]$ (+ 0.71V) (Jullapun, 2004). The present set of Ru(III)/(II) redox potential data of $[Ru(3aazpy)_2Cl_2]$ are higher than $[Ru(azpy)_2Cl_2]$. This suggests that the π-acidity order of the ligand is arranged follow:

3aazpy > azpy

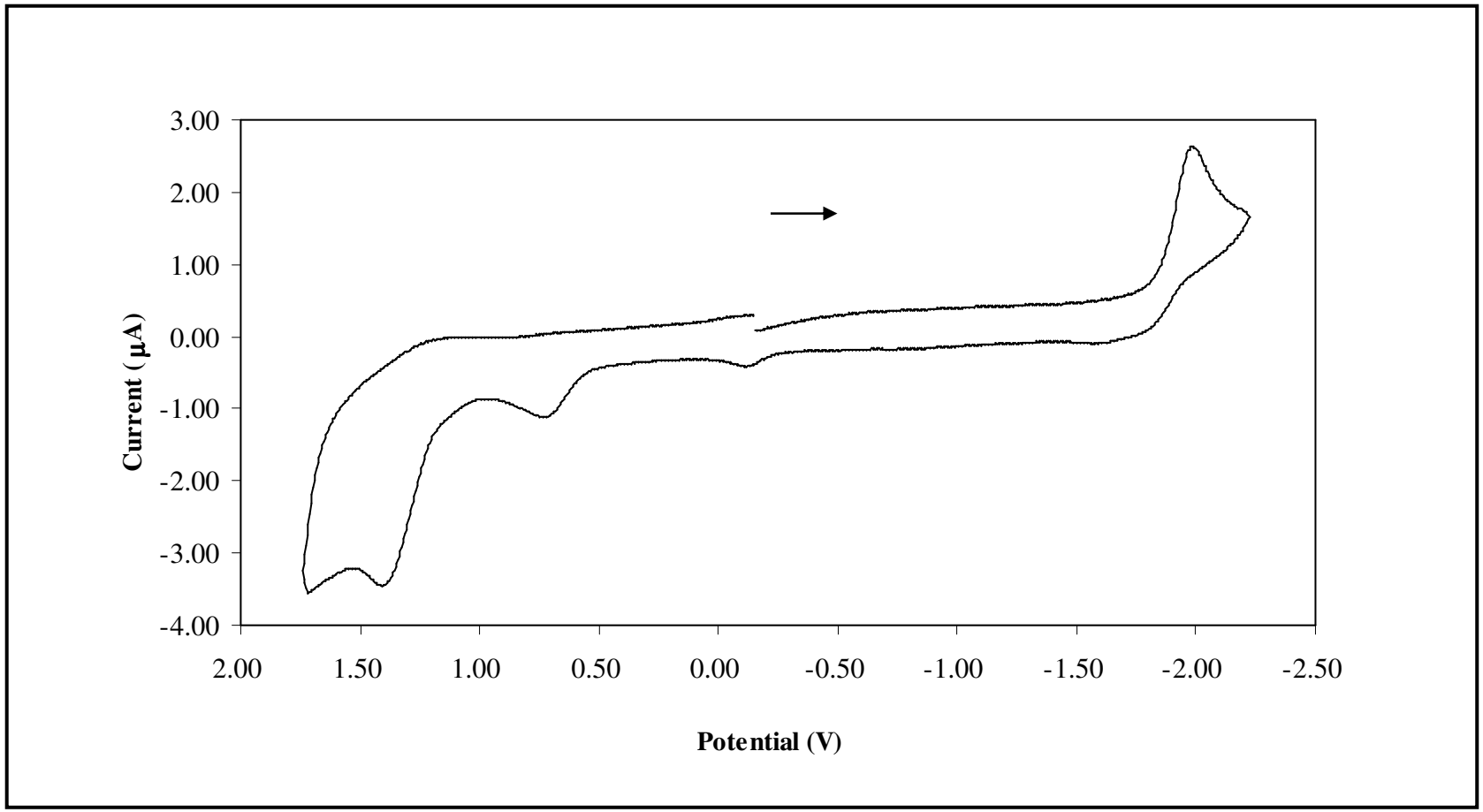

Figure 32. Cyclic voltammogram of 3aazpy in 0.1 M TBAH CH_2Cl_2 at scan rate 100 mV/s.

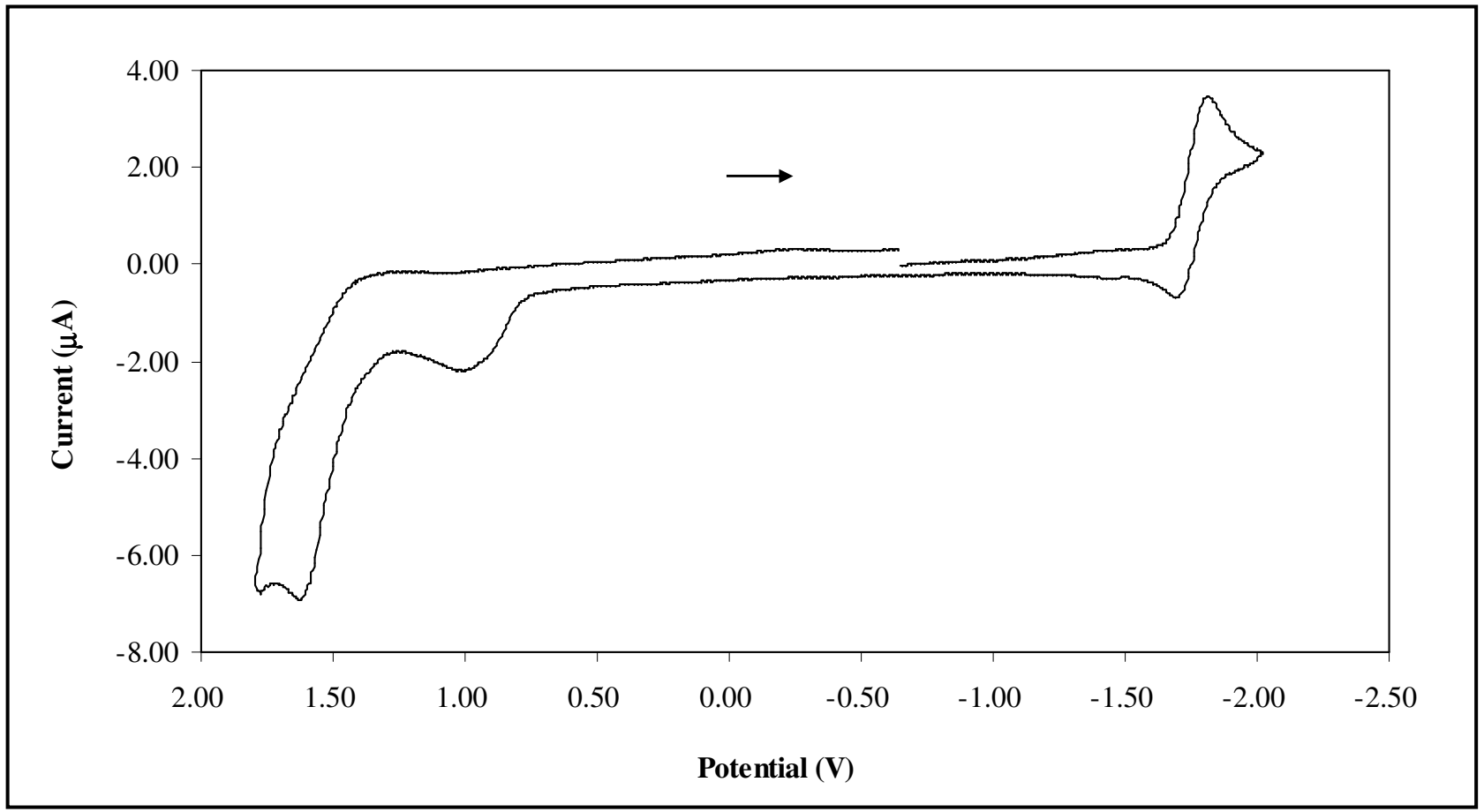

Figure 33. Cyclic voltammogram of 2a3pp in 0.1 M TBAH CH_2Cl_2 at scan rate 100 mV/s.

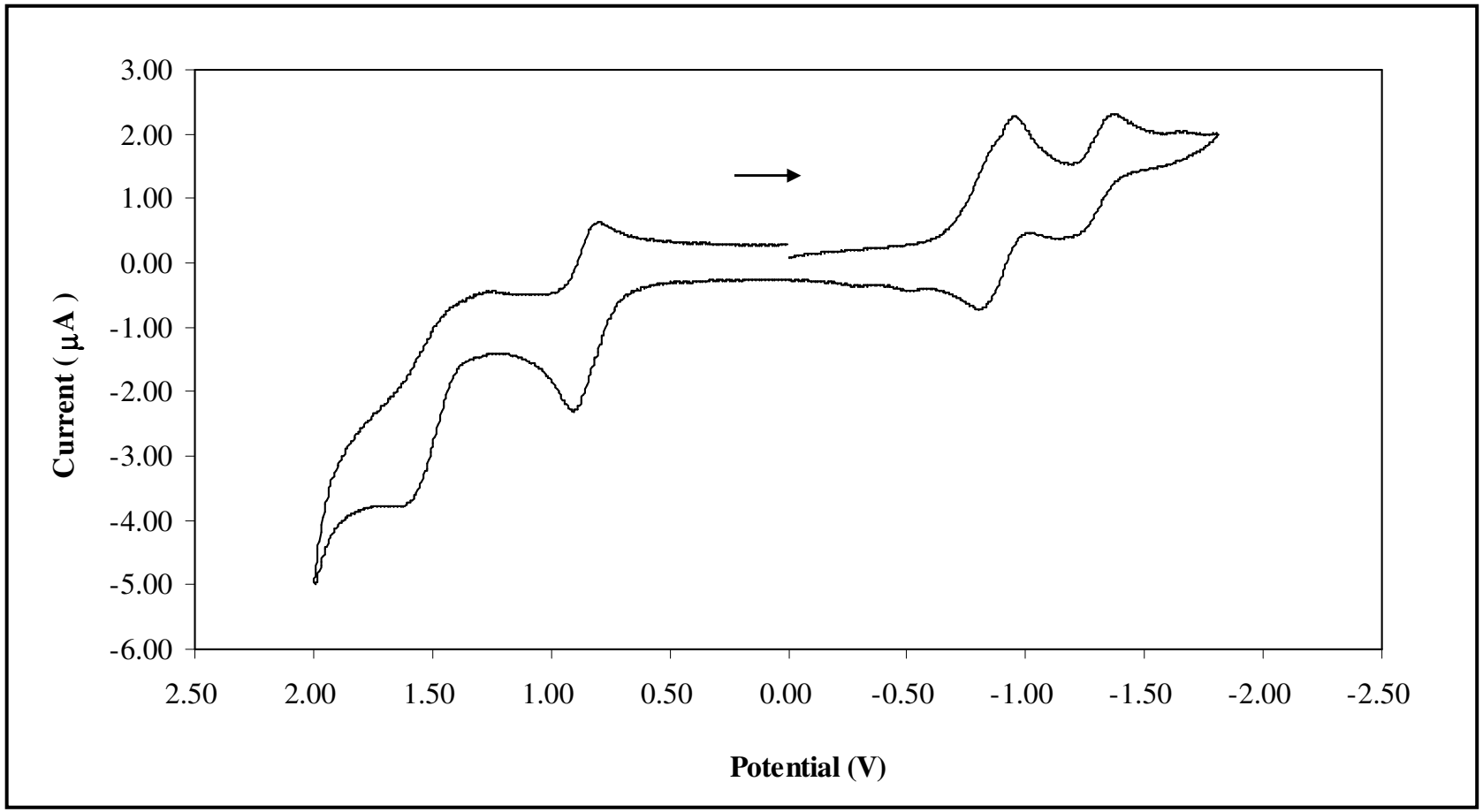

Figure 34. Cyclic voltammogram of *ctc*-[Ru(3aazpy)$_2$Cl$_2$] in 0.1 M TBAH CH_2Cl_2 at scan rate 100 mV/s.

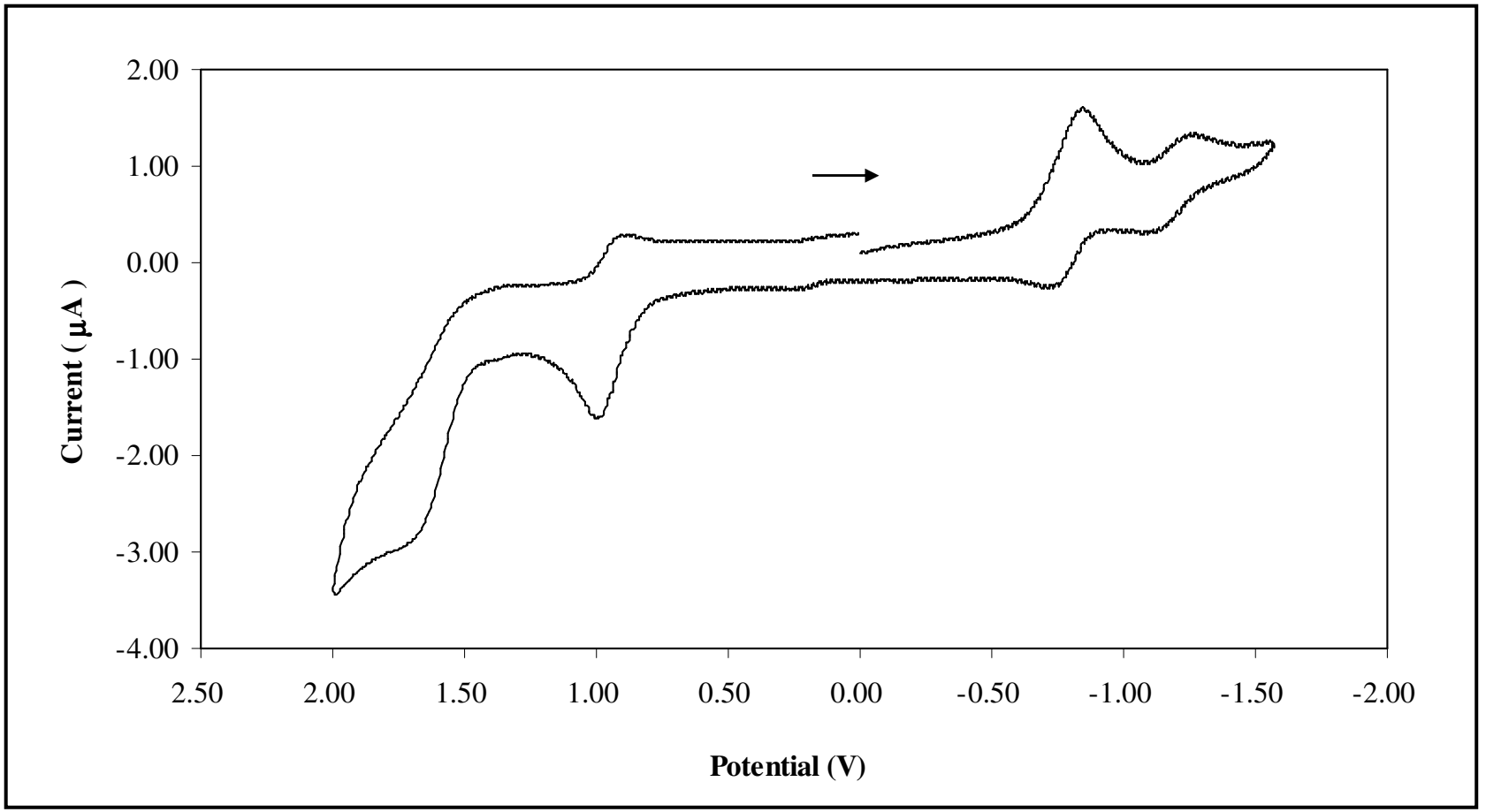

Figure 35. Cyclic voltammogram of *ccc*-[$Ru(3aazpy)_2Cl_2$] in 0.1 M TBAH CH_2Cl_2 at scan rate 100 mV/s.

3.2.6 X-ray Crystallography

X-ray crystallography is the most important technique to identify the geometry of compounds. The single crystals of both 3-amino-2-(phenylazo)pyridine and 2-amino-3-(phenylazo)pyridine were grown to obtain the suitable X-ray quality crystals for structure determination. X-ray diffraction data were collected on the APEX CCD diffractometer with the Xtal 3.7.1 program system and equipped with graphite monochromatized Mo Kα radiation (λ = 0.71073) at 293 K.

(a) X-ray structure of 3-amino-2-(phenylazo)pyridine

The single crystals of 3-amino-2-(phenylazo)pyridine were obtain by slow evaporation of a dichloromethane solution. The solid state structure of 3-amino-2-(phenylazo)pyridine is shown in Figure 36. The crystallographic data are shown in Table 14. Selected bond parameters are listed in Table 15.

In the title compound, the benzene ring (C6-C11), the azo group (N3-N4), and the substituted pyridine ring are not coplanar in the same plane. The angle between the planes of the pyridine ring and the azo group (C5-N3-N4) is 4.2(1)°, that between planes of the pyridine ring and the benzene ring is 19.59(6)°. The N3-N4 distance of the title compound is 1.265(2)Å, greater than that of the protonated azpy (1.248(4)Å)(Panneerselvam, K., *et al.,* 2000) and comparable with *trans*-bis(2-aminophenyl)diazene (1.2641(18)Å) (Bohle, D. S., *et al.*, 2007). In addition the bond length of C5-N3 1.400(2)Å is relative short compare with *trans*-bis(2-aminophenyl)diazene (Bohle, D. S., *et al.*, 2007), It indicates that there are some delocalization of electron density into the N=N π* orbitals.

Table 14. Crystallographic data of the 3-amino-2-(phenylazo)pyridine

Empirical formular	$C_{11}H_{10}N_4$	
Formular weight	198.25	
Temperature	293 K	
Wavelength	0.71073 Å	
Crystal system	Orthorhombic	
Space group	*Pbca*	
Unit cell dimensions	a = 11.8408(9) Å	$\alpha = 90°$
	b = 11.9798(9) Å	$\beta = 90°$
	c = 14.4198(11) Å	$\gamma = 90°$
Volume	2045.5(3) $Å^3$	
Z	8	
Density	1.288 mg/m^3	
Absorption coefficient	0.083 mm^{-1}	
Goodness-of-fit on F^2	1.03	
R	0.088	
wR	0.091	

Table 15. Selected bond lengths (Å) and angles (°) for the 3-amino-2-(phenylazo)pyridine

N(1)-C(1)	1.437(6)	N(2)-C(7)	1.404(5)
C(7)-C(8)	1.420(6)	N(1)-N(2)	1.256(5)
C(1)-C(2)	1.382(7)	C(7)-N(4)	1.340(5)
C(8)-N(3)	1.335(6)	C(1)-C(6)	1.378(7)
C(2)-C(3)	1.380(8)	C(8)-C(9)	1.411(7)
C(9)-C(10)	1.369(7)	C(3)-C(4)	1.36(1)
C(4)-C(5)	1.375(9)	C(10)-C(11)	1.374(7)
C(11)-N(4)	1.314(6)	C(5)-C(6)	1.388(8)

C(1)-N(1)-N(2)	114.2(4)	N(2)-C(7)-C(8)	126.3(4)
N(2)-C(7)-N(4)	111.1(3)	N(1)-C(1)-C(2)	115.4(4)
N(1)-C(1)-C(6)	125.4(4)	C(8)-C(7)-N(4)	122.6(4)
C(7)-C(8)-N(3)	123.9(4)	C(2)-C(1)-C(6)	119.3(5)
C(1)-C(2)-C(3)	120.7(6)	C(7)-C(8)-C(9)	115.7(4)
N(3)-C(8)-C(9)	120.4(4)	C(2)-C(3)-C(4)	120.0(6)
C(3)-C(4)-C(5)	119.9(6)	C(8)-C(9)-C(10)	120.2(4)
C(9)-C(10)-C(11)	119.3(5)	C(4)-C(5)-C(6)	120.7(6)
C(1)-C(6)-C(5)	119.4(5)	C(10)-C(11)-N(4)	122.8(5)
C(7)-N(4)-C(11)	119.4(4)	N(1)-N(2)-C(7)	115.5(3)

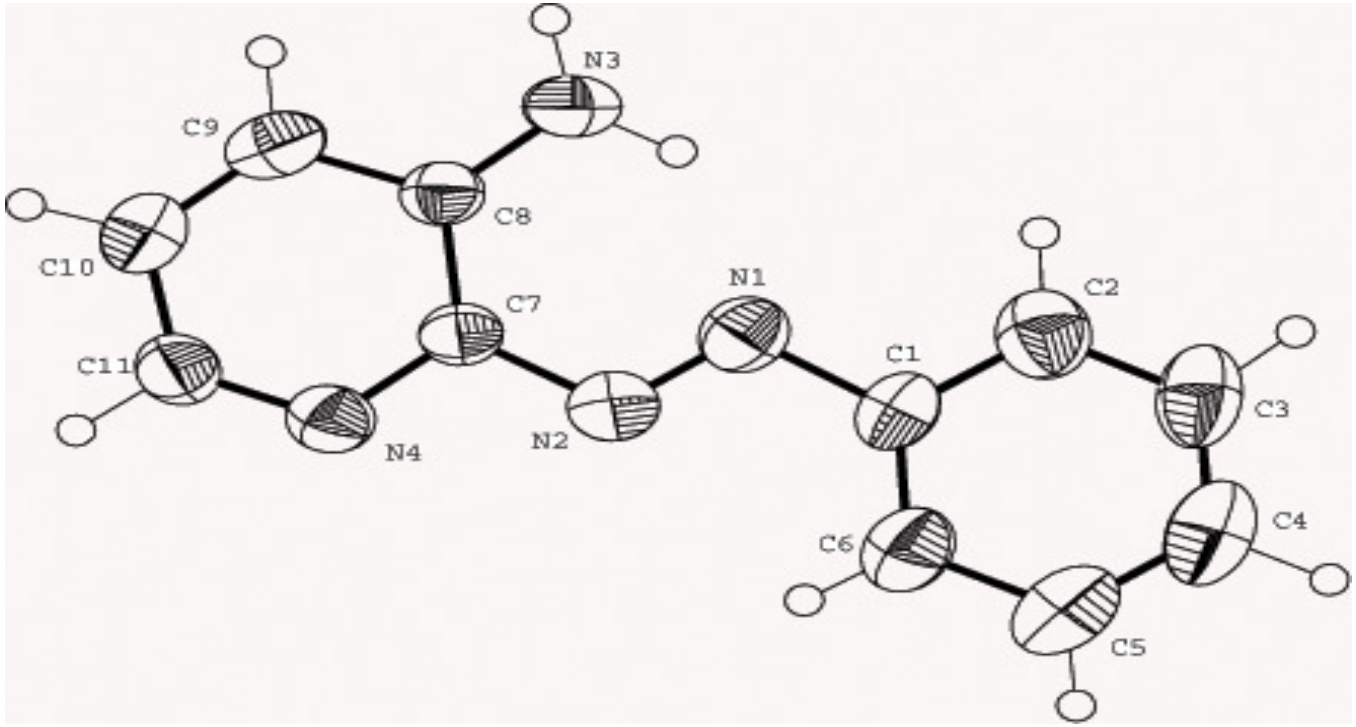
N3
C9
C8
C10
C7
N1
C2
C11
C1
C3
N4
N2
C4
C6
C5

Figure 36. The structure of 3-amino-2-(phenylazo)pyridine.

(b) X-ray structure of 2-amino-3-(phenylazo)pyridine

The X-ray quality single crystals were grown by slow diffusion of hexane into acetone solution of the compound. The structure of 2-amino-3-(phenylazo)pyridine is shown in Figure 37. The crystallographic data are shown in Table 16 and the selected bond parameters are listed in Table 17.

Table 16. Crystallographic data of the 2-amino-3-(phenylazo)pyridine

Empirical formular	$C_{11}H_{10}N_4$
Formula weight	198.25
Temperature	293 K
Wavelength	0.71073 Å
Crystal system	Monoclinic
Space group	$P2_1/n$
Unit cell dimensions	a = 5.1288(5) Å $\alpha = 90°$
	b = 16.5784(15) Å $\beta = 95.185°$
	c = 11.8055(11) Å $\gamma = 90°$
Volume	999.68(16) $Å^3$
Z	4
Density (calculated)	1.317 mg/m^3
Absorption coefficient	0.091 mm^{-1}
Goodness-of-fit on F^2	0.904
R	0.042
wR	0.048

Table 17. Selected bond lengths (Å) and angle (°) for the 2-amino-3-(phenylazo)pyridine

C1-N1	1.351(2)	N3-N4	1.265(2)
N4-C6	1.429(2)	C1-N2	1.334(2)
C1-C5	1.431(2)	C6-C7	1.393(2)
C6-C11	1.381(2)	N1-C2	1.326(2)
C2-C3	1.381(2)	C7-C8	1.382(2)
C8-C9	1.378(3)	C3-C4	1.373(2)
C4-C5	1.386(2)	C9-C10	1.377(3)
C10-C11	1.384(2)	C5-N3	1.400(2)

N1-C1-N2	116.5(1)	C5-N3-N4	117.3(1)
N3-N4-C6	113.5(1)	N1-C1-C5	120.6(1)
N2-C1-C5	122.9(1)	N4-C6-C7	123.5(1)
N4-C6-C11	116.6(1)	C1-N1-C2	118.8(1)
N1-C2-C3	124.5(1)	C7-C6-C11	119.9(1)
C6-C7-C8	119.4(2)	C2-C3-C4	117.4(2)
C3-C4-C5	120.8(1)	C7-C8-C9	120.8(2)
C8-C9-C10	119.7(2)	C1-C5-C4	117.8(1)
C1-C5-N3	127.2(1)	C9-C10-C11	120.3(2)
C6-C11-C10	120.0(2)	C4-C5-N3	114.9(1)

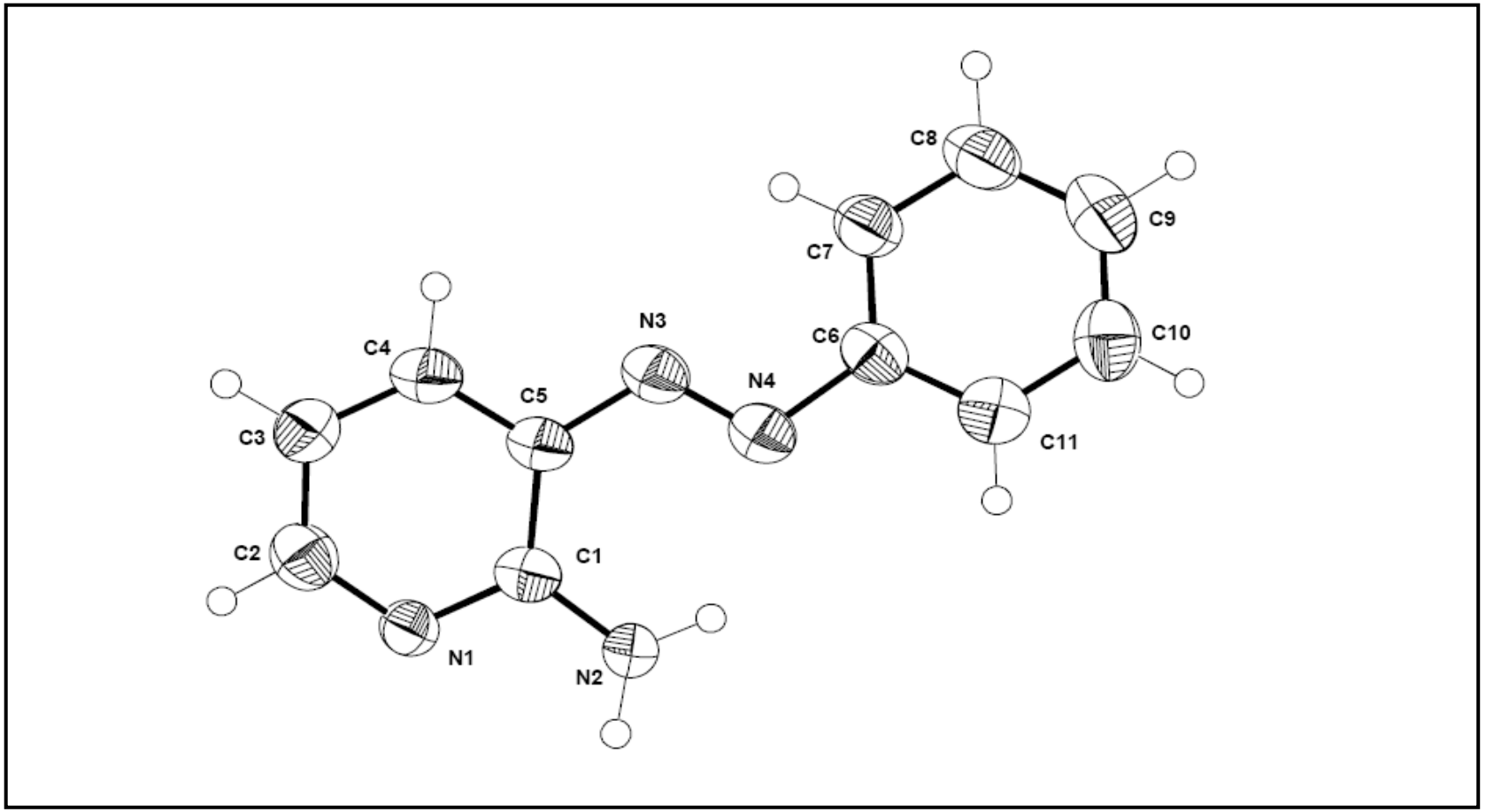

Figure 37. The structure of 2-amino-3-(phenylazo)pyridine.

4 CONCLUSION

The azoimine functionalized ligand 3-amino-2-(phenylazo)pyridine (3aazpy) was synthesized and reacted with $RuCl_3.3H_2O$ in DMF under refluxing condition. Two isomers of the composition $[Ru(3aazpy)_2Cl_2]$ have been chromatographically separated and are established as having *cis-trans-cis* (ctc) and *cis-cis-cis* (ccc) configurations with reference to the order of coordination pairs as Cl; N(pyridine), N and N(azo), N'. All of compounds were characterized by using elemental analysis, Infrared spectroscopy, UV-Visible absorption spectroscopy, 1D and 2D NMR spectroscopy and their electrochemical properties were studied by cyclic voltammetry. The solid state molecular structure of the two compounds, 3aazpy and 2a3pp were determined by X-ray crystallography.

From the results of elemental analysis, the analytical data of the compound corresponded to the calculated values.

The ligand exhibited a sharp band at 1399 cm^{-1}, corresponding to an N=N stretching mode. In the two complexes, ν(N=N) was red shifted by 80-90 cm^{-1} , which was a good indication of N-coordination. Solution electronic spectra of the complexes revealed that the *ctc* and *ccc* complexes exhibited highly intense MLCT transitions. The energy of the MLCT transition is an allowed transition. The ^{1}H, ^{13}C and DEPT NMR spectra between the ligand and complexes were compared in order to study the structures and the stereochemistry of the compounds. Results of 2D NMR experiments, ^{1}H-^{1}H COSY and ^{1}H-^{13}C HMQC, corresponded with the 1D NMR data. Redox studies of the 3aazpy revealed that the free ligand displayed one quasireversible two electron reduction at -1.78 mV. Nonetheless, the reduction potential of the ruthenium complexes showed a positive shift from the free ligand.

The X-ray structural studies confirmed both structures of 3aazpy and 2a3pp.

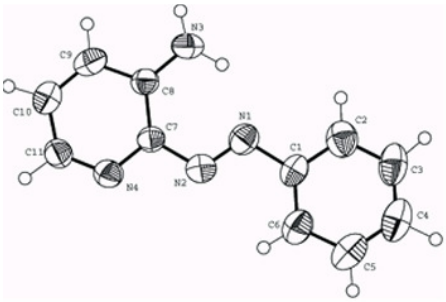

3aazpy

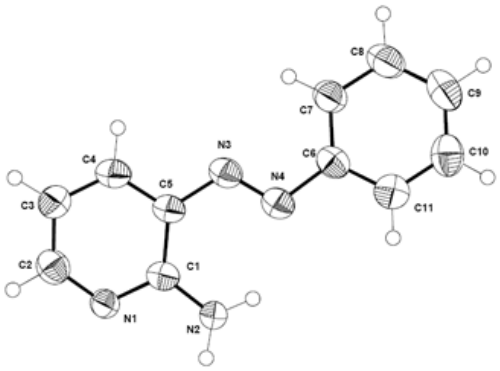

2a3pp

REFERENCES

Barf, G.A. and Sheldon, R.A. 1995. Ruthenium(II) 2-(phenylazo)pyridine complexes as epoxidation catalysts. *Journal of Molecular Catalysis A: Chemical* **98**: 143-146.

Bohle D. S., Dorans K. S., and Fotie J. 2007. *trans*-Bis(2-aminophenyl)diazene. *Acta Cryatallographica Section E* **E63**: o889-o890.

Changsaluk, U. 2008. Syntheses and Characterization of Ruthenium(II) Complexes with 5-Methyl-2-(phenylazo)pyridine Ligand. Ph. D. Inorganic Chemistry, Prince of Songkla University. (Unpublished)

Das, A., Peng, S. M. and Bhattacharya, S. 2000. Chemistry of 2-(Phenylazo)pyridine Complexes of Osmium: Synthesis, Characterization and Reactivities. *Polyhedron* **19**: 1227-1232.

Das, C., Saha, A., Hung, C. H., Lee, G. H., Peng, S. M. and Goswami, S. 2003. Ru(II) Complexes of 2-[(4-(Arylamino)phenyl)azo]pyridine Formed via Regioselective Phenyl Ring Amination of Coordinated 2-(Phenylazo)pyridine: Isolation of Products, X-ray Structure, and Redox and Optical Properties. *Inorganic Chemistry* **42**: 198-204.

Hansongnern, K., Tempiam, S., Liou, J.-C., Liao, F.-L., and Lu. T.-H. 2003. Crystal Structure of 2-(4'-*N, N*-Dimethylaminophenylazo)pyrimidine. *Analytical Sciences* **19** : x13-x14.

Hotze, A.C.G., Velders, A. H., Ugozzoli, F., Biagini-Cingi, M., Manotti-Lanfredi, A.M., Haasnoot, J. G. and Reedijk, J. 2000. Synthesis, Characterization, and Crystal Structure of α-[$Ru(azpy)_2(NO_3)_2$] (azpy = 2-(Phenylazo)pyridine) and the Products of Its Reactions with Guanine Derivatives. *Inorganic Chemistry* **39**: 3838-3844.

Jullapan, T. 2004. Synthesis and characterization of Ruthenium with 2-(phenylazo)benzothiazole ligands. M. Sc. Inorganic Chemistry, Prince of Songkla University. (Unpublished)

Kamar, K. K., Saha, A., Castineiras, A., Hung, C. H. and Goswami, S. 2002. Chromium Complexes of an Isomeric N-donor Ligand, 2-[(N-Arylamino)phenylazo]pyridine: Amination Reactions, X-ray Structure, and Redox Properties. *Inorganic Chemistry* **41**: 4531-4538.

Krause, R. A. and Krause, K. 1980. Chemistry of Bipyridyl-like Ligands. Isomeric Complexes of Ruthenium(II) with 2-(Phenylazo)pyridine. *Inorganic Chemistry* **19**: 2600-2603.

Krause, R. A. and Krause, K. 1984. Chemistry of Bipyridyl-like Ligands. 3. Complexes of Ruthenium(II) with 2-((4-Nitrophenyl)azo)pyridine. *Inorganic Chemistry* **23**: 2195-2198.

Lu, T. H., Misra, T. K., Lin, P. C., Liao, F. L. and Chung, C. S. 2003. Synthesis and X-ray Characterization of Two Isomeric Dichloro bis-{1-(phenylazo)isoquinoline} Complexes of Ruthenium(II). *Polyhedron* **22**: 535-541.

Misra T. K., Das D., Sinha, C., Ghosh, P. and Pal C. K. 1998. Chemistry of Azoimidazoles: Synthesis, spectral Characterization, Electrochemical Studies and X-ray Crystal Structure of Isomeric Dichloro Bis[1-alkyl-2-azrylazo)-imidazole] Complexes of Ruthenium(II). *Inoreganic Chemistry* **37**: 1672-1678.

Otsuki, J., Omokawa, N., Yoshiba, K., Yoshikawa, I., Akasaka, T., Suenobu, T., Takido, T., Araki, K. And Fukuzumi, S. 2003. Synthesis and Structural, Electrochemical, and Optical Properties of Ru(II) Complexes with Azobis(2,2'-bipyridine). *Inorganic Chemistry* **42**: 3057-3066.

Pal, S., Misra, T. K., Sinha, C., Slawin, A. M. Z. And Woollins, J. D. 2000. Ruthenium(II) Complexes of α-Diimines: Synthesis, Spectral Characterisation, Electrochemical Properties and Single-crystal X-ray Structure of bis-(2,2'-Bipyridine) {1-benzyl-2-(*p*-tollylazo)imidazole}ruthenium(II) perchlorate. *Polyhedron* **19**: 1925-1933.

Panneerselvam, K., Hansongnern, K., Rattanawit, N., Liao, F.-L. and Lu, T.-H. 2000. Crystal Structure of the [Protonated 2-(phenylazo)pyridine and Protonated 2-(4-hydroxyphenylazo)pyridine(3:1)]tetrafluoroborate. *Analytical Sciences* **16**: 1107-1108.

Saha, A., Das, C., Mitra, K. N., Peng, S.-M., Lee, G. H., Goswami, S. 2002. Synthesis, structure and redox properties of isomeric $[RuCl_2(L)_2]$ (L = *N*-aryl-1,2-arylenediimine) complexes formed by the oxidative dimerization of coordinated aromatic amines. *Polyhedron* **21**: 97-104.

Sahavisit, L. 2008. Syntheses and Characterization of Ruthenium(II) Complexes with 5-Chloro-2-(phenylazo)pyridine Ligand. Ph. D. Inorganic Chemistry, Prince of Songkla University. (Unpublished)

Santra, P. K., Misra, T. K., Das, D., Sinha, C., Slawin, A. M. Z. And Woollins, J. D. 1999. Chemistry of Azopyrimidine. Part II. Synthesis, Spectra, Electrochemistry and X-ray Crystal Structures of Isomeric dichloro bis-[2-(Arylazo)pyrimidine] Complexes of Ruthenium(II). *Polyhedron* **18**: 2869-2878.

Santra, P. K., Sinha, C., Sheen, W. J., Liao, F. L. and Lu, T. H. 2001. Reaction of $Ru(PPh_3)_3Cl_2$ with 2-(Arylazo)pyrimidine. Spectral and Redox Characterisation of the Products. Part V. Single Crystal X-ray Structure of $Ru(PPh_3)_2(papm)Cl_2$ (papm = 2-(Phenylazo)pyrimidine). *Polyhedron* **20**: 599-606.

Senapoti, S., Ray, U. S., Santra, P. K., Sinha, C., Alexandra, M. Z. S. And Woolins, J. D. 2002. Osmium-azopyrimidine Chemistry. Part VII: Synthesis, Structure Characterisation and Electrochemistry. *Polyhedron* **21**: 753-762.

Velders, A. H., Kooijman, H., Spek, A. L., Haasnoot, J. G., Vos, D. D. and Reedijk, J. 2000. Strong Differences in the in Vitro Cytotoxicity of Three Isomeric Dichlorobis(2-phenylazopyridine)ruthenium(II) Complexes. *Inorganic Chemistry* **39**: 2966-2967.

Velders, A. H., Schilden, K. V., Hotze, A. C. G., Kooijman, H., and Spek, A. L. 2004. Dicholrobis(2-phenylazopyridine)ruthenium(II) complexes of four isomers. *Dalton Trans* : 448-455.

Viñas C., Anglès P., Sánchez G., Lucena N., Teixidor F., Escriche L., Casabó J., Piniella J. F., Alvarez-Larena A., Kivekäs R. and Sillanpää R. 1998. Ruthenium(II) Complexes with NS_2 Pyridine-Based Dithia-Containing Ligands. Proposed Possible Structural Isomers and X-ray Confirmation of Their Existence. *Inorganic Chemistry* **37**: 701-707.

A. Cut off solvents

Table 18. The solvents for UV-Visible spectrum and the minimum values for measurement

Solvents	λ(nm)
CH_2Cl_2	230
$CHCl_3$	245
CH_3CN	195
DMF	270
DMSO	265

B. Bond distances (Å) and bond angles (°)

Table 19. The bond distances (Å) and angles (°) of the 3-amino-2-(phenylazo)pyridine

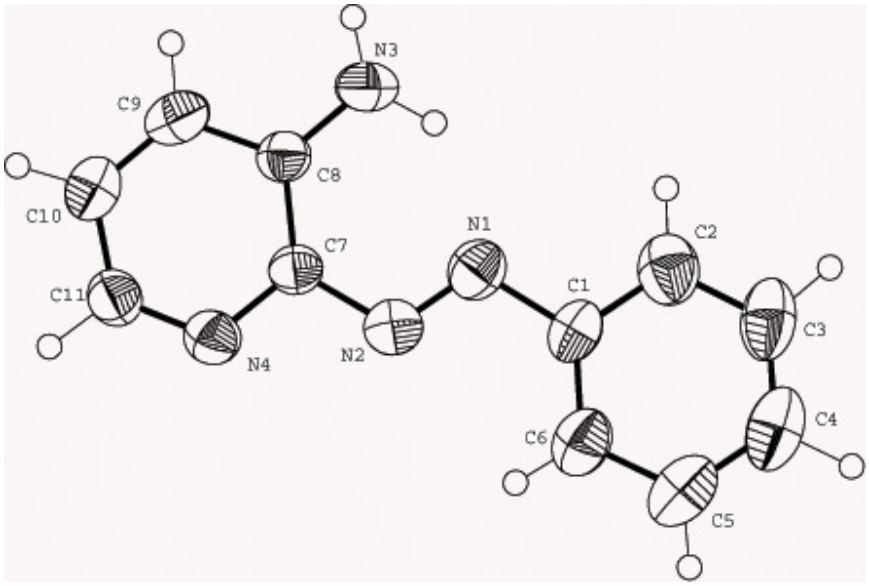

Bond distances and bond angle (°)

Atoms	Distance (Å)	Atoms	Angle (°)
N(1)-C(1)	1.437(6)	C(1)-N(1)-N(2)	114.2(4)
N(1)-N(2)	1.256(5)	N(1)-C(1)-C(2)	115.4(4)
C(1)-C(2)	1.382(7)	N(1)-C(1)-C(6)	125.4(4)
C(1)-C(6)	1.378(7)	C(2)-C(1)-C(6)	119.3(5)
C(2)-C(3)	1.380(8)	C(1)-C(2)-C(3)	120.7(6)
C(3)-C(4)	1.360(1)	C(1)-C(2)-H(2)	117.0(3)
C(4)-C(5)	1.375(9)	C(3)-C(2)-H(2)	122.0(3)
C(5)-C(6)	1.388(8)	C(2)-C(3)-C(4)	120.0(6)
N(2)-C(7)	1.404(5)	C(2)-C(3)-H(3)	114.0(3)
C(7)-C(8)	1.420(6)	C(4)-C(3)-H(3)	126.0(3)
C(7)-N(4)	1.340(5)	C(3)-C(4)-C(5)	119.9(6)
C(8)-N(3)	1.335(6)	C(3)-C(4)-H(4)	116.0(3)
C(8)-C(9)	1.411(7)	C(5)-C(4)-H(4)	124.0(3)
C(9)-C(10)	1.369(7)	C(4)-C(5)-C(6)	120.7(6)
C(10)-C(11)	1.374(7)	C(4)-C(5)-H(5)	119.0(4)
C(11)-N(4)	1.314(6)	C(6)-C(5)-H(5)	120.0(4)
		C(1)-C(6)-C(5)	119.4(5)
		C(1)-C(6)-H(6)	120.0(3)
		C(5)-C(6)-H(6)	121.0(3)

Table 19. (Continued)

Atoms	Distance (Å)	Atoms	Angle (°)
C(2)-H(2)	0.960(5)	N(1)-N(2)-C(7)	115.5(3)
C(3)-H(3)	0.950(6)	N(2)-C(7)-C(8)	126.3(4)
C(4)-H(4)	0.960(6)	N(2)-C(7)-N(4)	111.1(3)
C(5)-H(5)	0.920(6)	C(8)-C(7)-N(4)	122.6(4)
C(6)-H(6)	0.910(5)	C(7)-C(8)-N(3)	123.9(4)
N(3)-H(31)	0.860(5)	C(7)-C(8)-C(9)	115.7(4)
N(3)-H(32)	0.880(4)	N(3)-C(8)-C(9)	120.4(4)
C(9)-H(9)	0.900(4)	C(8)-N(3)-H(31)	117.0(3)
C(10)-H(10)	0.930(5)	C(8)-N(3)-H(32)	113.0(3)
		H(31)-N(3)-H(32)	129.0(4)
		C(8)-C(9)-C(10)	120.2(4)
		C(8)-C(9)-H(9)	115.0(3)
		C(10)-C(9)-H(9)	125.0(3)
		C(9)-C(10)-C(11)	119.3(5)
		C(9)-C(10)-H(10)	120.0(3)
		C(11)-C(10)-H(10)	121.0(3)
		C(10)-C(11)-N(4)	122.8(5)
		C(10)-C(11)-H(11)	118.0(3)
		N(4)-C(11)-H(11)	119.0(3)
		C(7)-N(4)-C(11)	119.4(4)

Non-Hydrogen Positional and Isotropic Displacement Parameters

Atom	x/a	y/b	z/c	U(eq) A**2
N(1)	0.0875(3)	0.4588(3)	0.3972(3)	* 0.053(2)
C(1)	-0.0010(4)	0.5168(4)	0.3490(3)	* 0.054(3)
C(2)	-0.0744(5)	0.4499(5)	0.2994(4)	* 0.065(3)
C(3)	-0.1638(5)	0.4959(6)	0.2514(4)	* 0.074(4)
C(4)	-0.1801(5)	0.6081(6)	0.2520(4)	* 0.074(4)
C(5)	-0.1079(5)	0.6757(6)	0.3012(4)	* 0.074(4)
C(6)	-0.0175(5)	0.6307(5)	0.3497(4)	* 0.063(3)
N(2)	0.1537(3)	0.5215(3)	0.4410(2)	* 0.046(2)
C(7)	0.2413(4)	0.4672(3)	0.4887(3)	* 0.042(2)
C(8)	0.2573(4)	0.3501(3)	0.4960(3)	* 0.044(2)
N(3)	0.1908(4)	0.2748(4)	0.4553(4)	* 0.068(3)
C(9)	0.3509(5)	0.3157(4)	0.5494(4)	* 0.057(3)
C(10)	0.4187(4)	0.3934(4)	0.5913(4)	* 0.057(3)
C(11)	0.3962(4)	0.5048(4)	0.5787(4)	* 0.055(3)
N(4)	0.3101(3)	0.5411(3)	0.5297(3)	* 0.051(2)

Hydrogen Positional and Isotropic Displacement Parameters

Atom	x/a	y/b	z/c	U(eq) A**2
H(2)	-0.061(4)	0.371(5)	0.301(4)	0.09(2)
H(3)	-0.209(5)	0.443(5)	0.219(4)	0.09(2)
H(4)	-0.243(5)	0.635(4)	0.216(4)	0.09(2)
H(5)	-0.116(5)	0.752(5)	0.297(4)	0.10(2)
H(6)	0.031(4)	0.675(4)	0.381(3)	0.06(2)
H(9)	0.361(3)	0.241(4)	0.554(3)	0.05(1)
H(10)	0.480(4)	0.370(4)	0.627(4)	0.07(2)
H(11)	0.448(4)	0.559(4)	0.608(4)	0.08(2)
H(31)	0.201(4)	0.206(5)	0.470(3)	0.07(2)
H(32)	0.134(4)	0.305(4)	0.424(3)	0.05(1)

Table 20. The bond distances (Å) and angles (°) of the 2-amino-3-(phenylazo)pyridine

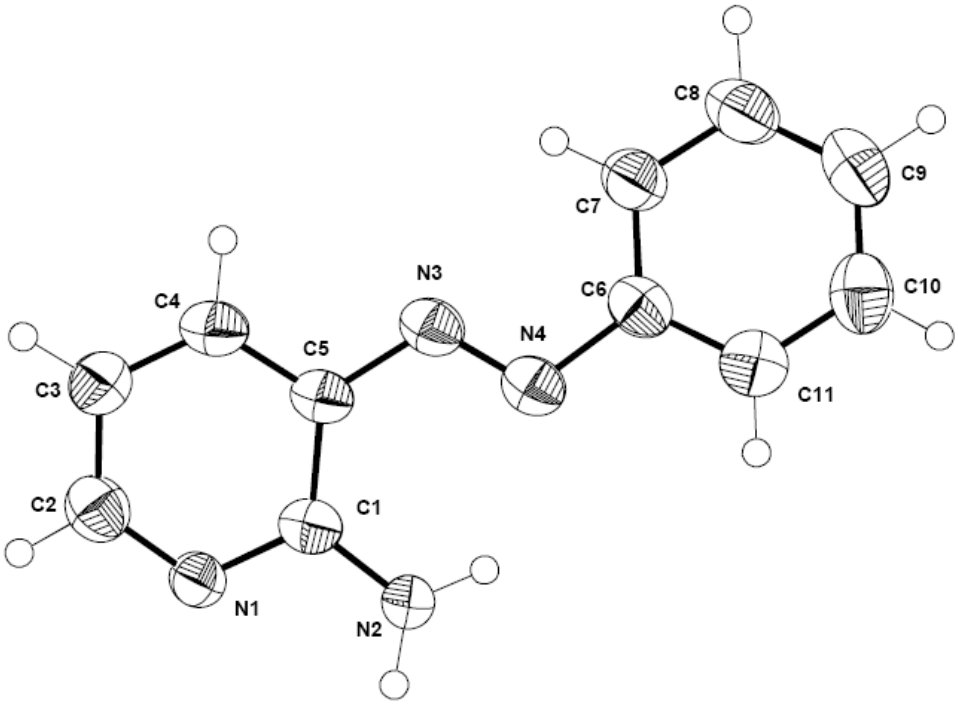

Bond distances and bond angle (°)

Atoms	Distance (Å)	Atoms	Angle (°)
C(1)-N(1)	1.350(19)	N(1)-C(1)-N(2)	116.48(12)
C(1)-N(2)	1.334(2)	N(1)-C(1)-C(5)	120.65(13)
C(1)-C(5)	1.430(18)	N(2)-C(1)-C(5)	122.87(13)
N(1)-C(2)	1.326(2)	C(1)-N(1)-C(2)	118.79(12)
N(2)-H(2Na)	0.880(2)	C(1)-N(2)-H(2Na)	118.50(12)
N(2)-H(2Nb)	0.880(2)	C(1)-N(2)-H(2Nb)	118.20(13)
C(2)-C(3)	1.381(2)	H(2Na)-N(2)-H(2Nb)	123.30(18)
C(2)-H(2)	0.963(16)	N(1)-C(2)-C(3)	124.47(15)
C(3)-C(4)	1.373(2)	N(1)-C(2)-H(2)	115.00(10)
C(3)-H(3)	0.972(18)	C(3)-C(2)-H(2)	120.60(10)
C(4)-C(5)	1.386(2)	C(2)-C(3)-C(4)	117.41(15)
C(4)-H(4)	0.976(17)	C(2)-C(3)-H(3)	121.10(10)
C(5)-N(3)	1.400(18)	C(4)-C(3)-H(3)	121.40(10)
N(3)-N(4)	1.264(17)	C(3)-C(4)-C(5)	120.83(14)
N(4)-C(6)	1.429(18)	C(3)-C(4)-H(4)	121.90(10)
C(6)-C(7)	1.393(2)	C(5)-C(4)-H(4)	117.20(10)
C(6)-C(11)	1.381(2)	C(1)-C(5)-C(4)	117.80(13)
C(7)-C(8)	1.382(2)	C(1)-C(5)-N(3)	127.22(13)
C(7)-H(7)	0.947(17)	C(4)-C(5)-N(3)	114.93(12)

Table 20. (Continued)

Atoms	Distance (Å)	Atoms	Angle (°)
C(8)-C(9)	1.378(3)	C(5)-N(3)-N(4)	117.32(11)
C(8)-H(8)	0.990(2)	N(3)-N(4)-C(6)	113.53(11)
C(9)-C(10)	1.377(3)	N(4)-C(6)-C(7)	123.49(14)
C(9)-H(9)	0.960(19)	N(4)-C(6)-C(11)	116.62(13)
C(10)-C(11)	1.384(2)	C(7)-C(6)-C(11)	119.86(14)
C(10)-H(10)	0.960(2)	C(6)-C(7)-C(8)	119.35(16)
C(11)-H(11)	0.969(18)	C(6)-C(7)-H(7)	119.40(10)
		C(8)-C(7)-H(7)	121.20(10)
		C(7)-C(8)-C(9)	120.77(17)
		C(7)-C(8)-H(8)	118.60(12)
		C(9)-C(8)-H(8)	120.60(12)
		C(8)-C(9)-C(10)	119.68(17)
		C(8)-C(9)-H(9)	120.50(12)
		C(10)-C(9)-H(9)	119.80(12)
		C(9)-C(10)-C(11)	120.35(18)
		C(9)-C(10)-H(10)	121.40(12)
		C(11)-C(10)-H(10)	118.30(12)
		C(6)-C(11)-C(10)	119.98(16)
		C(6)-C(11)-H(11)	118.70(10)
		C(10)-C(11)-H(11)	121.20(10)

Non-Hydrogen Positional and Isotropic Displacement Parameters

Atom	x/a	y/b	z/c	U(eq) A**2
C(1)	0.6853(3)	0.51572(8)	0.1757(1)	* 0.0422(7)
N(1)	0.4786(2)	0.46709(8)	0.1468(1)	* 0.0481(7)
N(2)	0.7879(3)	0.5538(1)	0.0905(1)	* 0.0594(9)
C(2)	0.3717(3)	0.4271(1)	0.2282(1)	* 0.0507(9)
C(3)	0.4586(3)	0.4309(1)	0.3422(1)	* 0.0515(9)
C(4)	0.6662(3)	0.48099(9)	0.3731(1)	* 0.0478(8)
C(5)	0.7833(3)	0.52547(8)	0.2922(1)	* 0.0412(7)
N(3)	0.9807(2)	0.57816(7)	0.3360(1)	* 0.0442(6)
N(4)	1.0943(2)	0.61988(8)	0.2654(1)	* 0.0454(7)
C(6)	1.2800(3)	0.67585(8)	0.3177(1)	* 0.0441(7)
C(7)	1.2886(3)	0.6982(1)	0.4317(1)	* 0.0529(9)
C(8)	1.4734(4)	0.7536(1)	0.4744(2)	* 0.061(1)
C(9)	1.6475(4)	0.7870(1)	0.4054(2)	* 0.063(1)
C(10)	1.6362(3)	0.7655(1)	0.2925(2)	* 0.061(1)
C(11)	1.4521(3)	0.7103(1)	0.2482(1)	* 0.0518(9)

Hydrogen Positional and Isotropic Displacement Parameters

Atom	x/a	y/b	z/c	U(eq) A**2
H(2)	0.223(3)	0.394(1)	0.203(1)	0.054(4)
H(3)	0.371(3)	0.401(1)	0.399(2)	0.065(5)
H(4)	0.737(3)	0.487(1)	0.452(1)	0.061(5)
H(7)	1.166(3)	0.676(1)	0.478(1)	0.059(5)
H(8)	1.477(4)	0.769(1)	0.555(2)	0.078(6)
H(9)	1.776(4)	0.825(1)	0.436(2)	0.074(6)
H(10)	1.752(4)	0.789(1)	0.242(2)	0.074(6)
H(11)	1.447(3)	0.693(1)	0.170(2)	0.057(5)
H(2Na)	0.924(4)	0.585(1)	0.107(2)	0.066(5)
H(2Nb)	0.718(4)	0.545(1)	0.021(2)	0.072(6)

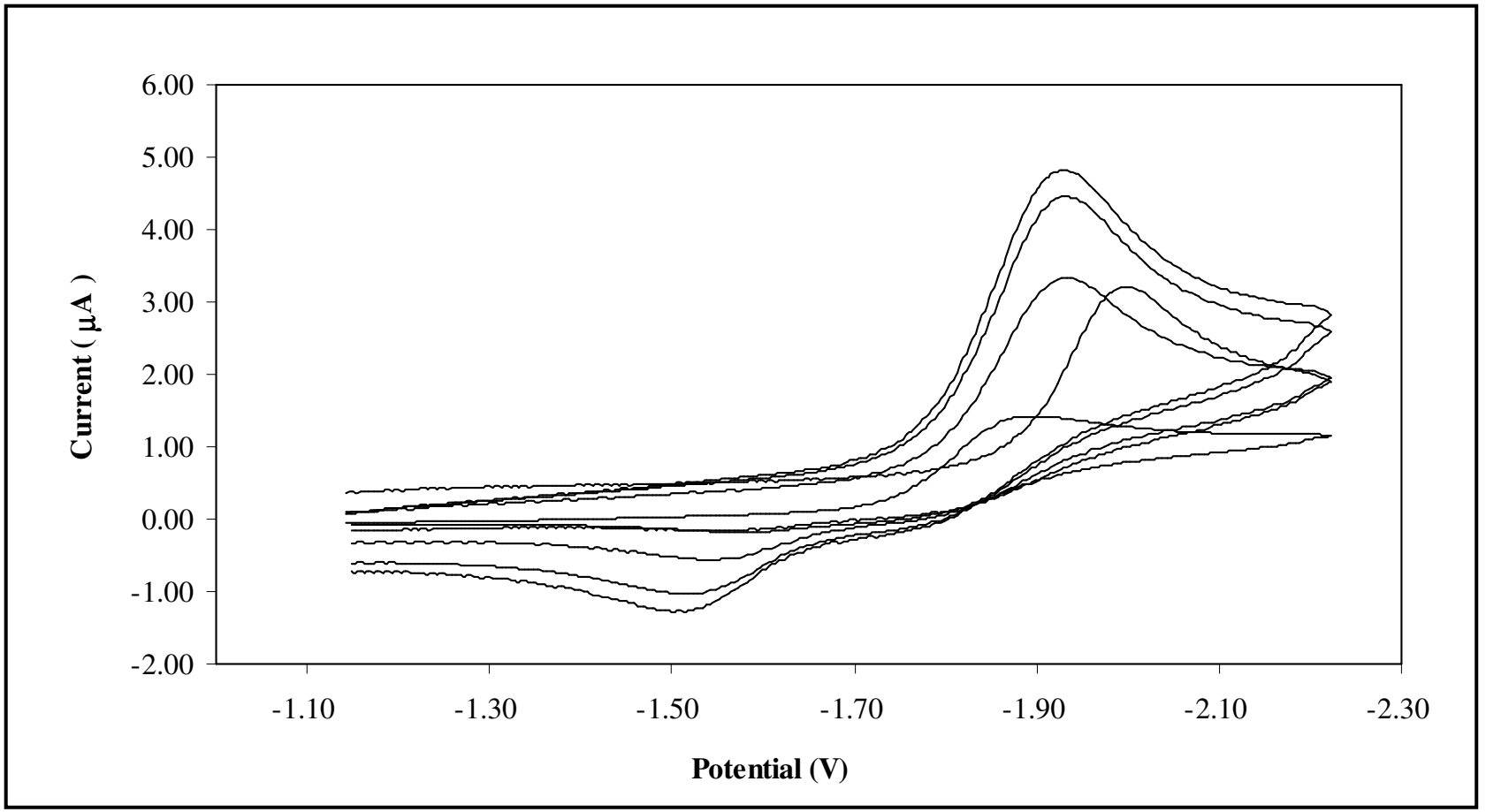

Figure 38. Cyclic voltammogram of 3aazpy with various scan rates 50-500 mV/s in the reduction range.

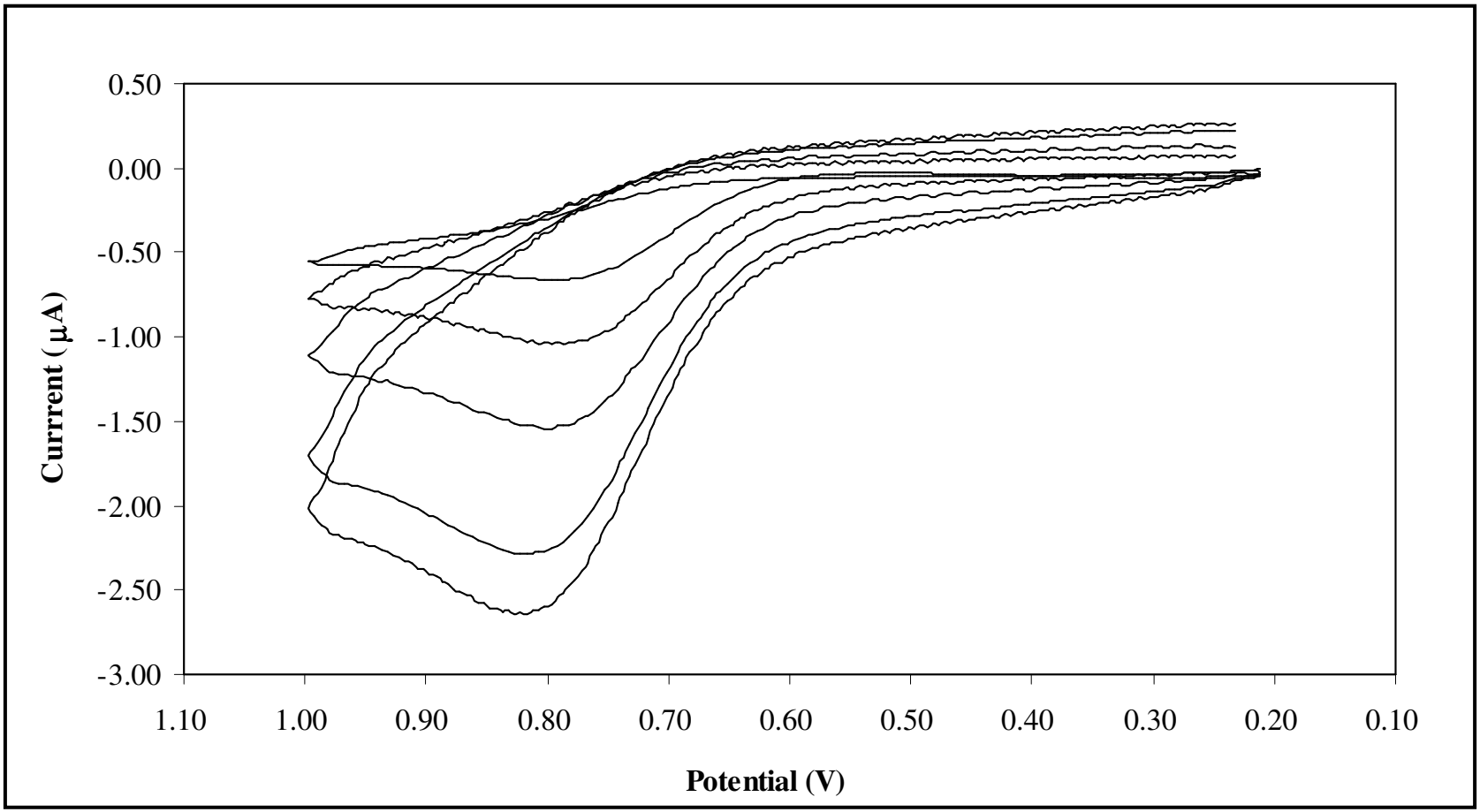

Figure 39. Cyclic voltammogram of 3aazpy with various scan rates 50-500 mV/s in the oxidation range.

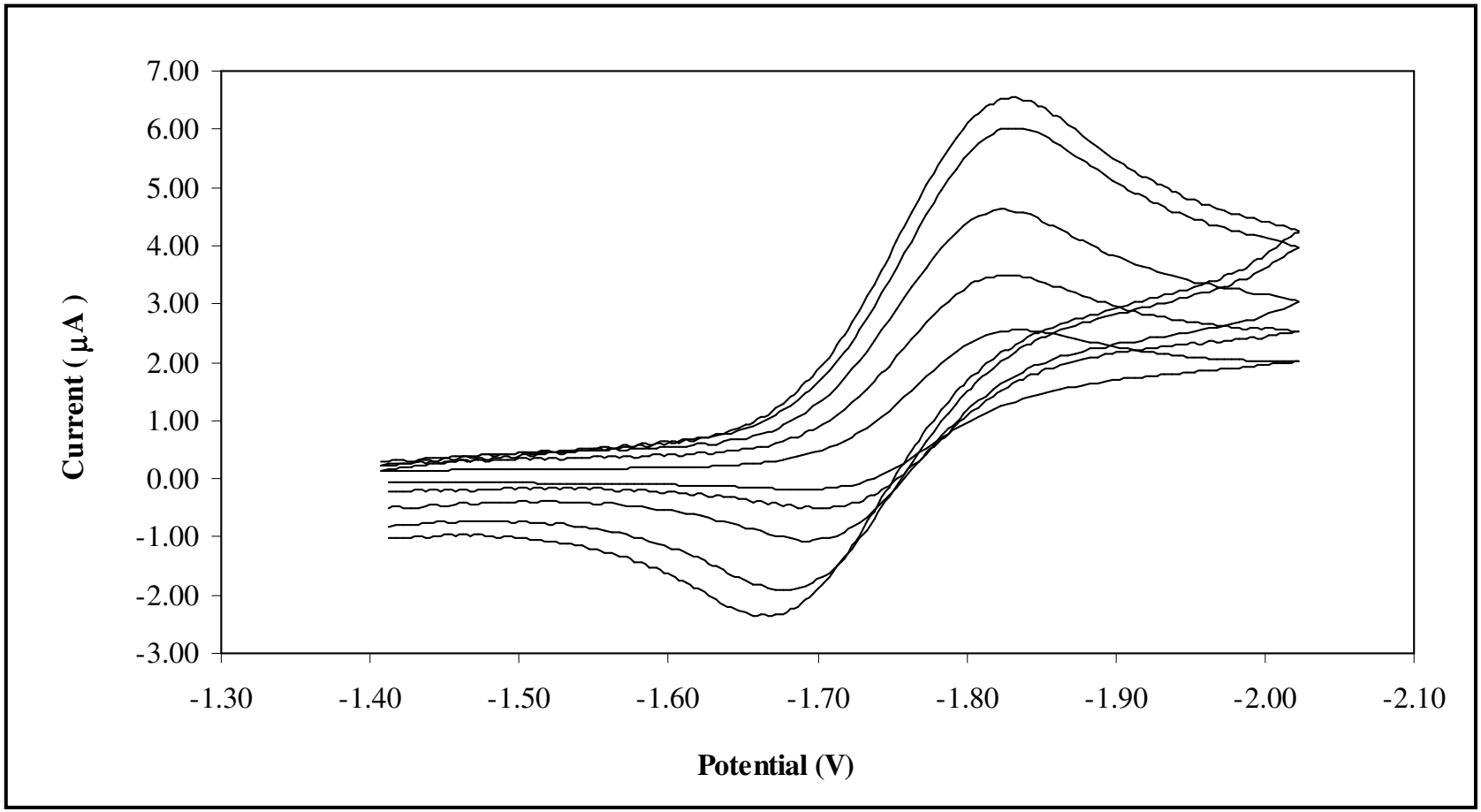

Figure 40. Cyclic voltammogram of 2a3pp with various scan rates 50-500 mV/s in the reduction range.

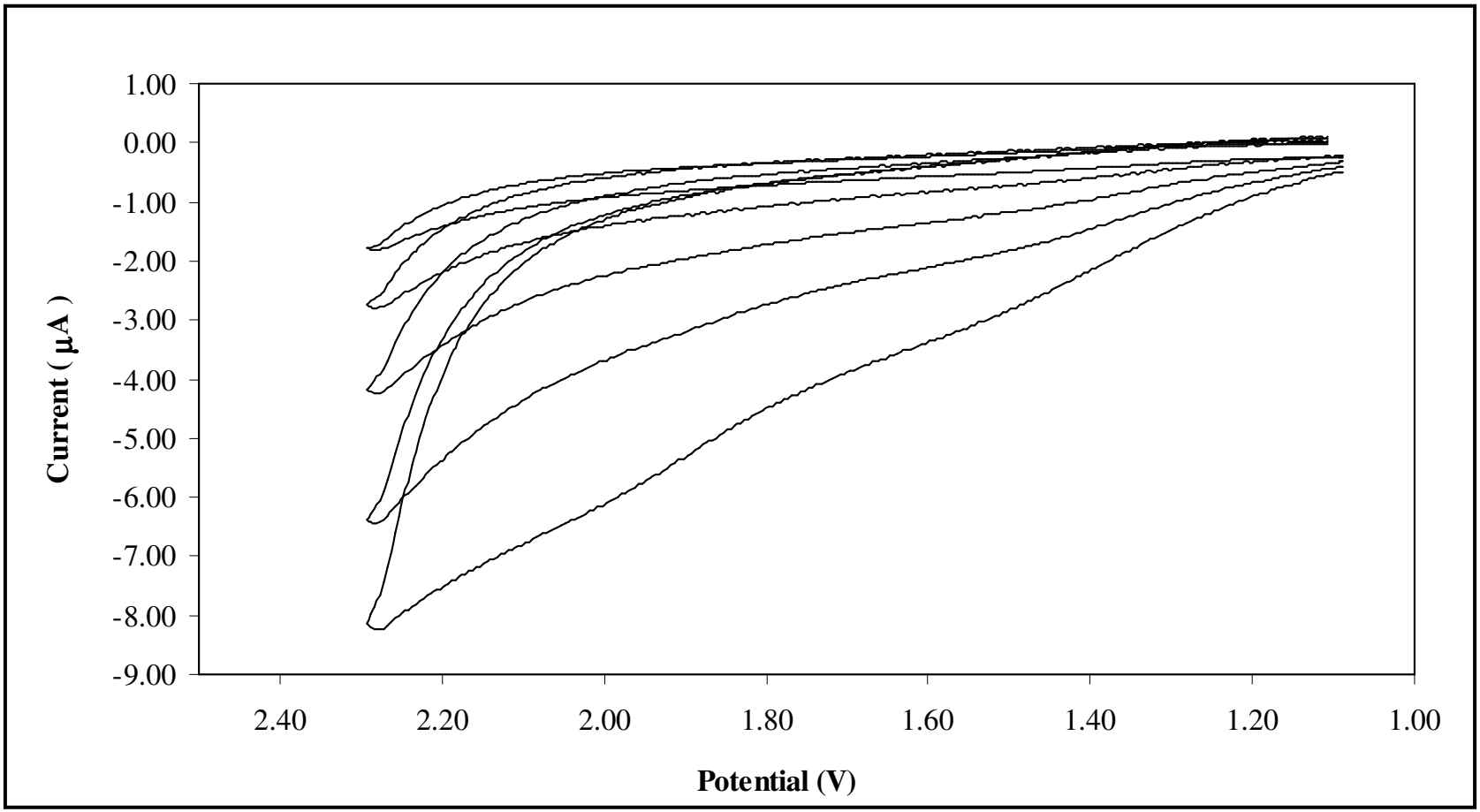

Figure 41. Cyclic voltammogram of 2a3pp with various scan rates 50-500 mV/s in the oxidation range.

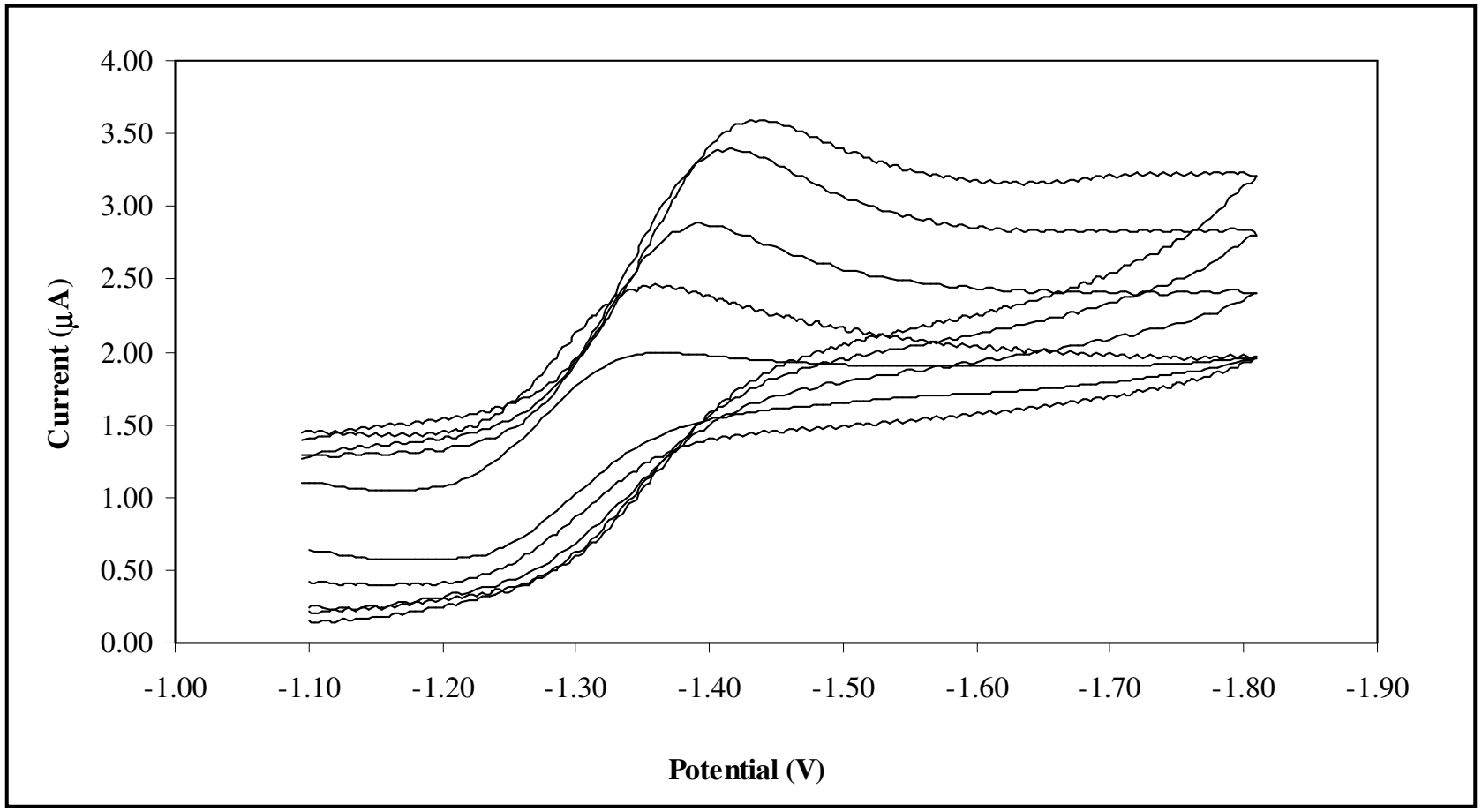

Figure 42. Cyclic voltammogram of *ctc*-[Ru(3aazpy)$_2$Cl$_2$]-couple I in the reduction ranges with various scan rate 50-500 mV/s.

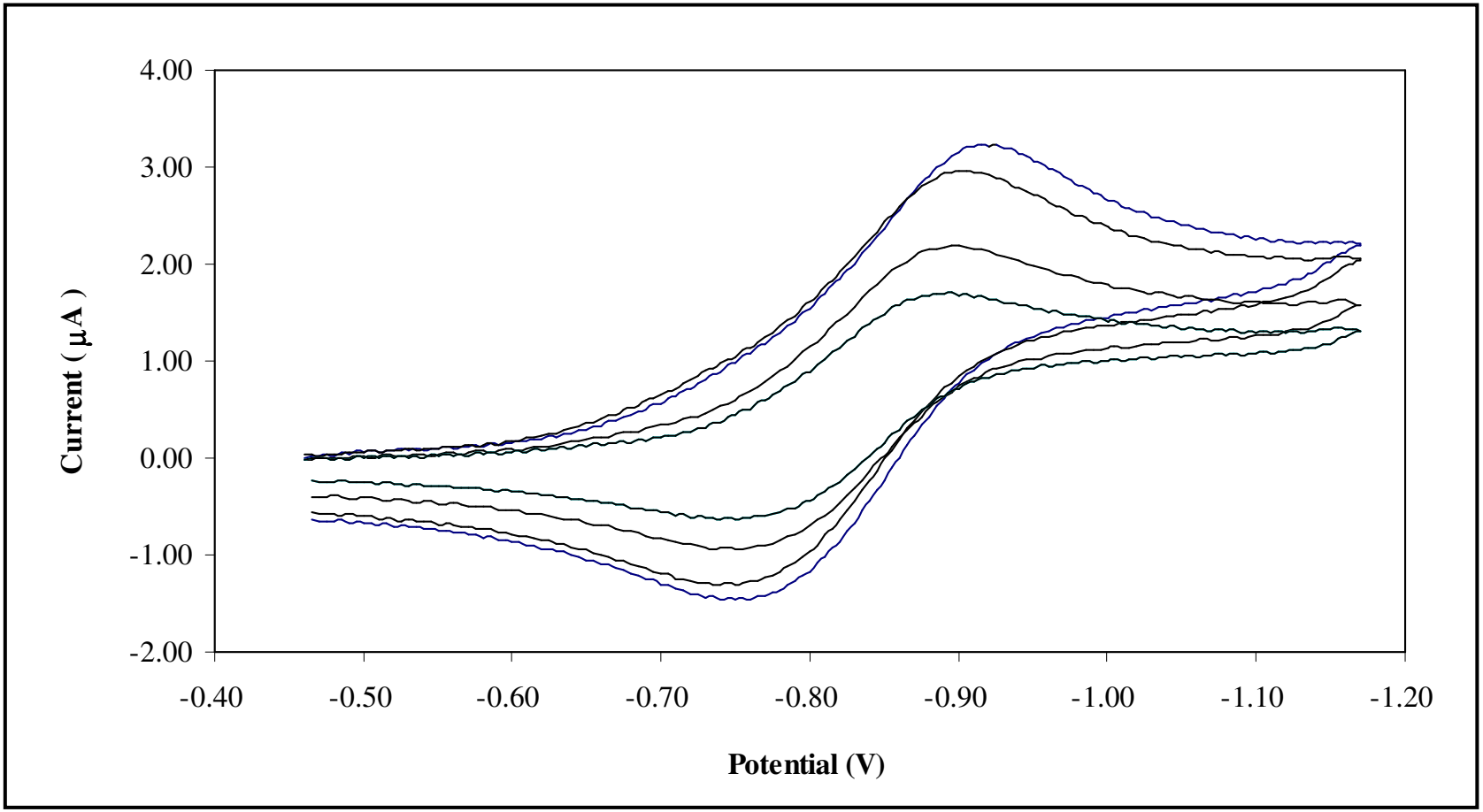

Figure 43. Cyclic voltammogram of *ctc*-[Ru(3aazpy)$_2$Cl$_2$]-couple II in the reduction ranges with various scan rate 50-500 mV/s.

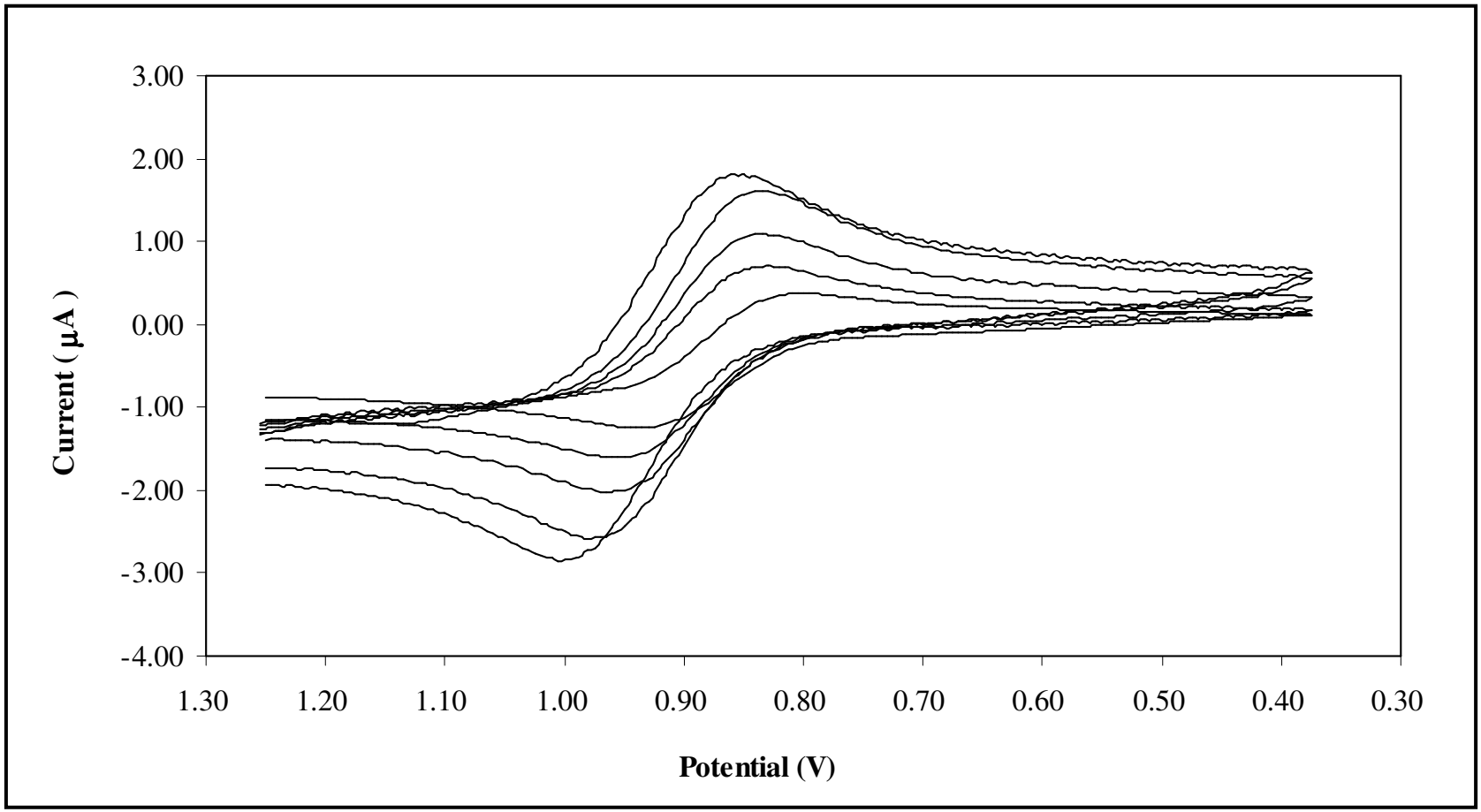

Figure 44. Cyclic voltammogram of *ctc*-[Ru(3aazpy)$_2$Cl$_2$] in the oxidation range with various scan rates 50-500 mV/s.

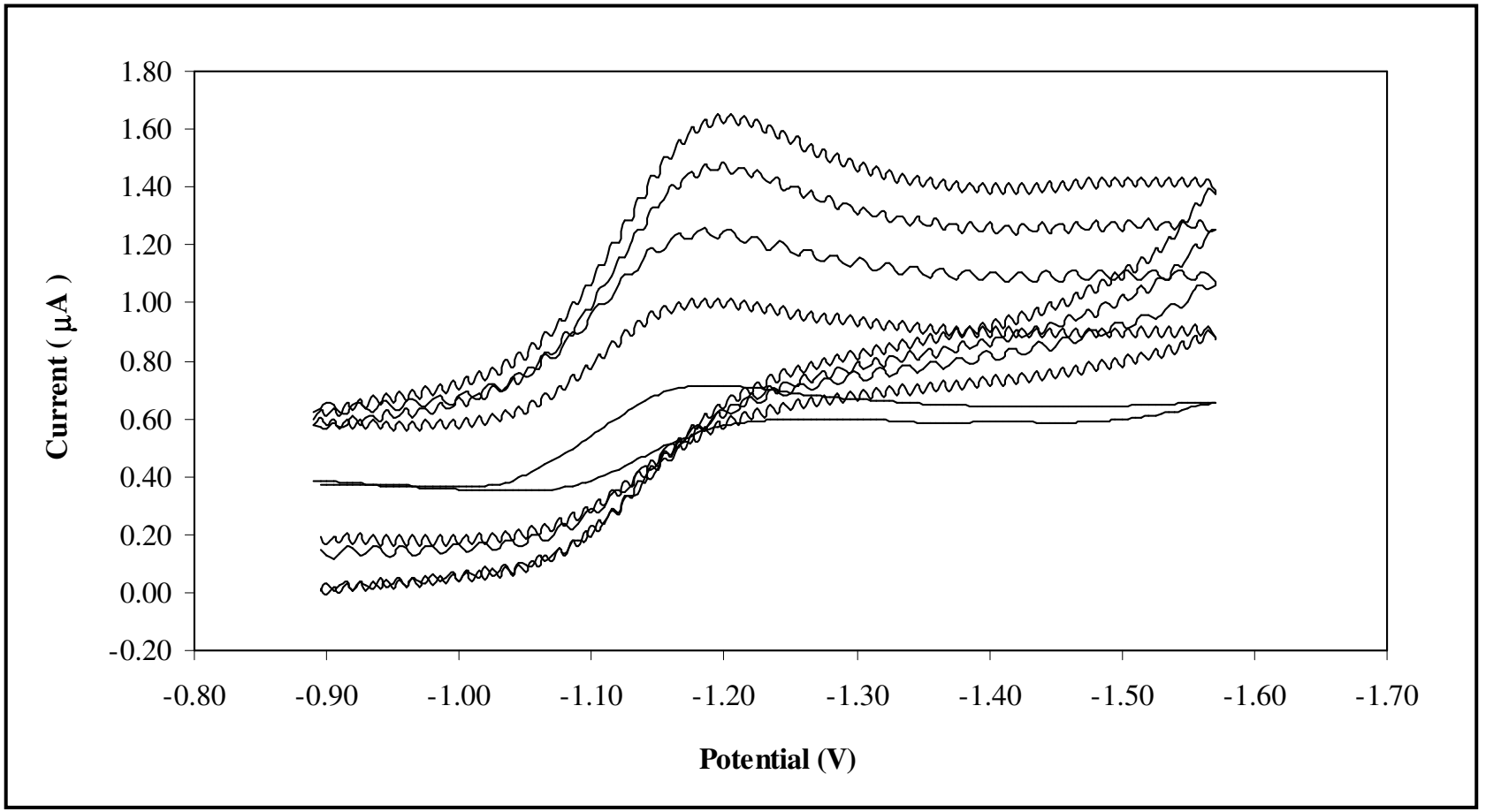

Figure 45. Cyclic voltammogram of *ccc*-[Ru(3aazpy)$_2$Cl$_2$]-couple I in the reduction range with various scan rates 50-500 mV/s.

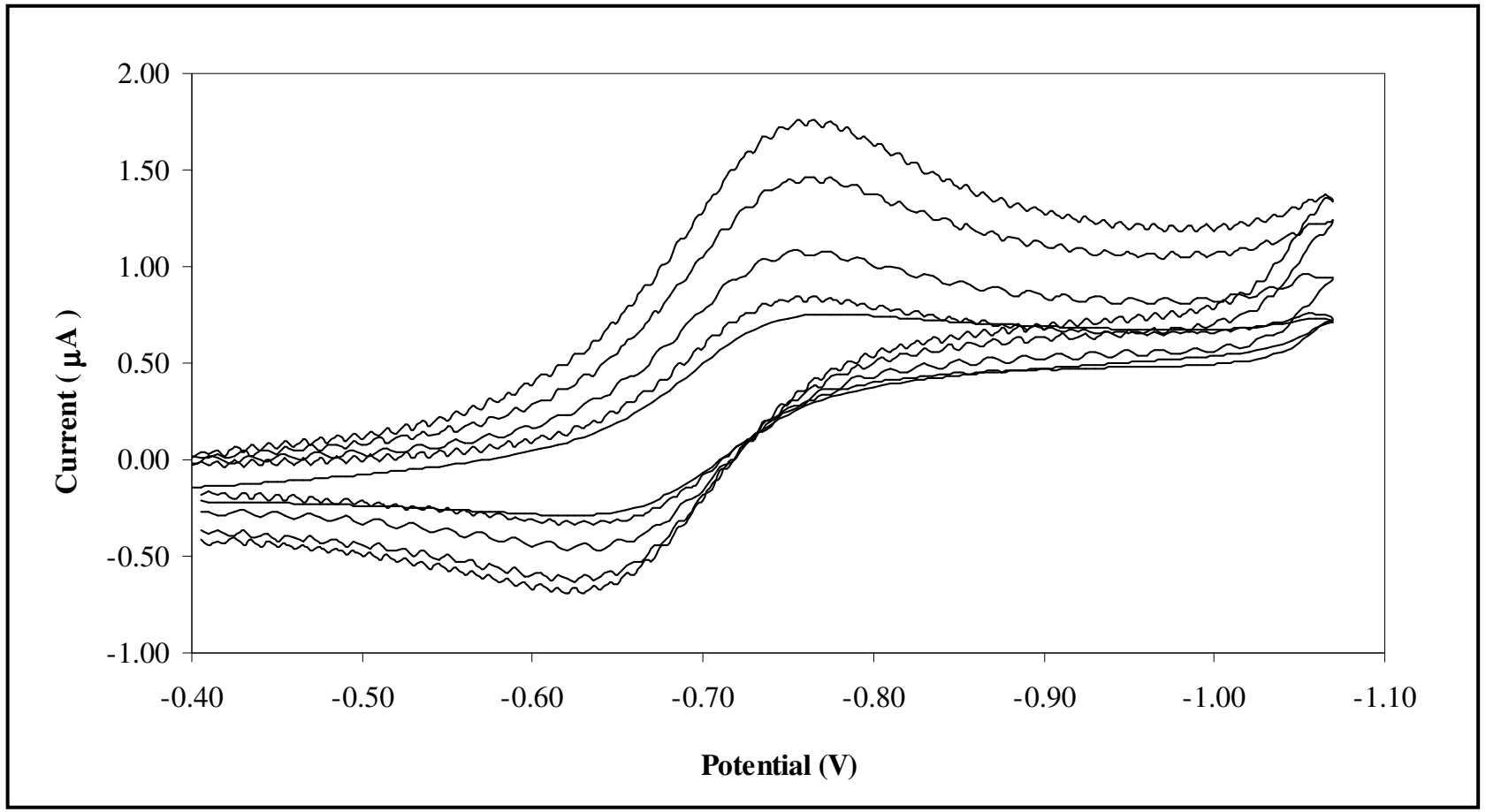

Figure 46. Cyclic voltammogram of *ccc*-[Ru(3aazpy)$_2$Cl$_2$]-couple II in the reduction range with various scan rates 50-500 mV/s.

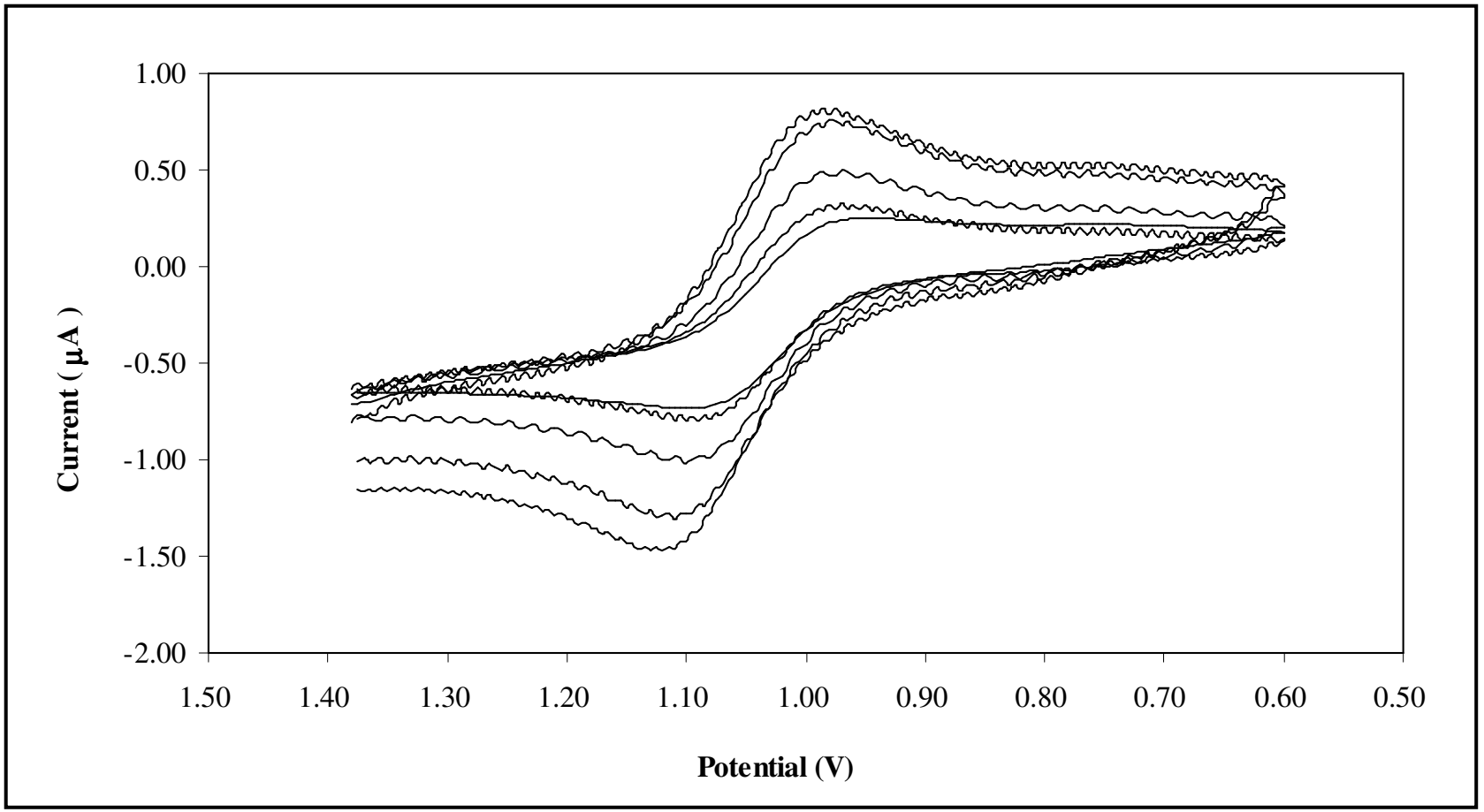

Figure 47. Cyclic voltammogram of *ccc*-[Ru(3aazpy)$_2$Cl$_2$] in the oxidation range with various scan rates 50-500 mV/s.

VITAE

Name Miss Supojjanee Sansook

Student ID 4910220089

Educational Attainment

Degree	Name of Institution	Year of Graduation
Bachelor of Science (Chemistry)	Prince of Songkla University	2005

Scholarship Awards during Enrolment

Center of Excellence for Innovation in Chemistry (PERCH-CIC): Commision on Higher Education, Ministry of Education

Teaching Assistance (TA)

List of Publication and Proceeding

Poster presentation

Sansook S. and Hansongnern K.* "Synthesis and Characterization of 3-Amino-2-(phenylazo)pyridine Ligand", Pure and Applied Chemistry International Conference, Bangkok, Thailand, January 30 – February 1, 2008, 104.